MARMARA UNIVERSITY
INSTITUTE FOR GRADUATE STUDIES
IN PURE AND APPLIED SCIENCES

MULTI-OBJECTIVE OPTIMIZATION AT A CRUDE NOVEL LIPASE CATALYZED FAME PRODUCTION:

KRIGING AS AN ALTERNATIVE TO RSM

CEYDA KULA

Ph.D. THESIS
Department of Bioengineering

Thesis Supervisor
Assoc. Prof. Dr. Nihat Alpagu SAYAR

ISTANBUL, 2018

MARMARA UNIVERSITY
INSTITUTE FOR GRADUATE STUDIES
IN PURE AND APPLIED SCIENCES

MULTI-OBJECTIVE OPTIMIZATION AT A CRUDE NOVEL LIPASE CATALYZED FAME PRODUCTION:

KRIGING AS AN ALTERNATIVE TO RSM

CEYDA KULA

Ph.D. THESIS
Department of Bioengineering

Thesis Supervisor
Assoc. Prof. Dr. Nihat Alpagu SAYAR

ISTANBUL, 2018

MARMARA UNIVERSITY
INSTITUTE FOR GRADUATE STUDIES IN PURE AND APPLIED SCIENCES

Ceyda KULA, a Doctor of Philosophy student of Marmara University Institute for Graduate Studies in Pure and Applied Sciences, defended her thesis entitled "Multi-objective optimization at a crude novel lipase catalyzed FAME production: Kriging as an alternative to RSM", on September 28, 2018 and has been found to be satisfactory by the jury members.

Jury Members

Assoc. Prof. Nihat Alpagu SAYAR (Advisor)
Marmara University ....(SIGN)................

Prof. Dr. Nazlı ARDA (Jury Member)
İstanbul University ....(SIGN)................

Prof. Dr. Dilek KAZAN (Jury Member)
Marmara University ....(SIGN)................

Prof. Dr. Ayşegül TOPAL SARIKAYA (Jury Member)
İstanbul Yeni Yüzyıl University ....(SIGN)................

Prof. Dr. Ahmet Alp SAYAR (Jury Member)
Marmara University ....(SIGN)................

APPROVAL

Marmara University Institute for Graduate Studies in Pure and Applied Sciences Executive Committee approves that Ceyda KULA be granted the degree of Doctor of Philosophy in Department of Bioengineering, Bioengineering Program on .08.10.2018.. (Resolution no: .2018/25-03..).

Director of the Institute

Prof. Dr. Bülent EKİCİ

ACKNOWLEDGEMENTS

I would like to first say a very big thank to my PhD supervisor, Assoc. Prof. Nihat Alpagu SAYAR for all the support, contributions and encouragement he gave me during these past six years.

I would like to express my sincere thanks to Prof. Dr. Dilek KAZAN and Prof. Dr. Nazlı ARDA for their valuable advices and contributions during this work. And also I would like to thank the jury members of my thesis for their attention.

I would like to thank Prof. Dr. Ahmet Alp SAYAR not only for his contributions to my thesis but also for his support and advices.

I would like to express my sincere thanks to my dear friends Orkun PİNAR, Fatma Gizem AVCI, Fatma Ece ALTINIŞIK KAYA, Ceyhun BEREKETOĞLU for their priceless intimacy and support.

I am also very grateful to all those at Marmara University Bioengineering Department faculty members who were always so helpful and supportive during the past six years.

I would like to express my gratitude to TÜBİTAK-BİDEB 2211 for providing the PhD Scholarship during my thesis work.

Financial support provided by Marmara University, Scientific Research Projects Committee (BAPKO) FEN-C-DRP-080415-0124 is gratefully acknowledged.

Finally, words cannot express how grateful I am to my parents for their encouragements, deep love, endless patience and everlasting support during the days of hard study.

September, 2018 **Ceyda KULA**

TABLE OF CONTENTS

ÖZET

SAFLAŞTIRILMAMIŞ YENİ BİR LİPAZ İLE KATALİZLENEN FAME ÜRETİMİNİN ÇOK HEDEFLİ OPTİMİZASYONU: RSM'E ALTERNATİF OLARAK KRIGING

Biyodizel özellikle transport sektörü açısından petrol kaynaklı dizel yakıtlara yenilenebilir ve potansiyel olarak sürdürülebilir bir alternatiftir. Biyodizel, ham, rafine veya atık yağlar ile hayvansal yağlar gibi çeşitli hammaddeler kullanılarak, katalitik olmayan ısıl yöntemler, homojen ya da heterojen kimyasal dönüşümler ve biyokatalitik dönüşümler ile üretilebilmektedir. Atık pişirme yağından elde edilen biyokatalitik biyodizel üretiminin ticari olarak uygulanabilirliği, hammaddedeki trigliseritlerin transesterifikasyonunu ve serbet yağ asitlerinin esterifikasyonunu katalizleyen lokal ve ekonomik olarak üretilme potansiyeli olan yeni lipazların mevcudiyetine bağlıdır. Bu açıdan, farklı kaynaklardan değişik özelliklere sahip farklı lipazların taranması, seçilmesi ve geliştirilmesi, lipaz katalizli biyodizel üretiminin cazip hale gelmesinde temel bir görevdir.

Yeni lipazlar için erken değerlendirme deneyleri, değişen reaksiyon sıcaklığı, alkil reseptör substrat mol oranı ve enzim miktarı altında zamana bağlı değişimleri gözlemlemek için uygulanmaktadır. Bu erken dönem deneylerinden elde edilen ön veriler, yeni lipazların hızlı ve etkili bir şekilde değerlendirilmesini kolaylaştırmak için uygun modelleme ve optimizasyon şeması içinde kullanılmalıdır. Geleneksel olarak, düşük mertebeden polinom modellerine dayanan yanıt yüzey yöntemi, verim gibi tek hedefli optimizasyon için kullanılır. Bu çalışmada, Kriging ve Pareto-front çok hedefli optimizasyonunu kullanan alternatif bir modelleme ve optimizasyon yaklaşımı, geleneksel şemaya kıyasla her iki prosedürün uygulanabilirliği ve verimliliği ile ilgili konulara dikkat çekerek, yeni bir lipaza uygulanmaktadır. Kriging temelli modelleme ve optimizasyon yönteminin, sınırlı ön deneysel verilerin kullanılmasında avantajlı olduğu gösterilmiştir.

Anahtar Kelimeler: Biyodizel, lipaz, yanıt yüzey yöntemi, Kriging, çok hedefli optimizasyon

Eylül, 2018 **Ceyda KULA**

ABSTRACT

MULTI-OBJECTIVE OPTIMIZATION AT A CRUDE NOVEL LIPASE CATALYZED FAME PRODUCTION: KRIGING AS AN ALTERNATIVE TO RSM

Biodiesel is a renewable and potentially sustainable alternative to petroleum-based diesel, especially in the transportation sector. Biodiesel can be produced by non-catalytic thermal methods, homogenous or heterogenous chemical conversions, and biocatalytic transformations using various types of feedstock such as crude, refined or waste oils, or animal fats. Commercial feasibility of biocatalytic biodiesel production from waste cooking oil critically depends on the availability of novel lipases, which catalyze the transesterification of triglycerides and esterification of free fatty acids in the feedstock into fatty acid alkyl esters, with the potential to be locally and economically produced. In this respect, screening, selection, and development of different lipases with varying properties from different sources is an essential task towards making lipase-catalyzed biodiesel production an attractive endeavor. Early evaluation of novel lipases employs time progress experiments under varying reaction temperature, alkyl receptor to substrate molar ratio, and enzyme amount.

The preliminary data acquired from these early experiments need to be used within an appropriate modelling and optimization scheme to facilitate rapid and efficient evaluation of the novel lipase. Conventionally, response surface methodology based on low-order polynomial models is used for the optimization of a single objective like yield. In this work, an alternative modelling and optimization approach employing Kriging and Pareto-front multi-objective optimization is applied to a novel lipase, in comparison to the conventional scheme, highlighting the issues regarding the applicability and efficiency of both procedures. Kriging-based modelling and optimization methodology is shown to be advantageous in making use of limited preliminary experimental data.

Anahtar Kelimeler: Biodiesel, lipase, Response Surface Methodology, Kriging, multi-objective optimization

September, 2018 **Ceyda KULA**

CLAIM FOR ORIGINALITY

MULTI-OBJECTIVE OPTIMIZATION AT A CRUDE NOVEL LIPASE CATALYZED FAME PRODUCTION: KRIGING AS AN ALTERNATIVE TO RSM

In this work, a novel lipase produced by the yeast *Cryptococcus diffluens* (D44) was used in a biodiesel production system using waste cooking oil as a feedstock. The first part of the thesis focuses on the experimental evaluation of the performance of the novel lipase under varying operational conditions such as reaction temperature, methanol to oil molar ratio, and enzyme amount. Generally, the experimental design for similar studies is based on conventional statistical templates such as central composite designs. In this study, a manually-modified version of central composite design is used for the design of experiments. The manual modifications are specifically aimed at solving system specific experimental problems.

The second part of the thesis focuses on the modelling and optimization of the biodiesel productions system. The models generated are purely empirical and based solely on the data collected in the experimental part. In similar studies, response surface methodology based on low-order polynomial models is used almost exclusively. Another principle novelty of the current work is the application of an alternative modelling approach, namely Kriging, to the biodiesel production system. Models are generated using both the conventional low-order polynomial models and Kriging techniques. A comparison of the model evaluations hints that Kriging may be a better choice for these types of systems.

Furthermore, an overwhelming majority of optimization studies in the field performs single-objective optimization, often aiming to maximize biodiesel yield. In the current study, two process metrics are used which are product titer and temporal productivity. Alongside single-objective optimization of these two metrics separately, a multi-objective optimization scheme displaying the trade-off between the selected process metrics based on Pareto-fronts is applied. The applicability and usefulness of these optimization schemes based on the aforementioned modelling approaches is highlighted.

September, 2018 Assoc. Prof. Dr. Nihat Alpagu SAYAR Ceyda KULA

SYMBOLS

ml	: Milliliter
mg	: Milligram
mM	: Millimolar
M	: Molar
nm	: Nanometer
mmol	: Millimol
g	: Gram
rpm	: Revolutions per minute
min	: Minute
µg	: Microgram
U	: Unit
h	: Hour
L	: Liter
t	: Time
T	: Temperature

ABBREVIATIONS

Adj_R^2	: Adjusted R-Squared
CCD	: Central composite design
DoE	: Design of experiments
FAAE	: Fatty acids alkyl esters
FAME	: Fatty acid methyl esters
FFA	: Free fatty acid
FID	: Flame ionization detector
F_stat	: F Statistic
GC	: Gas chromatography
HPLC	: High-performance liquid chromatography
MS	: Mass spectrometry
MSE	: Mean of squared error
NMR	: Nuclear magnetic resonance
pNPP	: p-nitrophenyl palmitate
R^2	: R-squared
RMSE	: Root mean squared errors
SSE	: Sum of square error
SSR	: Sum of squares due to regression
SST	: Sum of squares about the mean
TG	: Triglyceride
TLC	: Thin layer chromatography
WCO	: Waste cooking oils

LIST OF FIGURES

LIST OF TABLES

1. INTRODUCTION

1.1. Biodiesel

In recent years, increasing demand for energy, the rising prices of petroleum and limited supply of fossil fuel reserves as well as global warming, climate change, increasing of carbon emissions and ever-growing environmental pollution problems are driving scientists to investigate renewable, commercial and environmentally friendly energy sources (Budžaki et al., 2018; Rafiei et al., 2018; Saeidi et al., 2016).

Among the various forms of bio-based fuels and renewable energy sources, biodiesel plays a major role and is a sustainable option for replacing oil-based energy and other fossil fuels due to its numerous environmental, economic and social benefits which include a non-toxic, biodegradable character and low greenhouse gases emission profile as well as its similarity with conventional diesel in energy content and chemical structure. Additionally, biodiesel is not accumulated in fresh water or soil, has low sulfur content and a higher flash point around 150ºC (Jatropha: 161.85ºC; karanja: 186.85ºC; microalgae: 124.85ºC; waste cooking oil: 195.85ºC) which makes it a safer fuel for both the environment and human contact. Thanks to all these characteristics, biodiesel has the potential to minimize environmental pollution and global warming significantly and also represents a strategic source of energy for the countries that do not have fossil fuel resources (Wang et al., 2017; Budžaki et al., 2018; Rafiei et al., 2018; Katre et al., 2018; Ding et al., 2018; Anwar et al., 2018; Tang et al., 2018; Gaurav et al., 2016; Pourzolfaghar et al., 2016; Canet et al., 2016; Guldhe et al., 2015).

Biodiesel is chemically defined as a mixture of fatty acids alkyl esters (FAAE) derived from a wide variety of potentially renewable feedstocks including edible and non-edible of vegetable oils, animal fats, waste cooking oils (WCO) or micro algal biomass, which is produced via different methods with the help of alcohol, in the presence of suitable catalytic systems with glycerol as byproduct (Budžaki et al., 2018; Andrade et al., 2017; Dhawane et al., 2018; Ding et al., 2018; Wu et al., 2016; Canet et al., 2016; Hoekman et al., 2012; Verma and Sharma, 2016; Gaurav et al., 2016). Based on the fatty acid composition of the oils used as the feedstocks, the fatty acid profile and properties of biodiesel are affected significantly (Knothe and Razon, 2017; Lam et al., 2010; Dharma et al., 2016). The most common fatty acid esters contained in biodiesel are palmitic (16:0), stearic (18:0), oleic (18:1, cis-9), linoleic (18:2, cis-9,12) and linolenic (18:3, cis-9,12,15) (Hoekman et al., 2012; Carvalho et al., 2012).

Nowadays, the major challenge for biodiesel production is economic feasibility. There are various factors that affect the overall cost of biodiesel production such as price of raw materials, catalyst, biodiesel processing including energy, consumable materials and labor (Lam et al., 2010; Ullah et al., 2016). Among these, the cost of the raw material is the major factor in biodiesel production. Specifically, it has been found that raw material alone represents 70-95% of the overall biodiesel production cost if the edible oils are used such as virgin vegetable oil (Wu et al., 2016; Gaurav et al., 2016; Wang et al., 2017; Tang et al., 2018). This is a major hurdle before profitable commercialization of biodiesel (Wu et al., 2016; Tang et al., 2018).

Currently, it is reported that >95% of biodiesel is produced from the edible oils (human food) (Muthukumaran et al., 2017). Soybean oil, sunflower oil, rapeseed oil, and palm oil are typically used as raw material (Sajid et al., 2016). Since these raw materials are also used as food, competition of edible oil with food consumption has been a global concern, using these cause difficulty for large scale production of biodiesel (Muthukumaran et al., 2017; Sajid et al., 2016).

In order to avoid this conflict between energy and food demand and eliminate the cost problem, the researchers are focusing their attention to examine low-cost nonedible raw materials such as Jatropha, Jojoba and Cotton seed oils and waste cooking oils. Using of these raw materials in biodiesel production has become an attractive interest because it decreases the production cost as well as allowing for compliance with ecological and ethical requirements (Pourzolfaghar et al., 2016; Muthukumaran et al., 2017).

Cost of biodiesel produced from nonedible oils is higher than petrodiesel in commercial scale due to raw material cost since they still require the use of land to grow crops (Gaurav et al., 2016; Ullah et al., 2016; Sajid et al., 2016). In order to ensure economic viability in biodiesel production, producers are focusing their attention on using WCO because a large amount of WCO is available around the world at a reasonable price or even free (Wang et al., 2017; Sajid et al., 2016; Kamel et al., 2018). It is reported that WCO is generated globally to an extent of 29 million tons per year (Katre et al., 2018).

WCO is not suitable for human consumption which also eliminates any considerations of the competition with food industry; whereas WCO is a suitable raw material for biodiesel production since both triglycerides and free fatty acids are converted to biodiesel (Aboelazayem et al., 2018; Budžaki et al., 2018). Moreover its usage may help minimise cost problem as well as reducing the environmental impacts of untreated WCO (Wang et al., 2017; Sajid et al., 2016; Aboelazayem et al., 2018). Therefore producing biodiesel from WCO is environmentally and economically beneficial (Kamel et al., 2018). Table 1 indicates fatty acid composition of waste cooking oil (Chhetri et al., 2008).

Table 1.1 Fatty acid composition of waste cooking oil

Fatty acid composition (wt%)	**Waste cooking oil**
Myristic (C14:0)	0.9
Palmitic (C16:0)	20.4
Palmitoleic (C16:1)	4.6
Stearic (C18:0)	4.8
Oleic (C18:1)	52.9
Linoleic(C18:2)	13.5
Linolenic(C18:3)	0.8
Arachidic (C20:0)	0.12
Eicosenic (C20:1)	0.84
Behenic (C22:0)	0.03
Erucic (C22:1)	0.07
Tetracosanic (C24:0)	0.04
Mean molecular wt (g/mol)	856

In production of biodiesel, alcohol as an acyl acceptor is one of the most important raw materials (Musa, 2016). Some utilized in producing biodiesel are methanol, ethanol, propanol, butanol, isopropanol, tert-butanol and octanol (Musa, 2016; Ezekannagha, 2017; Nejad and Zahedi, 2018; Talebian-Kiakalaieh et al., 2013). Methanol and ethanol are more often used among these alcohols in biodiesel production because the others are costly (Musa, 2016; Nejad and Zahedi, 2018; Amini et al., 2017). Between methanol and ethanol, methanol is mostly preferred in commercial biodiesel production due to its economic feasibility and accessibility as well as has physical and chemical advantages such as being a simple and polar compound and not containing complex organic compounds or sulfur (Andrade et al., 2017; Musa, 2016; Wang et al., 2017; Lam et al., 2010; Ezekannagha, 2017; Nejad and Zahedi, 2018; Lamba et al., 2017; Talebian-Kiakalaieh et al., 2013). Moreover methanol does not form azeotropes, therefore it is easily recycled whereas ethanol forms an azeotrope with water so it is expensive to purify the ethanol during recovery. Additionally, the yield of fatty acid ethyl esters is lower compared to methyl esters and separation of glycerol is a main constrain in the process of ethanolysis. Also regarding their characteristics as fuels, biodiesel fuels from methanol have slightly higher pour and cloud points and slightly lower viscosities than those obtained from ethanol (Musa, 2016; Ezekannagha, 2017; Amini et al., 2017). Since methanol is currently the preferred alcohol for this purpose, biodiesel is often referred to as the fatty acid methyl esters (FAME) (Tan et al., 2010; Lam et al., 2010; Knothe and Razon, 2017; Hoekman et al., 2012).

1.2.Biodiesel Production Processes

As indicated above, there are many raw materials used for biodiesel production. They can not be directly used as biodiesel because of their high viscosity. Four major techniques exist to reduce high viscosity of these raw materials and production for biodiesel as well as to eliminate any operational problems from its use in a common diesel engine including direct use and blending, microemulsions, thermal cracking (pyrolysis) and transesterification (alcoholysis). Among all these, the most commonly used and cost-efficient method for converting oils to biodiesel with higher quality is the transesterification which gains the highest attention in industrial scale for biodiesel production as the process is simple, and the physical characteristics of the biodiesel are very close to diesel fuel (Tang et al., 2018; Budžaki et al., 2018; Vyas et al., 2010; Narwal and Gupta, 2013; Gumba et al., 2016; César et al., 2017; Verma and Sharma, 2016; Christopher et al., 2014; Adewale et al., 2015; Yan et al., 2014; Rafiei et al., 2018; Ambat et al., 2018).

1.2.1. Transesterification

Transesterification is a reversible reaction that includes the conversion of one ester into another ester. It refers to the exchange of groups between alcohol of ester and another alcohol to yield fatty acid alkyl esters together with glycerol as bi-product which is also called alcoholysis (Nejad and Zahedi, 2018; Gumba et al., 2016; Sen et al., 2016). The most widely used process to produce FAME is transesterification, which is also known as methanolysis due to the use of methanol as the preferred alcohol, the reaction between triglycerides of the raw materials and methanol in the presence of a different catalysts including alkaline, acid, and biocatalysts (Guldhe et al., 2015; Budžaki et al., 2018; Andrade et al., 2017; Knothe and Razon, 2017; Sajid et al., 2016; Liew et al., 2014; Zarejousheghani et al., 2016; Ding et al., 2018). The detailed chemical reaction diagram for transesterification is illustrated in Figure 1.1.

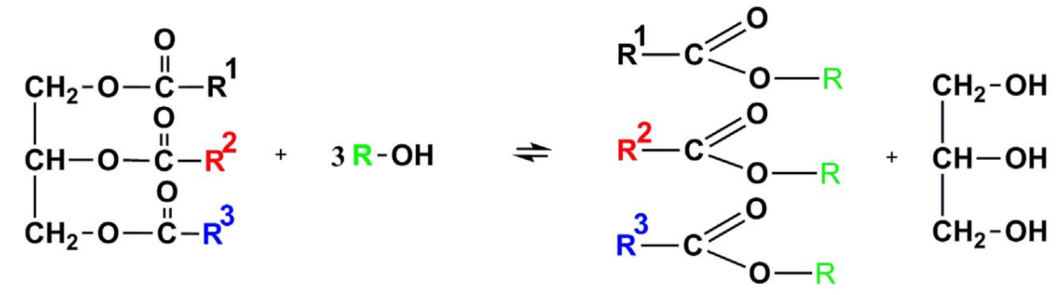

Triglyceride (TAG) Alcohol Alkyl Ester Glycerol

Figure 1.1 Schematic diagram of biodiesel (FAME) production through transesterification process (Price et al., 2016)

As shown, for each mol of triglyceride (TG), 3 mol of methanol are required to produce 3 mol of FAME and 1 mol of glycerol as byproduct (Andrade et al., 2017; Talebian-Kiakalaieh et al., 2013; Liew et al., 2014; Muthukumaran et al., 2017). Enhancing the methanol amount decreases the glycerol content as equilibrium is used to favour the forward reaction for biodiesel (Muthukumaran et al., 2017; Zarejousheghani et al., 2016; Vyas et al., 2010).

Conventionally, the transesterification process takes place by three consecutive reversible reactions. Firstly, it starts with the conversion of TG into diglyceride. As followed by the conversion of diglyceride into monoglyceride and finally monoglyceride converts into ester and glycerol. In all these reactions, produced esters are called as biodiesel (FAME) (Knothe and Razon, 2017; Gumba et al., 2016, Hamze et al., 2015; Zarejousheghani et al., 2016; Vyas et al., 2010; Dhawane et al., 2018).

Esterification works along with transesterification, which is the transformation of free fatty acid (FFA) to biodiesel in presence of an alcohol and water as the by-product (Christopher et al., 2014; Vyas et al., 2010; Gaurav et al., 2016). Moreover, biodiesel can be also produced by an interesterification of TG to biodiesel in presence of an ester (such as methyl/ethyl acetate) as the acyl acceptor. In this process, instead of glycerol, another triacylglycerol (triacetin) is formed as the by-product (Christopher et al., 2014; Kusumaningtyas et al., 2016). The detailed chemical reaction diagrams for esterification and interesterifcation are illustrated in Figure 1.2 and Figure 1.3, respectively.

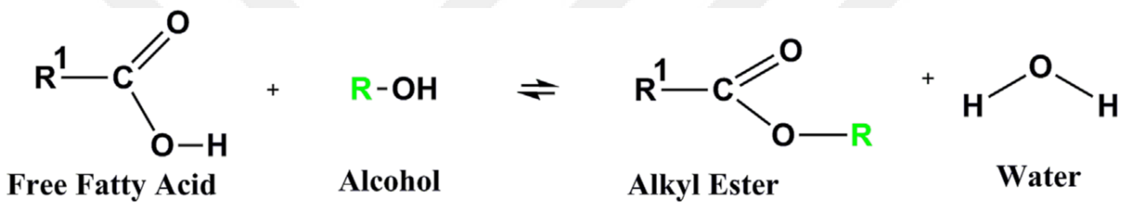

Figure 1.2 Schematic diagram of biodiesel production through esterification process (Price et al., 2016).

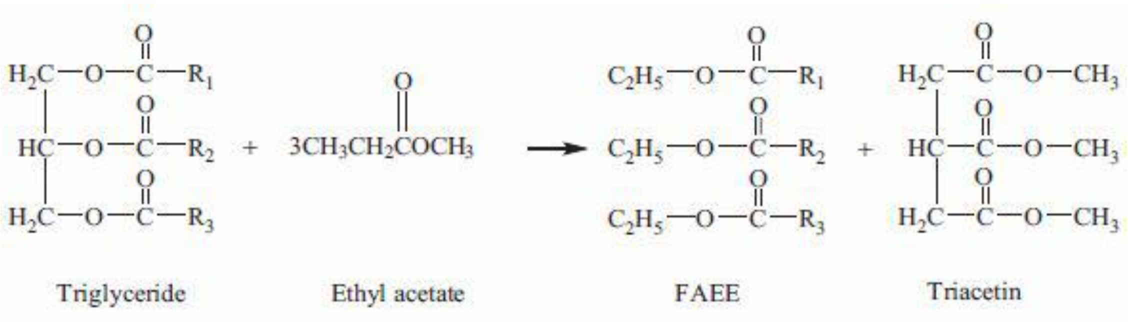

Figure 1.3 Schematic diagram of biodiesel production through interesterifcation process (Kusumaningtyas et al., 2016).

Selection of the catalyst is based on the properties of feedstock oil such as water content and total acid value (Aboelazayem et al., 2018; Dhawane et al., 2018). Depending on their solubility in the reaction mixture, catalysts used in biodiesel production are classified in two general categories which are homogenous and heterogeneous types. In homogeneous catalytic transesterification, the catalyst remains in the same phase, generally liquid phase, with the reactants during transesterification. On the other hand, if the catalyst remains in different phase like solid, immiscible liquid or gaseous phase with the reactants, the process is called heterogeneous catalytic transesterification (Ahmad Abbaszaadeh, 2012). The selection of the catalyst properly is an important parameter to lower the biodiesel production cost (Gumba et al., 2016).

1.2.1.1. Alkali-Catalyzed Transesterification

Homogeneous alkali-catalyzed transesterification has been the most commonly applied method used at laboratory, pilot and industrial scales since it can be operated under mild conditions like relatively low reaction temperature (60-65ºC) and atmospheric pressure to achieve significant conversion and high quality biodiesel in a short reaction time. The alkaline metal hydroxides and alkoxides as well as sodium or potassium carbonates such as sodium hydroxide, sodium methoxide, potassium hydroxide, and potassium methoxide have been majorly used for producing biodiesel due to their high catalytic activity, relatively low cost and widely favorable characteristics (Wu et al., 2016; Stojković et al., 2014; Tubino et al., 2016; Abbaszaadeh et al., 2012; Zhang et al., 2003; Aransiola et al., 2014; Budžaki et al., 2018). Although the homogeneous alkaline system supplies many advantages, it also results in many limitations (Lee et al., 2016; Budžaki et al., 2018). The main bottleneck of alkaline catalyzed-reactions are reported to be high sensitivity to the purity of the feedstock. When the feedstocks contain a high percentage of free fatty acids or water, the biodiesel production using homogenous alkaline catalyzis is usually badly affected. The presence of water favors the formation of FFAs by hydrolysis of TGs and biodiesel into diglycerides. The free fatty acids can rapidly react with alkaline in the media to form soaps and create serious problems for product separation (Ahmed et al., 2015; Zhang et al., 2003; Leung et al., 2010; Aboelazayem et al., 2018). It is commonly observed that saponification is an unfavourable side reaction which reduces the amount of biodiesel produced because the catalyst is consumed and the biodiesel is difficult to separate from the reaction mixture (Balat and Balat, 2010; Aboelazayem et al., 2018). There are various reports about the effect of FFA and water content in feedstock for reactions with alkali catalysts. Leung et al. (2010) reported that, the maximum acceptable amount of FFAs in feedstock is below

2.5 wt%. If the feedstock has FFA content over 2.5 wt%, a pretreatment step is necessary before the transesterification process. Canakci et al. (2001) reported that, in order to carry out the alkali-catalyzed reaction, the optimum FFA and water levels in feedstocks are below 1 wt% and 0.5 wt%, respectively. Borugadda and Goud (2012) reported that, if the FFA content in feedstock reaches 3 wt%, the alkaline-catalyzed transesterification process is not suitable to produce esters. Hence, it is clear that the FFAs and water content in feedstock should be as low as possible (FFAs < 3 wt% and water < 0.5 wt%) for homogenous alkaline catalysis, otherwise the yield of FAMEs would reduce significantly. Thus, since the average level of FFAs in WCO is on the order of 10–15%, alkaline-catalyst may not be suitable to be used for biodiesel production via transesterification process (Ahmed et al., 2015; Lotero et al., 2005; Zhang et al., 2003; Hajjaria et al., 2017; Katre et al., 2018; Anwar et al., 2018; Lam et al., 2010). Moreover, when the homogenous alkaline catalysis is used, separation of product, recovery of the liquid catalyst from biodiesel and glycerol, washing process of esters for purification are other major problems. During the washing process, high amounts of unfavorable alkali waste water is generated (0.2 ton of waste water per ton of biodiesel is produced) which makes the process expensive, complicated and environmentally unfriendly (Fjerbaek et al., 2009; Meher et al., 2013; Mardhiah et al., 2017; Leung et al., 2010). Heterogeneous alkali catalysts, which generally are found in solid form, have been tried to overcome the drawbacks of the homogeneous alkali catalysts as mentioned above. Many heterogeneous alkali catalysts have been used for the transesterification of oils such as basic zeolites, alkaline earth metal oxides and hydrotalcites. Heterogeneous alkali catalysts are promising for the transesterification reaction because they are non-corrosive, recyclable and in addition to this, these catalysts are useful for feedstocks with high free fatty acid content. Moreover, some solid heterogeneous catalysts could be rapidly separated from the product by filtration, which reduces the washing requirement. By using a heterogeneous catalyst, the cost of processing is lowered by the fact that the catalyst is easily separated, recovered and reused (Meher et al., 2013; Mardhiah et al., 2017; Leung et al., 2010; Borugadda and Goud, 2012; Aboelazayem et al., 2018). However, using heterogeneous alkali catalyst has some limitations such as slower rates because the reaction mixture creates a three-phase system which inhibits the reaction due to diffusion limitation, high molar ratio of alcohol to oil requirement, high reaction temperature with pressure and relatively high cost (Leung et al., 2010; Liu et al., 2008; Shimada et al., 2002; Kulkarni, et al., 2006; Chen et al., 2012; Serio et al., 2007; Kawashima et al., 2009).

1.2.1.2. Acid-Catalyzed Transesterification

In another scenario, biodiesel is produced by transesterification of triglycerides with alcohol in the presence of homogeneous and heterogeneous acid-catalysts. The most commonly used homogeneous acid catalysts in biodiesel production process are HCl, BF_3, H_2SO_4, H_3PO_4 and $FeSO_4$ (Ullah et al., 2016, Gumba et al., 2016). Among these H_2SO_4 and HCl are commonly employed at concentration ranges of 0.5–1 wt% with temperatures of 60–100°C (Gumba et al., 2016; Yun et al., 2013).

Acid catalysts are another option for the feedstock oil with high concentrations of free fatty acids (>1%) and moisture (>0.5%) such as waste cooking oil, as they can catalyze both the transesterification and esterification reactions simultaneously and inhibit the saponification reaction and lead to the higher yield of esters (Andrade et al., 2017; Lamba et al., 2017; Amini et al., 2017; Ullah et al., 2016; Yun et al., 2013).

On the downside, this process has some disadvantages such as the necessity of more steps in which is more energy demanding and economically unfavorable; also reaction rates are slow, and the use of acids can cause equipment damage. Additionally, huge amounts of wastewater are generated during the biodiesel production and separation of the catalyst from the product stream is difficult. And also, higher amounts of methanol are required in acid mediated transesterification processes (Budžaki et al., 2018; Andrade et al., 2017; Amini et al., 2017; Gumba et al., 2016; Yun et al., 2013).

Main heterogeneous acid catalysts are zirconium oxide, titanium oxide, zeolites, sulfonic ion-exchange resin, sulfonic modified mesostructure silica, sulfonated carbon-based catalyst, heteropolyacids (Amini et al., 2017). They allow easy product separation and greater recyclability. However, in addition to longer reaction time and higher temperature requirement, they are relatively rare metals hence the catalyst fabrication is costly (Gumba et al., 2016).

1.2.1.3. Enzymatic Transesterification

The enzymatic transesterification process is a promising alternative as a biological approach for biodiesel production with a range of advantages over the chemical approaches (Andrade et al., 2017; Ali et al., 2017; Wang et al., 2017; Babaki et al., 2017). These include relatively low reaction temperature, pressure and waste, quality glycerol by-product, relative less dependence to process water and acidity value, more simple, purification process, easy catalyst removal, high substrate specificity and lower alcohol to oil ratio (Andrade et al., 2017; Ali et al., 2017; Wang et al., 2017; Tacias-Pascacio et al., 2017). Moreover, enzymes can transesterify TG and esterify FFA simultaneously, thus the additional free fatty acid esterification step is not necessary which is necessary in alkali/acid catalytic processing (Andrade et al., 2017; Tacias-Pascacio et al., 2017; Ali et al., 2017; Selvakumar and Sivashanmugam, 2017). In the presence of enzymes, TG from oils react with alcohol to produce FAAE and glycerol. The overall process of transesterification includes three reversible reactions as mentioned above. In the presence of a small amount of water, enzymes catalyze the hydrolysis of TG into FFAs and glycerol. These FFA can be esterified by enzymes, reacting with alcohol to produce FAAE (Andrade et al., 2017). Additionally, it is advantageous to use enzymatic catalyzis in order to process WCO because of its high FFA content (Ali et al., 2017; Tacias-Pascacio et al., 2017; Gumba et al., 2016).

1.3.Lipase Enzyme

Lipases (triacylglycerol acyl hydrolases, EC 3.1.1.3) are a class of enzymes that catalyze hydrolysis, esterification (FFA to FAAE) and transesterification (TGs to FAAE). This ability of lipases allows them to be employed as biocatalyst in biodiesel production (Pollardo et al., 2018; Budzaki et al., 2017; Ullah et al., 2016). It is the fact that lipase can use WCO as a substrate without its previous pre-treatment which is significant in their use in biodiesel production (Budzaki et al., 2017; Yan et al., 2014).

Lipases are ubiquitous and many microorganisms such as bacteria, yeast and fungi are known to produce lipases. So, the potential number of candidates to be evaluated as biocatalysts for biodiesel production is very high. Moreover, lipases show varying catalytic properties depending on their source and the substrate they are used with (Bajaj et al., 2010). Therefore, screening and selection for an ideal lipase for the development of a feasible, robust, stable and cost-effective biocatalyst is a time-consuming and experimental work-intensive effort (Ghaly et al., 2010). Lipases can be used in crude, partially-purified and purified forms (Suwanno et al., 2017; Ugur et al., 2014; Ali et al., 2017). Purification increases the specific activity of the enzymes while adding to the difficulty of production cost. So, there is a trade-off between the effort put in for purification and the resulting gains in process performance. Also, for each new lipase-substrate system, optimization of process conditions is necessary as varying properties of these systems require different operating conditions for optimal performance (Hama and Kondo, 2013; Amini et al., 2017). Choosing an organic solvent or a solvent-free system, selection of the acyl-acceptor, molar ratio of the substrates, biocatalyst concentration, temperature, and reaction duration are amongst the most important factors (Szczesna-Antczak et al., 2009). In this respect, it is important to design rapid workflows that integrate optimization of these factors for biodiesel production at various levels of biocatalyst and process development.

Microbial lipases, especially yeast lipases, are extensively used for biodiesel production. The most widely used yeast lipases in biodiesel synthesis are the lipase B from the yeast *Candida antarctica*, *Candida rugosa*, *C. antarctica* A and *Candida* sp. 99–125. Lipases obtained from filamentous fungi such as *Rhizomucor miehei* lipase, *Rhizopus oryzae* lipase, *Thermomyces lanuginosus* lipase, *Aspergillus niger* lipase and *Penicillium expasum* lipase have also been studied for biodiesel production. In general, free and immobilized lipases are two main forms of biocatalysts used in biodiesel synthesis (Aguieiras et al., 2015).

Free lipases present the advantage of easy and low-cost preparation which consist of liquid formulations or powder enzymes obtained by freeze-drying. In order to prevent the addition of water to the reaction medium, the solution containing the free lipase can be freeze-dried. The freeze-drying process is considered necessary in order to dehydrate the lipase enzyme solution because the uncontrolled water content causes the hydrolysis which is an undesirable process for transesterifcation reaction (Aguieiras et al., 2015). However, although free enzymes are significantly cheaper than immobilized lipases, in many cases they have poor operational stability (Yan et al., 2014). Despite the advantages of immobilized lipases such as increased thermal stability, enhanced number of available active sites and easy recovery making it possible to carry out continuous processes, these biocatalysts are expensive since their preparation requires costly steps (Bajaj et al., 2010; Ullah et al., 2016). Moreover, the mass transfer limitation and the effect of alcohol in contact with the immobilized biocatalyst are the other negative aspects (José et al., 2011).

As mentioned above, theoretically, a stoichiometric ratio of alcohol to oil (3:1) is needed to completely convert the substrate. High concentrations of alcohol may lead to higher yields, but can also significantly reduce the activity of lipases. For methanol, it has been demonstrated that *C. antarctica* lipase is already inactivated by methanol/oil ratios of 0.5:1 or higher (Shimada et al., 1999). Enzyme inhibition by methanol can be overcome by overdosing the lipase, which however is not a cost-effective solution to the problem (Fjerbaek et al., 2009). It was also reported that some lipases such as those from *Pseudomonas* sp. were more tolerant to alcohol than others e.g. from *T. lanuginosus* (Fjerbaek et al., 2009). Since it is known that various lipases have shown different levels of tolerance towards the organic solvent, development of more tolerant enzymes is one of the important aspects in biodiesel production (Wang et al., 2017). In order to do this, the properties of *Cryptococcus diffluens* D44 lipase which was isolated from petroleum sludge, has been examined. Highlighting the fact that it has high activity and stability in the presence of organic solvents, lipase of *C. diffluens* D44 can be considered in potential applications in biodiesel production using oily substrates. The considerable stability of D44 lipase in aqueous methanol, which can reach up to 20%, makes *C. diffluens* D44 lipase a good candidate for biodiesel production, since moderate reaction conditions and lower organic solvent concentrations are required for oil-based biofuel production. Considering all these points, D44 lipase can be recognized as a potential additive for oil-based production of biodiesel (Yılmaz and Sayar, 2015).

The lipases of known three-dimensional structure have molecular weights in the range of 19-60 kDa. The three-dimensional structure of lipase consists of the catalytic triad which includes Ser, Hys and Asp/Glu. The residue is contained in the well-conserved Gly-X-Ser-X-Gly motif. Where X can be histidine or tyrosine. The protected motif is located between a β-sheet and an **α**-helix. The three-dimensional structure of lipases suggests that (3-D) has an **α**/β-hydrolase fold. Lipases usually consist of a central β-layer that forms eight different β-bands (β1-β8) linked by six α-helix. The active site contains amino acids, serine, aspartic acid (or glutamic acid) and histidine. The nucleophilic serine residue is contained in the highly conserved pentapeptide (G-X-S-X-G) sequence at the C-terminal end of the β5 strand. This pentapeptide sequence forms a characteristic β-turn-α motif, termed a nucleophilic elbow. The catalytic activity is influenced by the cap structure formed by the triple α-band. The separation of this structure is essential for the initiation of catalytic activity. With the formation of the interface with activity of the lipases, the lid structure is lifted and the lipase enzyme becomes active (Kapoor and Gupta, 2012; Christopher et al., 2014; Narwal and Gupta, 2013; Gupta et al., 2004; Jaeger et al., 1999; Borrelli and Trono, 2015; Guldhe et al., 2015).

This situation; opening of the lid following contact with the hydrophobic substrate at the interface between oil and water, is followed by activation of the lipase. The nucleophilic effect on the serine residue by neighboring histidine and the Ser-O atom make a nucleophilic attack on the carbonyl carbon atom of the substrate. Transition state tetrahedral intermediate formation is O-stabilized by the two peptides in the NH group. The proton is separated from the alcohol component of the substrate and transferred to the histidine. The serine residue of the enzyme is esterified with the acid component of the substrate to form the covalent intermediate (acyl enzyme). The water molecules are activated by neighboring histidine residues and the resulting hydroxyl group makes a nucleophilic attack on the carbonyl carbon atom of the covalent intermediate. The proton is transferred to the oxygen atom of the active serine residue by the histidine residue, the ester bond between the serine and acyl component is broken and the acyl product is released (Yan et al., 2014; Christopher et al., 2014; Guldhe et al., 2015).

Lipases can be examined in three different groups based on the substrate specificity. These include 1,3-specific, fatty acid-specific, and non-specific lipases. The 1,3-specific lipases hydrolyze ester bonds in the position 1 and 3 of TGs. It is reported that the use at such lipase, *T. lanuginosus* 1,3-specific lipases produces a transesterification yield of 90%. The fatty acid-specific lipases are specific to the fatty acids on the side chain of the acylglycerols and disrupt the ester bonds formed by these fatty acids. These lipases provide the elution of the specific compounds targeted in organic synthesis designs, especially in interesterification reactions. For non-specific lipases, enzymes entering this group can hydrolyze acyl groups at all positions of triglycerides. In partial hydrolysis reactions, diacyl and monoacylglycerol are formed as intermediates. After complete hydrolysis of triacylglycerols, glycerol and fatty acids are present in the reaction medium as product. For optimal biodiesel production, lipases should be able to convert all three forms of glycerides (mono-, di-, and tri-glycerides) to biodiesel, hence, they need to be non-stereospecific and to efficiently catalyze the esterification of FFA (Christopher et al., 2014; Kapoor and Gupta, 2012).

Water is a very important factor in the enzyme-catalyzed process, because water maintains the three dimensional structure of the enzyme and can directly affect the enzyme structure and activity. Hence the water amount in the reaction mixture affects both reaction rate and equilibrium yield in lipase-catalyzed transesterification (Christopher et al., 2014; Bankovic-Ilic et al., 2012; Chesterfield et al., 2012). Generally, minimum amount of water is necessary for biocatalytic activity that is specific for a given lipase. Transestercation is not possible in absence of water as the formation of enzyme substrate complexes (lipase-oil) proceeds only in presence of oil–water interface. At the optimum water content, minimum hydrolysis and maximum transesterification occur. The optimal water content for *C. antarctica* and *T. lanuginosa* lipase was 2% whereas 20% water was required for maximum transesterification by *Candida sp.* 99–125 lipase (Christopher et al., 2014).

1.4.Waste Cooking Oil

Cost of biodiesel produced from vegetable oil by transesterification is higher than petro-diesel due to raw material cost. This is a major hurdle before profitable commercialization of biodiesel. Use of WCO as raw material will help alleviate this problem as well as reducing the environmental impacts of untreated WCO (Yan et al., 2014; Babaki et al., 2017; Hamze et al., 2015).

Using WCO as biodiesel feedstock become popular nowadays due to the fact that WCO are available around the world from restaurants or public companies cheaply or even free. Moreover waste cooking oil as a feedstock does not compete directly with food accessibility. Therefore production of biodiesel from waste cooking oils ensures not only a solution to environmental corcerns, but it also enhances the economics of high-cost biodiesel production (Ambat et al., 2018; Hamze et al., 2015).

While the average level of FFAs in WCO is on the order of 10–15%, chemical methods such as alkali catalysts may not suitable to be used for biodiesel production via transesterification process, is overcome the specific limitations of alkali transesterification technology including using low-cost and waste feedstock containing high FFA can instead be done by an enzymatic reaction and subsequently the system cost will decrease (Babaki et al., 2017; Amini et al., 2017; Adewale et al., 2015).

1.5.GC-MS

Some chromatographic methods can be used to analyze biodiesel. These include thin layer chromatography (TLC), gas chromatography (GC), high-performance liquid chromatography (HPLC) and nuclear magnetic resonance (NMR) (Carvalho et al., 2012).

TLC can be used for the initial qualitative analysis of biodiesel. It is the simplest method and has some limitations that include low accuracy and sensitivity to humidity (Ambat et al., 2018). GC method is the most commonly used method for characterizing biodiesel products due to its high accuracy in differentiating components and analyzing minor and major compounds quantitatively (Hamze et al., 2015; Haigh et al., 2014; Ambat et al., 2018).

Flame ionization detector (FID) and mass spectrometry (MS) detectors have been combined with gas chromatography for this purpose (Ambat et al., 2018; Haigh et al., 2014). MS detectors are useful because they can also provide structural information based on the contained library (Haigh et al., 2014).

This analytical technique ensures the distribution area corresponding to each component in the produced sample. The obtained FAME (biodiesel) can be determined by direct comparison with the standard mixture and the percentage of individual FAME is made in relation to total area of the chromatogram. It is analyzed with help of the distribution area result from GC analysis (Carvalho et al., 2012; Ambat et al., 2018).

1.6.Modelling and Optimization

Biocatalytic biodiesel production requires optimal performance to be commercially feasible. Thus, optimization of lipase-catalyzed FAME production is a critical task for the design and development of biodiesel production processes. Reliable optimization of such complex systems necessitates appropriate modelling of these multivariate phenomena. The methodology for the appropriate modelling and subsequent model-based optimization of biodiesel production systems forms an important issue that bridges the exploratory experimental work with quantified process design. So, the methodology has to be correctly chosen and well understood.

In biocatalytic biodiesel production optimization studies, the input variables that are generally considered are numerous such as reaction time, alcohol-to-oil molar ratio, enzyme concentration, water content, and reaction temperature (Amini et al., 2017). Esp. in situations where complex substrates such as waste cooking oil is used, case-by-case optimization becomes very important (Hama and Kondo, 2013). Also, the importance of experimental design and its relationship to the modelling techniques used is paramount for these systems (Yu et al., 2015).

Generally, biodiesel optimization studies follow the conventional response surface methodology based on low-order polynomial models (Shieh et al., 2003). Response surface methodology is a set of mathematical and statistical techniques used to establish an adequate functional relationship between an output of a system (also called a response) and several related control variables (inputs). The functional relationship is described in terms of low-order polynomial models which are generally of the first or second degree (Khuri and Mukhopadhyay, 2010). Although the low-order polynomial models do not carry any mechanistic information about the system, their behaviour usually approximates many types of natural systems. Also, the availability of many mathematical tools for the manipulation of these models make them a versatile choice for optimization studies.

The first step in response surface methodology is the design of experiments required to collect the input data. There are many available statistical designs for this purpose but Box-Wilson type central composite designs are most commonly encountered in the modelling and optimization of multivariate natural systems. For a system with four independent variables, the number of experiments are usually around the order of twenty. For example, Rodriguez et al. (2008) have modelled the lipase-catalyzed ethanolysis of soybean oil in a solvent-free system using a central composite design and response surface methodology. They have chosen reaction temperature, reaction time, substrate molar ratio, enzyme content and added water are their independent variables, looking at yield as the response. For the five independent variable system, they have conducted 50 experiments to generate the input data for a second-degree polynomial model. The reported goodness of fit statistics for this study were satisfactory with an R^2 of 0.8, F-value of 5.17, and a p-value less than 0.0001.

Similarly, Ismail et al. (2017) conducted a response surface methodology-based optimization of Novozyme 435-catalyzed transesterification of waste cooking oil with methanol in a solvent-free medium. The experimental design for this study was also based on a central composite design. They also employed five independent variables which were methanol to oil molar ratio, enzyme concentration, reaction temperature, reaction time, and mixing rate. They have observed two responses which were biodiesel yield and percentage conversion. The model used for this study was also a second-order polynomial. Thirty-two experiments were run to collect the input data and the reported goodness of fit statistics include R^2 values for the two responses (0.9979 and 0.9940), p-values (both less than 0.0001), and F-values (268.07 and 257.02).

Similar optimization studies exist for biodiesel production systems using alternative types of catalysis such as KOH catalysis. Ferella et al. (2010) optimized the transesterification of rapeseed oil using response surface methodology based on a full factorial design with three independent variables which were catalyzed concentration, reaction temperature, reaction time. A total of seventeen experiments were conducted to collect the input data and a second-order polynomial model was generated. Additionally, they have conducted each experiment twice and reported the arithmetic mean of the two replications. This is a step that is generally not required when running statistically designed experiments. The reported goodness of fit statistic was R^2 with a value of 0.97.

Another recent example is the optimization of biodiesel production from waste cooking oil using a lipase purified from a *Pseudomonas* species (Ali et al., 2017). A central composite design-based study was conducted within a response surface methodology scheme to analyse the effect of four independent variables (reaction temperature, methanol to oil molar ratio, amount of lipase, and rotation speed) on FAME yield. Thirty experiments were run to collect the input data and a second-order quadratic polynomial model was generated. The computed goodness of fit statistics in this study were a p-value of less than 0.0001 and a corresponding R^2 of 0.9907. The same biodiesel production system was also the subject of an optimization study integrating a Plackett-Burman experimental design for the selection of medium components affecting the lipase production with a subsequent optimization of the concentrations of the selected components based on a Box-Behnken design (Ali et al., 2015). This study is a good example of the power of statistical experimental design integrated with response surface methodology.

As in the examples above, a trend that can be seen in an overwhelming portion of optimization studies of biodiesel production systems is the use of statistically designed experiments (commonly based on a central composite design) to generate a second-order polynomial model of the system comprising 3-5 independent variables. Depending on the number of input variables the number of experiments conducted vary between 17-50. For example, Silva et al. (2011) performed an optimization of transesterification of soybean oil with ethanol using a factorial design for four independent variables (reaction temperature, catalyzt concentration, reaction time, and molar ratio of alcohol in relation to oil) by conducting thirty experiments. As usual, the generated model was a second-order polynomial.

There are also examples of such optimization studies being used to compare different catalysts. In one such study, optimized palm oil fatty acid methyl ester (POFAME) production was compared using chemical catalysis with NaOH, KOH, and $NaOCH_3$; and enzymatic catalysis using Novozyme 435 (Mumtaz et al., 2014). Central composite response surface design was used to study four independent variables (catalyst/enzyme concentration, reaction time, reaction temperature, and alcohol to oil molar ratio). The response was biodiesel yield. The number of experiments for each catalysis system was 30. Similarly, response surface methodology-based comparison of various catalysis systems using alternative feedstocks can be found in the literature. Mumtaz et al. (2012) compared the performance of different catalysis systems (NaOH, KOH, $NaOCH_3$, Novozyme 435, and a novel lipase) using two different feedstocks (rice bran oil and sunflower oil). All models generated were second-order quadratic polynomial models with p-values of 0.0003 and lower; and R^2 values ranging from 0.8198 to 0.9958. The reported adj-R^2 values for these two cases were 0.6517 and 0.9918, respectively.

It is not unusual to observe R^2 values well over 0.9 for situations involving three independent variables and twenty experimental points as can be seen in another example with reactant molar ratio, enzyme loading, and shaking speed chosen as input variables (Sun et al., 2012). However, such goodness of fit statistics does not guarantee the most appropriate modelling approach for systems like biodiesel production where there are highly nonlinear relationships between the input variables. The mathematical structure of the second-order quadratic polynomials nicely characterises natural systems where the response behaves optimally within the design space away from the extremes. However, for some biodiesel production systems, the optimal points may lie close to the extreme sections of the design space. The best example for this situation is in regards of reaction temperature. For some lipases, the optimal temperature is close to 60°C which would constitute the upper end for the optimization range. In such a situation, the curvature of a second-order polynomial away from the optimal point as the polynomial nears the extreme points would be a disadvantage.

In other fields, such as geo-imaging, the abovementioned situation is more common. In these fields, alternatives to low-order polynomial-based response surface methodology exist. One of the most commonly applied alternatives is Kriging, which is an interpolation-based method which can be more useful when dealing with systems demonstrating highly-nonlinear relationships between the input variables and possible optimal behaviour at the extreme sections of the design space (Kleijnen, 2017). The use of this method is extremely rare in biotechnology field. One of the rare examples is the use of Kriging for the predictive modelling of pharmaceutical studies (Jia et al., 2009).

A final point to highlight in the literature review of biodiesel optimization studies is the predominance of single-objective optimization applications compared to multi-objective ones. All the examples discussed above model and optimize a single objective which is usually yield or conversion. However, it is important to consider the combined performance of more than one process metric to be able to design and develop feasible processes. It is easier to find examples of multi-objective optimization when considering process flowsheet design as in the example of multi-objective optimization of integrated biorefineries (Geraili and Romagnoli, 2015). There are many methods to perform multi-objective optimization (Giagkiozis and Fleming, 2015). Using Pareto fronts seems to be a preferable one when considering two objective that can be in a trade-off with each other such as product titer and productivity. For example, the product titer would increase as the reaction proceeds, but a decreasing accumulation would result in a lower overall productivity, thus creating a trade-off between the two process metrics. Multi-objective optimization gives a much clearer picture of the behaviour of the system under such conditions.

In a multi-objective optimization study of biodiesel production from waste cooking oil, transesterification temperature, residence time, and methanol to oil molar ratio were selected while the optimized objectives were functional exergy efficiency, universal exergy efficiency, normalised exergy deconstruction, and conversion efficiency (Aghbashlo et al., 2019). In another multi-objective optimization study regarding biodiesel production, the aim was to maximise ester production while minimising other by-products (Goharimanesh et al., 2016). Similarly, Karimi et al. (2016) performed a multi-objective optimization of biodiesel production using an immobilized lipase based on the two objectives of FAME content and exergy efficiency. Also, Almeida et al. (2015) demonstrated the difference between the application of single-, bi-, and tri-objective optimization of biodiesel production from mixtures of waste fish oil, palm oil, and waste frying oil.

2. MATERIAL AND METHOD

2.1.Materials

2.1.1. Laboratory equipment

Laboratory equipment used in this study and their suppliers are listed as in the Table 2.1.

Table 2.1 Laboratory Equipment and Suppliers

Equipment	Supplier
Autoclave	NÜVE OT 032
Balances	Mettler Toledo Denver Instrument
Centrifuges	Sigma 2-16KL Sigma 3-18K
Deepfreezer (-20)	Liebherr
Deepfreezer (-86°C)	Thermoscientific
Freeze-dryer	Christ Freeze Dryer-Alpha 1-2 Ld
Horizontal Laminar Flow Cabinet	ESCO ClassII type A2
Ice Machine	Arttex Bar Line
Incubator	Nuve FN 400, FN 500
GC-MS	Agilent Technologies 5973Network GC/MSD
Magnetic stirrers	Velp Scientifica WiseStir MSH-20A
Orbital Shaker	Thermoshake THO 500/1, Gerhardt Analytical Systems
pH meter	inoLab
Refrigerator	Arçelik

Table 2.1 continued

Equipment	Supplier
Spectrophotometer	Bio-Rad SmartSpec Plus
Vortex	Labnet
Water baths	Memmert Heto
Water purification systems	Elga PURELAB

2.1.2. Chemicals

Chemicals used in this study are listed in Table 2.2.

Table 2.2 Chemicals and Suppliers

Chemical	Supplier
Acetic acid	Sigma-Aldrich
Agar	Biomérieux
Bovine serum albumin	Sigma-Aldrich
D(+)-Glucose Monohydrate	Sigma-Aldrich
Glycerol extrapure	OmniLife Science
Hydrochloric acid 37%	Sigma-Aldrich
Isopropanol	Merck
Magnesium sulfate heptahydrate	Merck
Malt extract	Merck
Methanol	Sigma-Aldrich
n-Hexane	Merck
Olive oil	Tariş
p-nitrophenyl palmitate	Alfa Aesar
Peptone	Merck
Potassium dihydrogen phosphate	Sigma-Aldrich
Sodium acetate	OmniLife Science
Sodium carbonate	OmniLife Science

Table 2.2 continued

Chemical	Supplier
Sodium hydroxide	Merck
Sodium nitrate	Carlo Erba
Supelco 37 Component FAME Mix	Sigma-Aldrich
Yeast extract	Merck

2.1.3. Standard reference for gas chromatographic analyses

The standard reference for gas chromatographic analyses; The Supelco® 37-component fatty acid methyl ester (FAME) mix, TraceCERT®, in dichloromethane (varied conc.), ampule of 1 ml (CRM47885) is supplied from Sigma–Aldrich Company.

2.1.4. Buffers and solutions

Different buffers and solutions used in this study and their compositions are listed as below:

Table 2.3 Compositions of buffers and solutions used in the study

Buffer or solution	Composition
30% (v/v) glycerol solution	30 ml glycerol is mixed with 70 ml deionized and distilled water
Sodium acetate- acetic acid buffer pH 5.6	0.05 M, 3640 ml sodium acetate is mixed with 0.05 M, 360 ml acetic acid
Sodium carbonate solution	10.6 g sodium carbonate is dissolved in 100 ml deionized and distilled water

2.1.5. Yeast strain

Cryptococcus diffluens (D44) was kindly obtained on agar slants as a gift from by Assoc. Prof. Dr. Hüsniye Tansel Yalçın-Öztürk.

2.1.6. Waste cooking oil

The WCO used as the raw material for producing biodiesel was collected from the different restaurants and stored at room temperature. The crude waste cooking oil was filtered using filter paper to remove impurities from oil.

2.2. Methods

2.2.1. Storage and maintainance of Cryptococcus diffluens (D44)

The cells were spread on agar slants in order to make yeast culture stocks which would be stored and preserved at +4°C until used. Those stock cultures were used to inoculate liquid medium pre-cultures. Agar slants medium consisted of 0.3% malt extract (w/v), 0.3% yeast extract (w/v), 0.5% peptone (w/v), 1% glucose (w/v), 1.5% agar (w/v) with the pH: 6.2 ±0.2. Approximately 5 ml of medium was added into test tubes and they were sterilised at 121ºC and 1 atm for 15 minutes. The inoculation from the old agar slants to fresh ones was done using sterile inoculation loop. The slants were incubated at 28ºC until the colonies appeared. For long term storage, the cells were kept at -80˚C in 15% (v/v) glycerol stocks. In order to prepare the glycerol stocks, the cells were inoculated in precultivation medium which is composed of 0.3% malt extract (w/v), 0.3% yeast extract (w/v), 0.5% peptone (w/v), 1% glucose (w/v). After 16 hours incubation at 28˚C and 180 rpm shaking conditions, the cells were mixed 30% (v/v) sterile glycerol with a ratio of 1:1.

2.2.2. Production and lyophilisation of crude lipase

Production of lipase from *C. diffluens* D44 was carried out using the same medium and culture conditions as described by Yılmaz and Sayar, 2015. A loop-full of yeast from agar slants was aseptically transferred into a 100 ml erlenmayer flask containing 20 ml of precultivation medium. After 16 hours incubation at 28˚C and 180 rpm shaking conditions, 2% inoculum was transferred to a 250 ml erlenmayer flask containing 50 ml lipase production medium which contains 0.1% (w/v) Yeast extract, 3.0% (w/v) Peptone, 0.05% (w/v) $MgSO_4.7H_2O$, 0.1% (w/v) KH_2PO_4, 0.3% (w/v) $NaNO_3$ and olive oil 2% (v/v). The initial pH of lipase production medium was adjusted to 7.0. Expect olive oil, all the media were heat sterilized (121°C for 15 min). After cooling, the olive oil, previously sterilized by dry heat (180°C for 60 min), was added to the culture medium. Lipase production conditions was determined based on preliminary studies (Yılmaz et al., 2014).

For the lyophilisation process, all samples of yeast culture were centrifuged at 10,000 rpm and +4°C for 20 minutes and the supernatant was separated to be used as extracellular crude lipase. Lyophilisation process was carried out at Tubitak Marmara Research Center Genetic Eng&Bitech Institute.

2.2.3. Determination of lyophilised crude lipase activity

Enzyme activity of lyophilised crude lipase using p-nitrophenyl palmitate (pNPP) as substrate was measured. 30 mg of pNPP dissolved in 10 ml 2-Propanol were emulsified in 90 ml of 50mM sodium acetate, pH 5.6. 0.1 g of lyophilised enzyme was dissolved in 1 ml of 50mM sodium acetate buffer. 0.1 ml of dissolved enzyme solution were mixed with 2 ml of the pNPP-containing emulsion and incubated at 37°C for 3min. The reaction was stopped by adding 0.15 ml of 1M sodium carbonate solution and absorbance was measured spectrophotometrically at 410 nm against an enzyme free 50mM sodium acetate buffer solution. One lipase unit (U) is defined as the amount of enzyme that librates 1 μmol p-nitrophenol/min under assay conditions described. Protein content was determined according to the Bradford method (Bradford, 1976) recording the absorbance at 595 nm and using bovine serum albumin as a protein standard.

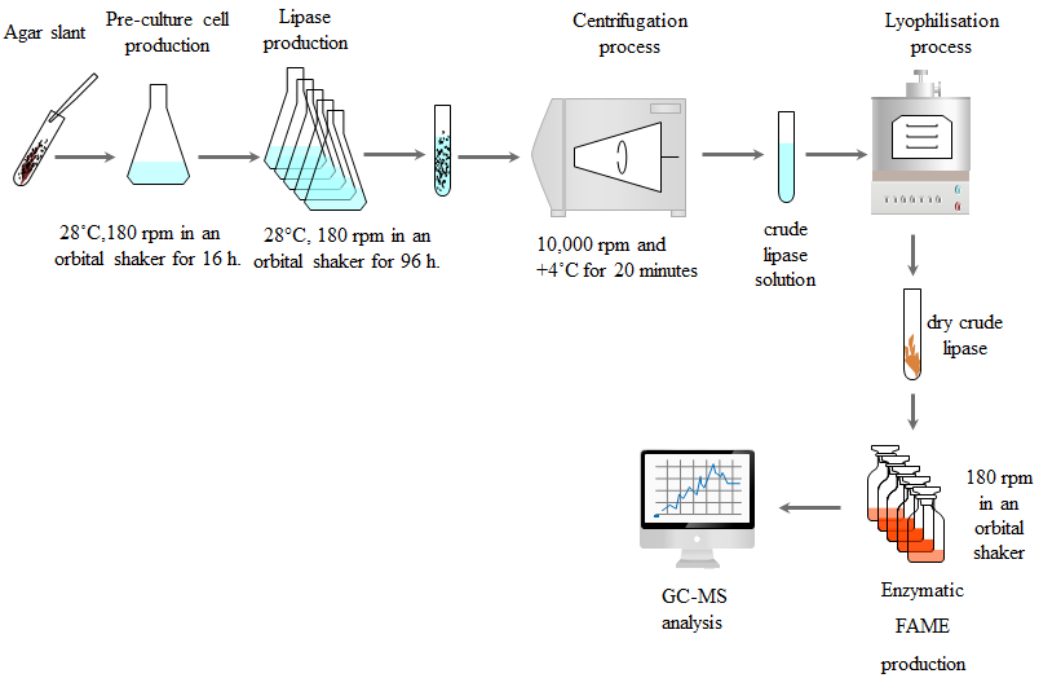

Figure 2.1 Flow diagram of from crude lipase to FAME production

2.2.4. Design of experiments (DoE)

The selected factors of interest (input variables) in evaluating the performance of the enzymatic biodiesel production system were reaction temperature (T), ratio by weight of lyophilised crude enzyme used to that of initial oil (E:O), and molar ratio of methanol added to that of initial oil (A:O). A 3-factor 5-level central composite design (CCD) was used to generate the experimental conditions to be tested. The general structure of CCD is given in Table 2.4.

Table 2.4 3-factor 5-level CCD

Experiment Number	Factor 1 (T)	Factor 2 (E:O)	Factor 3 (A:O)
1	-1.0000	-1.0000	-1.0000
2	-1.0000	1.0000	-1.0000
3	-1.0000	-1.0000	1.0000
4	-1.0000	1.0000	1.0000
5	1.0000	-1.0000	-1.0000
6	1.0000	1.0000	-1.0000

Table 2.4 continued

Experiment Number	Factor 1 (T)	Factor 2 (E:O)	Factor 3 (A:O)
7	1.0000	-1.0000	1.0000
8	1.0000	1.0000	1.0000
9	-1.6818	0	0
10	1.6818	0	0
11	0	0	-1.6818
12	0	0	1.6818
13	0	-1.6818	0
14	0	1.6818	0
15	0	0	0
16	0	0	0

Two repetitions of the central point (0,0,0) were considered satisfactory instead of the geometrically maximum six repetitions, resulting in a total of 16 experiments. Time (t) progress of each reaction was also monitored at 24 hour intervals up to 250 or 500 hours depending on the progress of the reactions resulting in a total of 220 data points.

For each data point, concentrations of three methyl ester fatty acids (C16:0, C18:1, C18:2) were measured as described below in Section 2.2.6 and total FAME titer was calculated as the summation of these three values. Also, productivity values were calculated by dividing the titers by time elapsed at each time point. A total of eight output metrics for each data point were acquired.

Table 2.5 Output metrics symbols (i = 1:8)

Symbols	Output Metrics
OM_1	C16:0 titer
OM_2	C18:1 titer
OM_3	C18:2 titer
OM_4	Total FAME titer
OM_5	C16:0 productivity

Table 2.5 continued

Symbols	Output Metrics
OM_6	C18:1 productivity
OM_7	C18:2 productivity
OM_8	Total FAME productivity

The data were collected in two sets. The small data set contains 16 points whose output metrics were taken at the time point where maximum total FAME titer was observed for each experiment. The large data set contains all of the 220 data points comprising time progress data for each experiment.

All experiments were conducted using 16 grams of initial waste cooking oil. Initially, input variable ranges were selected as follows based on commonly cited values in literature and previous experimentation (data not shown).

Table 2.6 Original input variable ranges

Independent variables	Symbols	Levels				
		-1.6818	**-1.0000**	**0**	**1.0000**	**1.6818**
Temperature (°C)	T	25	32	42.5	53	60
Crude enzyme to oil ratio (wt%)	E:O	10	28	55	82	100
Methanol to oil molar ratio	A:O	3.0:1	4.0:1	5.5:1	7.0:1	8.0:1

The following experimental design was generated using these ranges:

Table 2.7 Original DoE

Experiment Number	Factor 1 (T)	Factor 2 (E:O)	Factor 3 (A:O)
1	32	28	4.0
2	32	82	4.0
3	32	28	7.0

Table 2.7 continued

Experiment Number	**Factor 1 (T)**	**Factor 2 (E:O)**	**Factor 3 (A:O)**
4	32	82	7.0
5	53	28	4.0
6	53	82	4.0
7	53	28	7.0
8	53	82	7.0
9	25	55	5.5
10	60	55	5.5
11	42.5	55	3.0
12	42.5	55	8.0
13	42.5	10	5.5
14	42.5	100	5.5
15	42.5	55	5.5
16	42.5	55	5.5

After the completion of experiments 1, 3, 5, 7, 11, 12 and 13, a solubility limit problem regarding the crude enzyme was encountered for the experiments with high crude enzyme to oil ratios. Consequently, the DoE was manually modified to accommodate the already performed experiments along with further experiments within the allowable solubility limits. The manually modified DoE is given in Table 2.8.

Table 2.8 Manually modified DoE

Experiment Number	**Factor 1 (T)**	**Factor 2 (E:O)**	**Factor 3 (A:O)**
1	32	28	4.0
2	32	46	4.0
3	32	28	7.0
4	32	46	7.0
5	53	28	4.0

Table 2.8 continued

Experiment Number	Factor 1 (T)	Factor 2 (E:O)	Factor 3 (A:O)
6	53	46	4.0
7	53	28	7.0
8	53	46	7.0
9	25	32.5	5.5
10	60	32.5	5.5
11	42.5	55	3.0
12	42.5	55	8.0
13	42.5	10	5.5
14	42.5	55	5.5
15	42.5	32.5	5.5
16	42.5	32.5	5.5

Figures 2.2 and 2.3 show the distribution of experimental points scanning the 3-dimensional design space for the original and manually-modified DoEs, respectively.

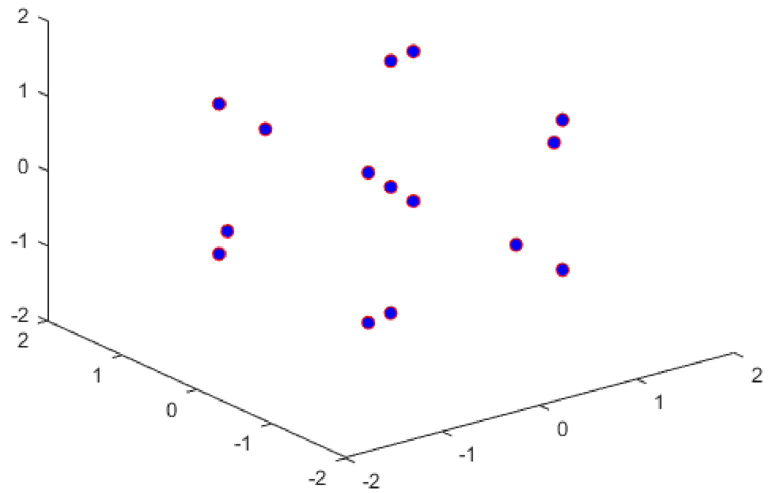

Figure 2.2 Original scanning of 3-dimensional design space

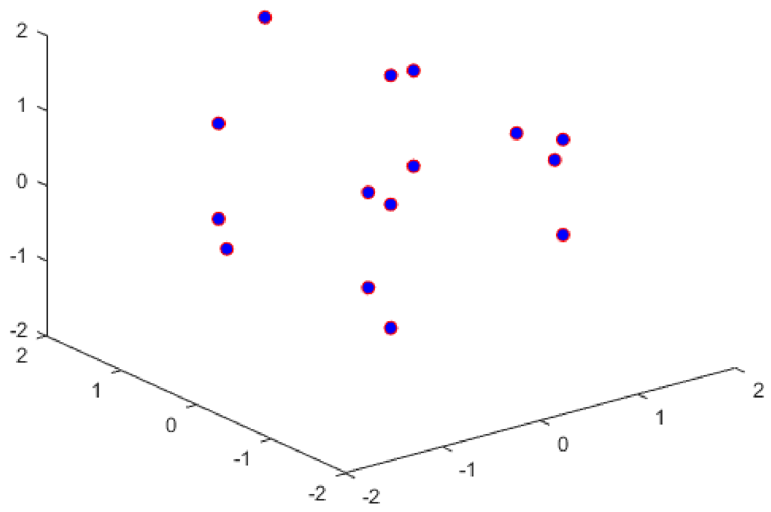

Figure 2.3 Modified scanning of design space

As can be seen from the figures, manually-modified DoE scans a satisfactorily equivalent section of the design space. Thus, the results acquired from the manually-modified DoE was used for further modelling and optimization exercises.

2.2.5. Enzymatic biodiesel production

All experiments were conducted in 100 ml screw-capped glass bottles placed at 180 rpm in an orbital shaker. 16 g of waste cooking oil mixed well with various amount of lyophilised crude lipase and methanol. Aliquots of the reaction mixture (200 µl) were withdrawn at various time intervals and mixed with hexane (1 ml). The mixture was centrifuged at 10,000 rpm for 15 min. The upper phase contained the desired FAME contents in hexane. The FAME composition of each sample was analyzed by the GC method as described below.

2.2.6. Determination of FAME using GC-MS

The methyl ester contents of reaction mixture were determined by gas chromatography in an Agilent Technologies 5973Network equipped with a mass detector (GC/MSD) and DB-Wax ms capillary column 30mx0.25mm x0.25µm (length x diameter x film thickness). Samples of 1 µl were injected into the capillary column with a split ratio of

50:1. Helium was employed as the carrier gas with flow rate of 1.0 ml/min. The temperatures of injector and detector were both maintained at 250^{0}C. The following temperature program was employed: 50^{0}C for 1 minute to 25^{0}C/min to 200^{0}C, 3^{0}C/min to 230^{0}C, 18 minutes and total time of the analysis was 35 min. An analytical standard Supelco® 37 Component FAME Mix was used to identify the peaks at different retention times.

Table 2.9 GC-MS quantitative result of Supelco® 37 Component FAME Mix

	C16:0	**C18:1**	**C18:2**
Area	74363198	79020869	48035538
Concentration (µg/ml)	619.0	418.3	211.4

Table 2.10 GC-MS quantitative result of Experimet Set of 6

Time (h)		C16:0	C18:1	C18:2
96	Area	17312046	83803209	57795690
	Concentration (µg/ml)	144.11	443.62	254.35
240	Area	39748327	193914230	132592321
	Concentration (µg/ml)	330.87	1026.49	583.53
360	Area	54664275	272404039	126245802
	Concentration (µg/ml)	455.03	1441.98	817.61

These numerical results were converted to g/l units via multiplication by 5 (dilution factor) and division by 1000 (ml to l conversion) for further use and reporting.

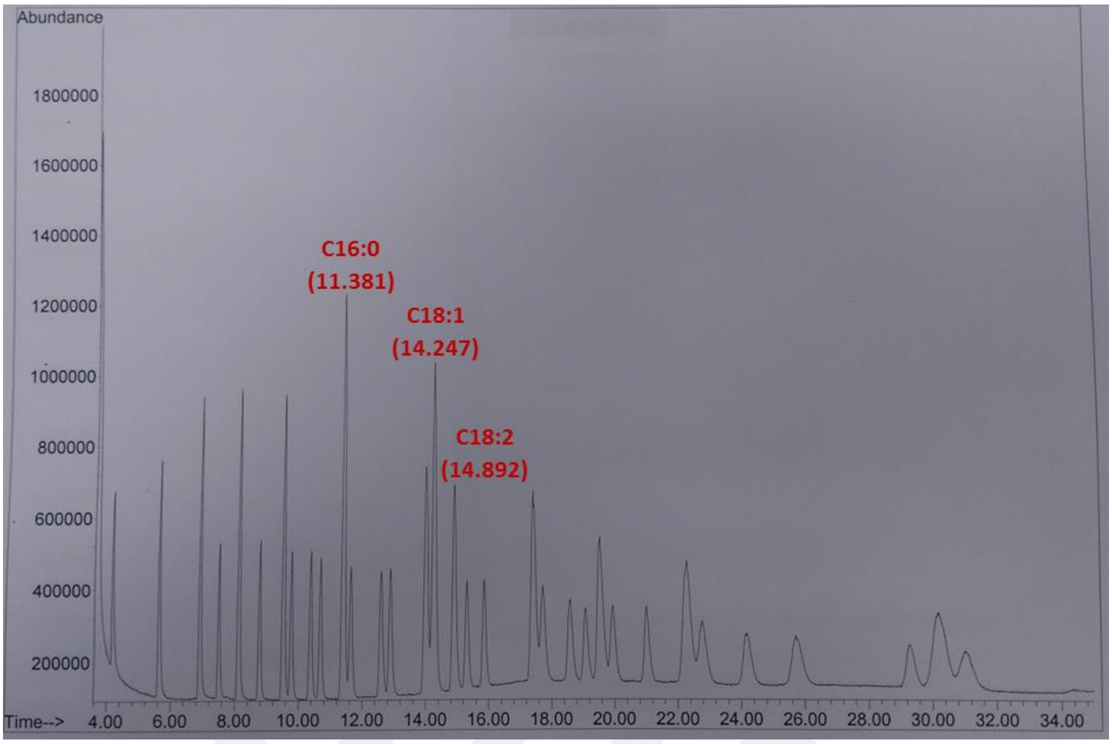

Figure 2.4 GC chromatogram of Supelco® 37 Component FAME Mix

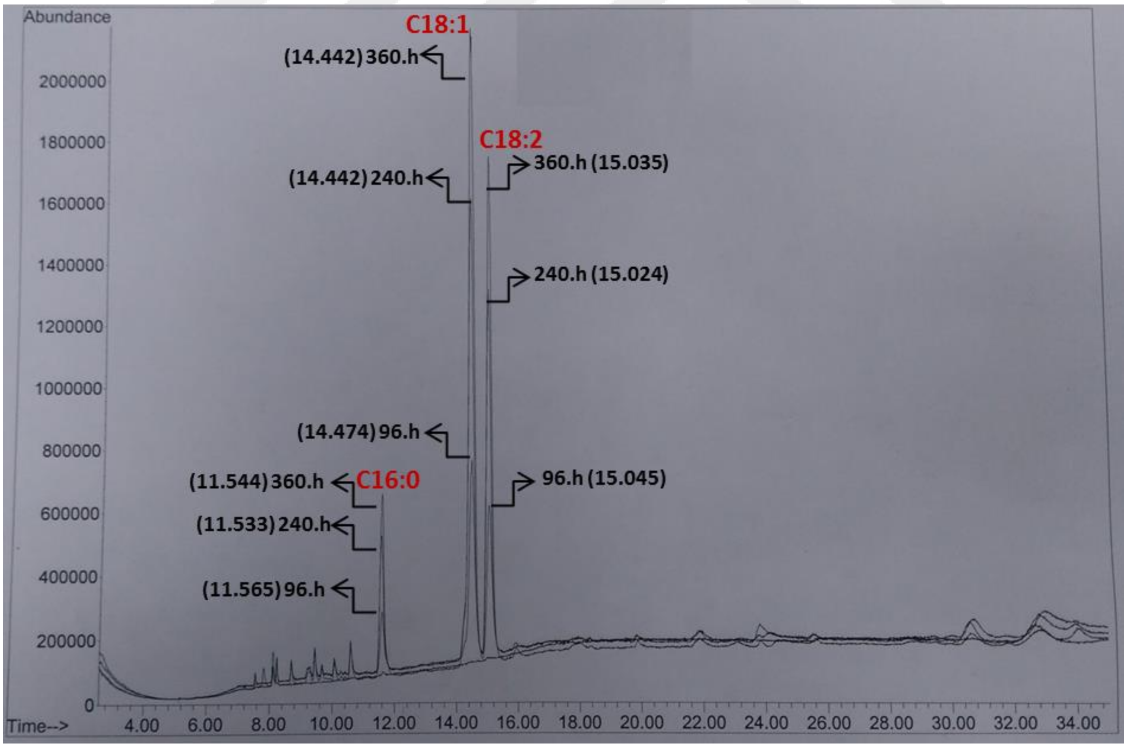

Figure 2.5 GC chromatogram of FAME production after 96, 240 and 360 h for Experiment Set of 6

2.2.7. Modelling and Optimization

2.2.7.1. Modelling

Two modelling approaches based on low-level polynomial RSM and Kriging were employed separately using two data sets to eight output metrics which were mentioned in Section 2.2.4. Two RSM models for the metrics were generated using the fitlm functionality of Matlab's Statistical and Machine Learning toolbox. The Kriging models for the metrics were generated with DACE toolbox which is an externally supplied toolbox operating under Matlab (Lophaven et al., 2002).

Table 2.11 Input variables symbols (j = 1:4)

Symbols	**Input Variables**
$\mathbf{IV_1}$	Time – t (h)
$\mathbf{IV_2}$	Temperature – T (°C)
$\mathbf{IV_3}$	Crude enzyme to oil ratio – E:O (%)
$\mathbf{IV_4}$	Methanol to oil molar ratio – A:O

Low-level polynomial model

Pure quadratic structure is shown as below:

$$OM_i^{pq} = \beta_{0,i}^{pq} + \beta_{1,i}^{pq}\,(IV_1) + \beta_{2,i}^{pq}\,(IV_2) + \beta_{3,i}^{pq}\,(IV_3) + \beta_{4,i}^{pq}(IV_4) + \beta_{5,i}^{pq}(IV_1)^2 + \beta_{6,i}^{pq}(IV_2)^2 + \beta_{7,i}^{pq}(IV_3)^2 + \beta_{8,i}^{pq}(IV_4)^2 \quad (2.1)$$

Quadratic structure is shown as below:

$$OM_i^{q} = \beta_{0,i}^{q} + \beta_{1,i}^{q}(IV_1) + \beta_{2,i}^{q}(IV_2) + \beta_{3,i}^{q}(IV_3) + \beta_{4,i}^{q}(IV_4) + \beta_{5,i}^{q}(IV_1)(IV_2) + \beta_{6,i}^{q}(IV_1)(IV_3) + \beta_{7,i}^{q}(IV_1)(IV_4) + \beta_{8,i}^{q}(IV_2)(IV_3) + \beta_{9,i}^{q}(IV_2)(IV_4) + \beta_{10,i}^{q}(IV_3)(IV_4) + \beta_{11,i}^{q}(IV_1)^2 + \beta_{12,i}^{q}(IV_2)^2 + \beta_{13,i}^{q}(IV_3)^2 + \beta_{14,i}^{q}(IV_4)^2 \quad (2.2)$$

where i, q, pq refer to the output metrics, quadratic structure and pure quadratic structure, respectively.

Kriging

The Kriging model is composed of a regression function and a correlation function. A zero order polynomial was selected as the regression function since this selection gave the best fit compared to first and second order polynomials. A Gaussian function was selected as the correlation function since error and deviations in natural and engineered systems often follow natural distribution. The Kriging model is as follows:

Full kriging equation:

$$f_1(IV_1, IV_2, IV_3, IV_4) + \varepsilon = C \tag{2.3}$$

Zero order polynomial regression function:

$$f_1(IV_1, IV_2, IV_3, IV_4) = \alpha \tag{2.4}$$

where C refers to a constant value and α refers to the parameter of the regression function.

Gaussian correlation function:

$$\varepsilon = e^{(-\theta_j d_j^2)} \tag{2.5}$$

where θ_j and d_j^2 refer to the parameters of the correlation function and squares of the residuals, respectively and *j* refers to the input variables.

Using two methods mentioned above, a total of 48 different models were developed. In the following table the model definitions were described.

Table 2.12 Model Descriptions

Model Number*	**Model Description**
Model-1	Pure quadratic model based on small data set for C16:0 titer
Model-2	Pure quadratic model based on small data set for C18:1 titer

Table 2.12 continued

Model Number*	**Model Description**
Model-3	Pure quadratic model based on small data set for C18:2 titer
Model-4	Pure quadratic model based on small data set for Total FAME titer
Model-5	Pure quadratic model based on small data set for C16:0 productivity
Model-6	Pure quadratic model based on small data set for C18:1 productivity
Model-7	Pure quadratic model based on small data set for C18:2 productivity
Model-8	Pure quadratic model based on small data set for Total FAME productivity
Model-9	Quadratic model based on small data set for C16:0 titer
Model-10	Quadratic model based on small data set for C18:1 titer
Model-11	Quadratic model based on small data set for C18:2 titer
Model-12	Quadratic model based on small data set for Total FAME titer
Model-13	Quadratic model based on small data set for C16:0 productivity
Model-14	Quadratic model based on small data set for C18:1 productivity
Model-15	Quadratic model based on small data set for C18:2 productivity
Model-16	Quadratic model based on small data set for Total FAME productivity
Model-17	Pure quadratic model based on large data set for C16:0 titer
Model-18	Pure quadratic model based on large data set for C18:1 titer
Model-19	Pure quadratic model based on large data set for C18:2 titer

Table 2.12 continued

Model Number*	Model Description
Model-20	Pure quadratic model based on large data set for Total FAME titer
Model-21	Pure quadratic model based on large data set for C16:0 productivity
Model-22	Pure quadratic model based on large data set for C18:1 productivity
Model-23	Pure quadratic model based on large data set for C18:2 productivity
Model-24	Pure quadratic model based on large data set for Total FAME productivity
Model-25	Quadratic model based on large data set for C16:0 titer
Model-26	Quadratic model based on large data set for C18:1 titer
Model-27	Quadratic model based on large data set for C18:2 titer
Model-28	Quadratic model based on large data set for Total FAME titer
Model-29	Quadratic model based on large data set for C16:0 productivity
Model-30	Quadratic model based on large data set for C18:1 productivity
Model-31	Quadratic model based on large data set for C18:2 productivity
Model-32	Quadratic model based on large data set for Total FAME productivity
Model-33	Kriging model based on small data set for C16:0 titer
Model-34	Kriging model based on small data set for C18:1 titer
Model-35	Kriging model based on small data set for C18:2 titer
Model-36	Kriging model based on small data set for Total FAME titer

Table 2.12 continued

Model Number*	**Model Description**
Model-37	Kriging model based on small data set for C16:0 productivity
Model-38	Kriging model based on small data set for C18:1 productivity
Model-39	Kriging model based on small data set for C18:2 productivity
Model-40	Kriging model based on small data set for Total FAME productivity
Model-41	Kriging model based on large data set for C16:0 titer
Model-42	Kriging model based on large data set for C18:1 titer
Model-43	Kriging model based on large data set for C18:2 titer
Model-44	Kriging model based on large data set for Total FAME titer
Model-45	Kriging model based on large data set for C16:0 productivity
Model-46	Kriging model based on large data set for C18:1 productivity
Model-47	Kriging model based on large data set for C18:2 productivity
Model-48	Kriging model based on large data set for Total FAME productivity

* In the remaining the text, each model will be referred to by its model number.

Evaluation of Goodness of Fit

For the evaluation and comparison of generated models, R^2, adjusted-R^2 (adj_R^2), root mean square error (RMSE), f_stat, and p_value statistics were used. The following equations show the calculations for these statistics.

- **Sum of square error (SSE)**

$$SSE = \sum_{i=1}^{n} (y_i - \hat{y}_i)^2 \tag{2.6}$$

where n is the number of observations, y_i is the value of the observation and $\hat{y}_i$ is the value obtained from the simulation.

- **Sum of squares about the mean (SST)**

$$SST = \sum_{i=1}^{n} (y_i - \bar{y})^2 \tag{2.7}$$

where $\bar{y}$ refers to the value of the mean of the observation.

- **Sum of squares due to regression (SSR)**

$$SSR = \sum_{i=1}^{n} (\hat{y}_i - \bar{y})^2 \tag{2.8}$$

- **R-squared (R^2)**

$$R^2 = 1 - \frac{SSE}{SST} \tag{2.9}$$

- **Mean of squared error (MSE)**

$$MSE = \frac{SSE}{v} \qquad v = n - m \tag{2.10}$$

where n and m refer to number of observation points and number of parameters in the model, respectively.

- **Root mean squared errors (RMSE)**

$$RMSE = \sqrt{MSE} \tag{2.11}$$

- **Adjusted R-Squared (adj_R^2)**

$$adj\_R^2 = 1 - \frac{SSE\ (n-1)}{SST\ (v)} \tag{2.12}$$

- **F Statistic (f_stat)**

$$f\_stat = {}^{\frac{SSR}{(m-1)}}\!\Big/_{MSE} \tag{2.13}$$

- $\boldsymbol{p - value}$

p_value is calculated based on f_stat depending upon cumulative F distribution.

2.2.7.2. Optimization

Single-objective optimization

For the single-objective optimization of each output metric a global search method was used. Due to the highly nonlinear behaviour of the system there is a significant possibility that local optima exist. Global search method is an appropriate method to deal with such a situation. The global search algorithm offered in Matlab's global optimization toolbox was used. The algorithm is as follows:

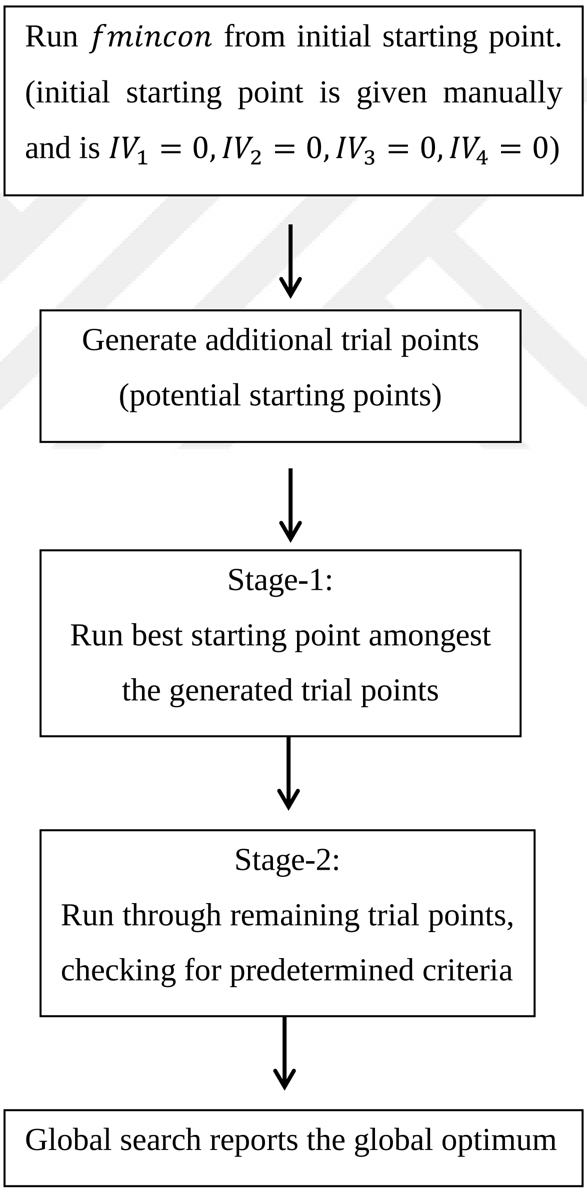

Figure 2.6 The algorithm figure

The algorithm uses Matlab's fmincon function which is an interior-point based optimization solver for constrained multivariate functions. The global search algorithm runs the optimization solver multiple times with varying starting points and compares the optima found in each run of the optimization solver. The comparison is based on predetermined criteria such as the total number of solver runs or minimum difference between multiple optima found and guides the direction of the global search. After the predetermined criteria have been achieved, the global search algorithm terminates, reporting the best optimum amongst all the optimal solutions.

Table 2.13 Table of constraints on input invariables for optimization

	Minimum	**Maximum**
IV_1	30	500
IV_2	25	60
IV_3	10	55
IV_4	3	8

These constraints are selected as they define the limits of experimental design space.

Multi-objective optimization

Amongst the eight output metrics modelled and optimized, two are most relevant from a process design perspective. These are total FAME titer achieved and the associated productivity. Often there exists a trade-off between these two metrics as longer reactions times usually mean higher titer but maybe at the expense of lower overall productivities. Because of this reason, it is an interesting idea to try to optimize the system with respect to both these metrics. Multi-objective optimization is applied for this purpose.

A Pareto front is generated to visualise the trade-off between the two metrics as the system is optimized for both metrics. The Pareto front shows the decrease in one of the metrics as the other one is maximized and vice versa. A Pareto front is a set of points in two-dimensional output metric plane that have noninferior output metric values. This means that on the Pareto front, the values of the two output metrics is as good as they can simultaneously be and leaving the Pareto front means sacrificing one of the output metrics.

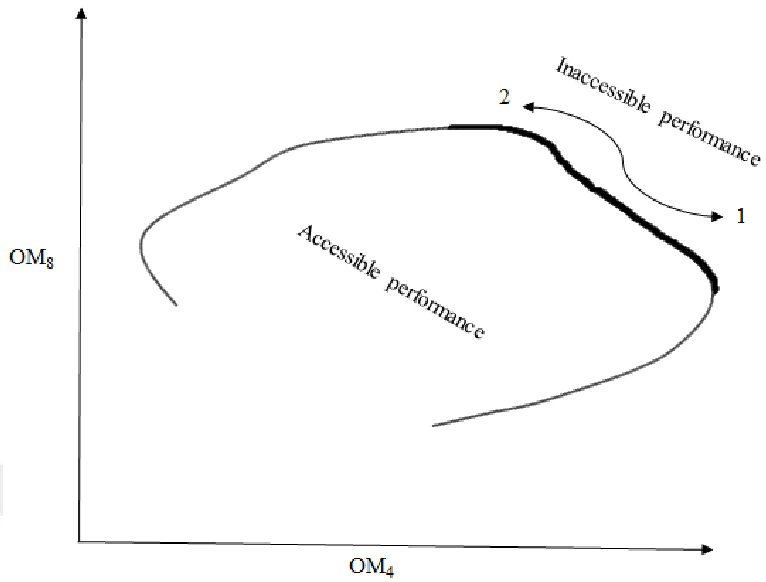

Figure 2.7 Generic Pareto Front

Direction 1 favours OM_4 over OM_8; direction 2 favours OM_8 over OM_4. In other words, for each point on the Pareto front, improvement in one output metric means degrading the other one. Any point in the accessible performance area and not on the Pareto front means that the system is performing under-optimally. The system cannot move into the inaccessible performance area.

Two Pareto fronts are generated for quadratic model and Kriging model based on the large dataset. Pareto fronts are generated using the gamultiobj functionality under Matlab's global optimization toolbox. The function uses a controlled, elitist genetic algorithm whose aim is to converge on an optimal Pareto front.

3. RESULTS AND DISCUSSION

3.1. Experimental Part

In the current study, the relationship between response methyl esters concentration and three reaction variables, which are effect of enzyme concentration, alcohol-to-oil molar ratio and reaction temperature, were evaluated by using a manually-curated, CCD-based experimental design. 16 g of WCO and stirring rate of 180 rpm were constant parameters for all reactions. Crude *C. diffluens* D44 lipase (44.53 U/min 0.62 mg/ml protein) was used.

Time-course reactions were monitored using gas chromatography–mass spectrometry. For all reactions, each individual ester concentration was monitored and quantified. Also total ester concentration was calculated.

It is known that the WCO is a suitable feedstock for biodiesel production. When WCO is analyzed for its fatty acid content, it is shown that palmitic C16:0 (20.4 %), oleic C18:1 (50.9 %) and linoleic C18:2 (13.5 %) acids are the three most common fatty acids (Chhetri et al., 2008). According to our results, it could be seen that the methyl esters of these three fatty acids were produced.

3.1.1. Experiment-1

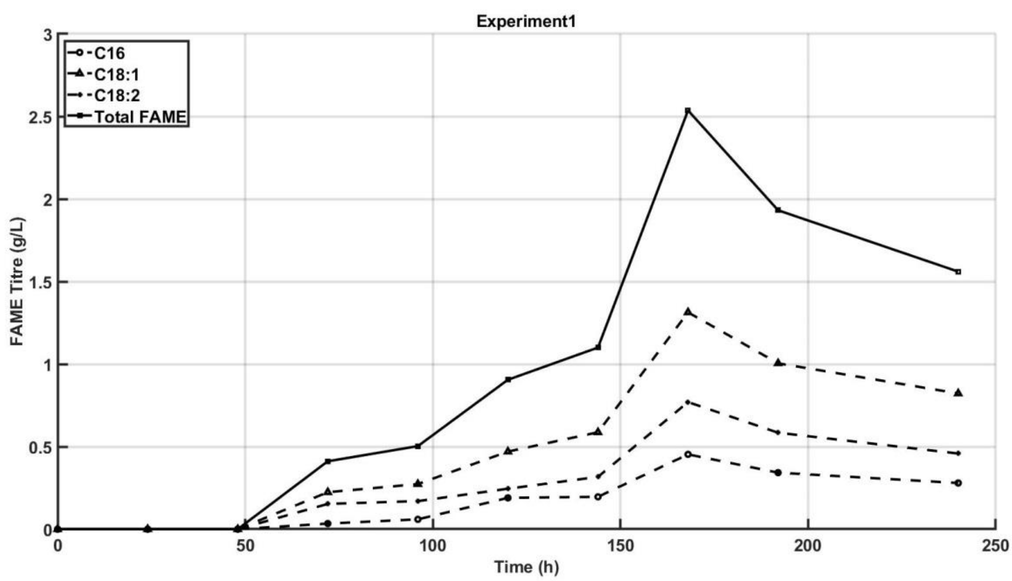

Figure 3.1 Time course profile of FAME concentration for the enzymatic methanolysis of WCO

In this work, the reaction conditions were investigated were a temperature of 32°C, *C. diffluens* D44 lipase with a concentration (wt% by weight of oil) 28 (%w/w), and methanol to WCO molar ratio of 4:1.

It is seen from the figure, no ester production is observed for the first 48 hours. Based on that fact, the enzyme-oil-methanol interaction starts after a certain time caused by the stirring effect and temperature. Under this reaction conditions, the enzyme-oil-methanol interaction takes at least 48 hours to start the ester production. As shown in the graph above between 48 and 144 hours there is an increasing rate in methanolysis reaction. When the FAME production is investigated between 144 and 168 hours, almost 2 and a half-fold rise in concentration is observed. The reason is due to the fact that after a while the temperature will reduce the viscosity of the oil which leads to a sufficient contact at the active site of enzyme surface between the oil and the methanol.

It shows the maximum total FAME concentration is observed at 168 hours as 2.5 g/l. Then total FAME concentration drops drastically from 2.5 g/l to 1.9 g/l due to a lack of substrate for the enzyme. In addition to that, when total FAME production at 192 and 240 hours was investigated, it was observed that the decreasing in concentration continued from 1.9 to 1.5 g/l. As a result, the total reaction time was set at 240 hours for this experiment.

For this reaction, methyl oleate (C18:1) is the major component of the biodiesel resulted from the methanolysis of WCO which is followed by methyl linoleate (C18:2) and methyl palmitate (C16:0), respectively. Thus, the change of methyl oleate yield has the most significant effect on the total ester yield. When each ester concentrations are quantified individually, it is observed that the maximum values are determined at 168 hour as 1.3, 0.8 and 0.4 g/l, respectively.

3.1.2. Experiment-2

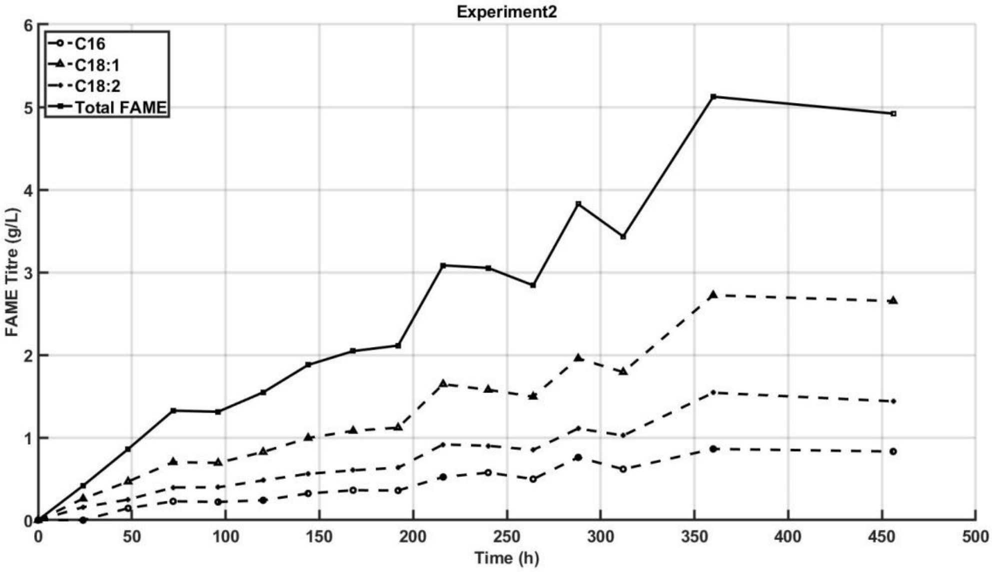

Figure 3.2 Time course profile of FAME concentration for the enzymatic methanolysis of WCO

In this study, the reaction conditions were investigated were a temperature of 32°C, *C. diffluens* D44 lipase with a concentration (wt% by weight of oil) 46 (%w/w), and methanol to WCO molar ratio of 4:1.

As shown in the graph above, the first findings of formation for methyl oleate (C18:1) and methyl linoleate (C18:2) are detected at 24 hours, it is thought that the production has begun early on during the experiment between 0 and 24 hours. However formation of methyl palmitate (C16:0) is observed after first 24 hours.

The reaction fluctuates up to 360 hours and maximum total FAME concentration is reached as 5.1 g/l at this time. Especially at 264 hours and at 312 hours sharp drop in concentrations are observed due to analytical measurement.

When each individual ester are examined, it is observed that they have almost the same pattern. Methyl oleate (C18:1) is the major component which is followed by methyl linoleate (C18:2) and methyl palmitate (C16:0), respectively. Maximum concentrations are quantified at 360 hours as 2.7, 1.5 and 0.9 g/l, respectively.

When the total FAME production between 360 and 456 hours was investigated, the concentration showed a slight decrease with time from 5.1 g/l to 4.9 g/l. As a result, the total reaction time was set at 456 hours for this experiment.

3.1.3. Experiment-3

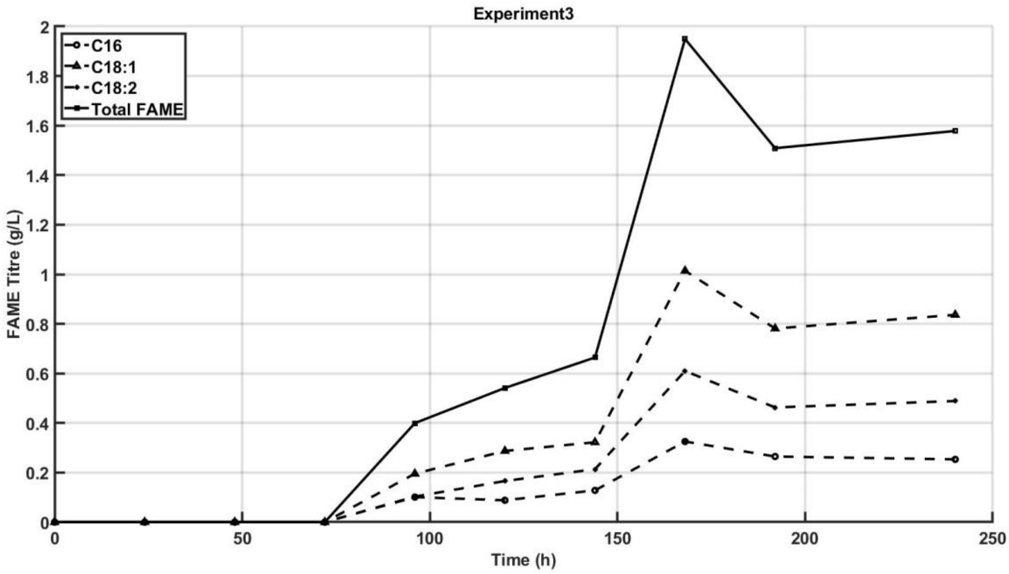

Figure 3.3 Time course profile of FAME concentration for the enzymatic methanolysis of WCO

In this work, the reaction conditions were investigated were a temperature of 32°C, *C. diffluens* (D44) lipase with a concentration (wt% by weight of oil) 28 (%w/w), and methanol to WCO molar ratio of 7:1.

It is observed from the figure that for the first 72 hours any ester production is not observed. The reason is due to the fact that, the enzyme-oil-methanol interaction starts after a certain time caused by the stirring effect and temperature. In this reaction conditions, the enzyme-oil-methanol interaction takes at least 72 hours to start the ester production.

Up to 144 hours the reaction takes place at an almost linear rate, at 168 hours the production rises substantially and almost 3-fold increase in concentration is observed. The reason is due to the fact that after a while the temperature will reduce the viscosity of the oil which leads to a sufficient contact at the active site of enzyme surface between the oil and the methanol.

As it is depicted in Figure 3.3 the maximum total FAME concentration is reached as 1.9 g/l at 168 hours. After that time, total FAME concentration drops from 1.9 g/l to 1.5 g/l.

Methyl palmitate (C16:0), methyl oleate (C18:1) and methyl linoleate (C18:2) are the components of the biodiesel resulted from the methanolysis of WCO, each ester concentrations are quantified individually as 0.3, 1.0 and 0.6 g/l at 168 hour, respectively.

Although when the total FAME production between 192 and 240 hours was investigated, a slight increase in concentration was observed, it was not enough to resume production. As a result, the total reaction time was set at 240 hours for this experiment.

3.1.4. Experiment-4

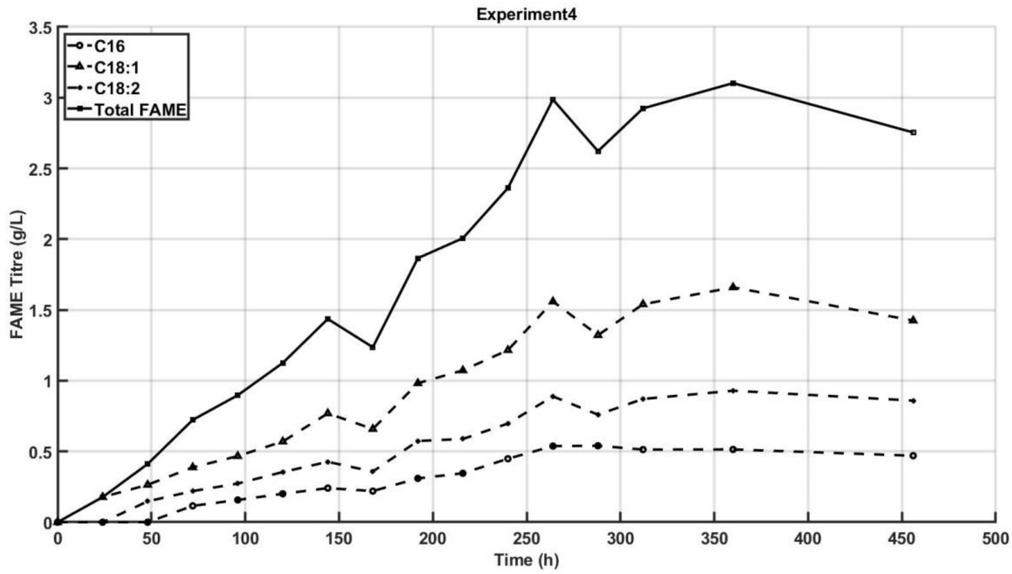

Figure 3.4 Time course profile of FAME concentration for the enzymatic methanolysis of WCO

In this work, the reaction conditions were investigated were a temperature of 32°C, *Cryptococcus diffluens* (D44) lipase with a concentration (wt% by weight of oil) 46 (%w/w), and methanol to WCO molar ratio of 7:1.

It is clear from the figure that enzymatic methanolysis of WCO takes place at a fluctuating rate up to 360 hours and maximum total FAME concentration is reached as 3.1 g/l under this conditions.

Although a relatively high rate methanol was used, inhibition was not observed due to the fact that *C. diffluens* D44 lipase was an organic solvent tolerant lipase (Yılmaz and Sayar, 2015).

When the production of esters are individually examined, the first findings of formation for methyl oleate (C18:1) are detected at 24 hours. However formation of methyl linoleate (C18:2) and methyl palmitate (C16:0) is observed after first 24 and 48 hours, respectively.

For methyl oleate (C18:1) and methyl linoleate (C18:2), while methanolysis reactions take place at an increasing rate till 360 hours, at 168 and 288 hours a slight decrease in concentrations are observed. Maximum individual ester concentrations are quantified as 1.7 and 0.9 g/l at 360 hours, respectively. In addition to that, production of methyl palmitate (C16:0) increases in an almost linear pattern during the reaction and reaches the maximum concentration as 0.6 g/l at 288 hours. However the concentration of methyl palmitate (C16:0) is determined as 0.5 g/l at 360 hours. For this reaction, methyl oleate (C18:1) is the major component of the biodiesel which is followed by methyl linoleate (C18:2) and methyl palmitate (C16:0), respectively. Thus, the change of methyl oleate concentration has the most significant effect on the total FAME concentration.

When the total FAME production between 360 and 456 hours was investigated, a slight decrease in concentration was observed. As a result, the total reaction time was set at 456 hours for this experiment.

3.1.5. Experiment-5

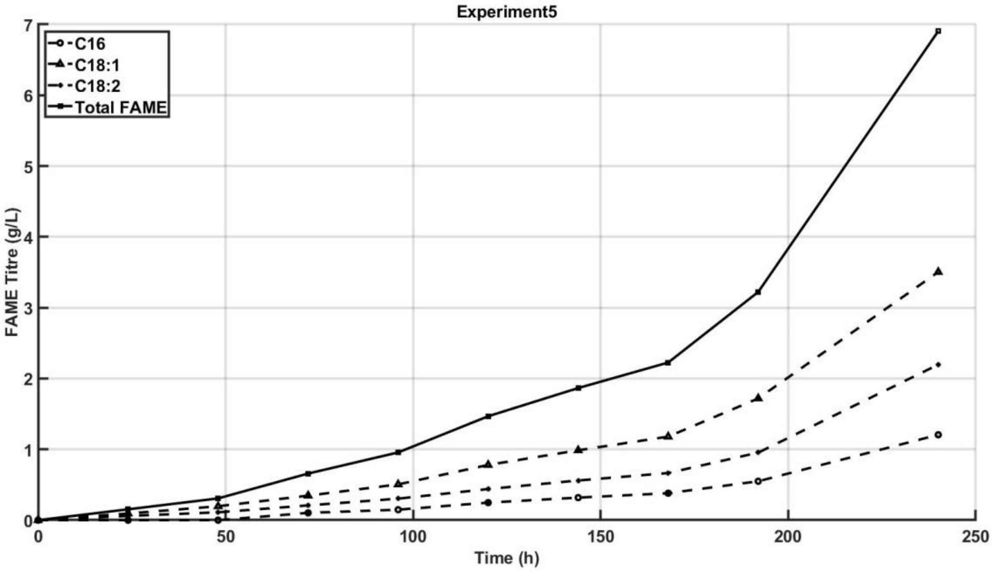

Figure 3.5 Time course profile of FAME concentration for the enzymatic methanolysis of WCO

In this work, the reaction conditions were investigated were a temperature of 53°C, *C. diffluens* (D44) lipase with a concentration (wt% by weight of oil) 28 (%w/w), and methanol to WCO molar ratio of 4:1.

The result of the experiment is shown in Figure 3.5 as the change in FAME concentration with time. It is seen from the figure, the first findings of formation for methyl oleate (C18:1) and methyl linoleate (C18:2) are detected at 24 hours.

Figure 3.5 represents that the FAME production gradually increases with increasing the reaction time. When the production patterns of each ester are examined individually, it is observed that they have all the same behavior. Methyl oleate (C18:1) is the major component which is followed by methyl linoleate (C18:2) and methyl palmitate (C16:0), respectively. Maximum concentrations are quantified as 3.5, 2.2 and 1.2 g/l at 240 hour, respectively. As it is depicted in Figure 3.5 the maximum total FAME concentration is reached as 6.9 g/l at that time.

When the FAME production is investigated between 192 and 240 hours, almost 2-fold increase in concentration is observed. The reason is due to the fact that after a while the temperature will reduce the viscosity of the oil which leads to a sufficient contact at the active site of enzyme surface between the oil and the methanol.

3.1.6. Experiment-6

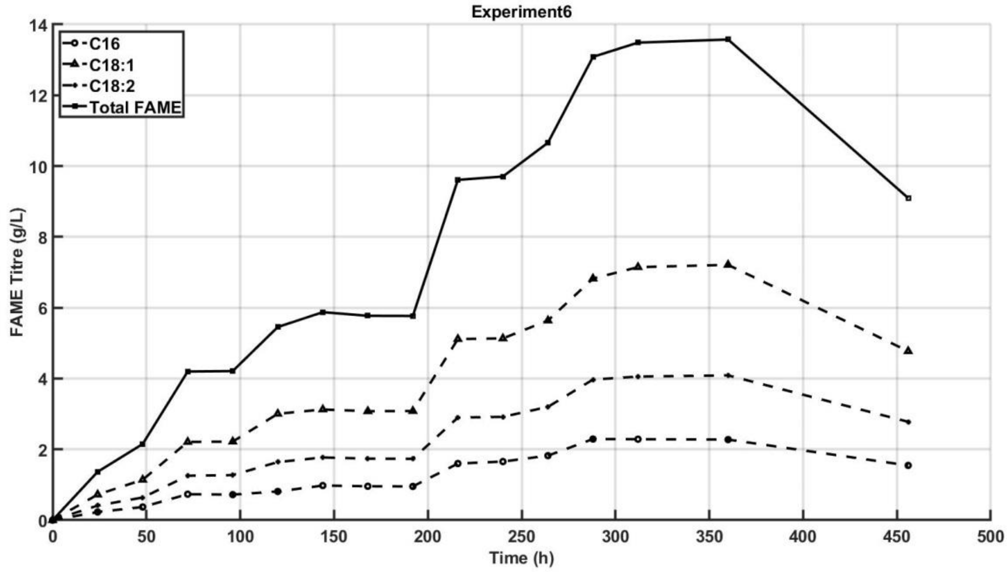

Figure 3.6 Time course profile of FAME concentration for the enzymatic methanolysis of WCO

In this work, the reaction conditions were investigated were a temperature of 53°C, *C. diffluens* (D44) lipase with a concentration (wt% by weight of oil) 46 (%w/w), and methanol to WCO molar ratio of 4:1.

As shown in the figure above, for the first 24 hours all the esters have begun to be produced. The enzymatic methanolysis of WCO fluctuates up to 360 hours and maximum total FAME concentration is reached as 13.6 g/l at that time. Then the total FAME concentration drops drastically from 13.6 g/l to 9.1 g/l. As a result, the total reaction time was set at 456 hours for this experiment.

When the esters were examined individually, the maximum concentration of methyl palmitate (C16:0) was determined as 2.3 g/l at 288 hours, remained constant up to 360 hours and showed an unsignificant decrease with time. However methyl oleate (C18:1) and methyl linoleate (C18:2) showed the almost same pattern with the total FAME production and they were reached the maximum concentrations as 7.2 g/l and 4.1 g/l at 360 hours, respectively. Especially sharp drop in concentration of methyl oleate (C18:1) was observed at 456 hours. For this reaction, methyl oleate (C18:1) is the major component of the biodiesel which is followed by methyl linoleate (C18:2) and methyl palmitate (C16:0), respectively. Thus, the change of methyl oleate concentration has the most significant effect on the total FAME concentration.

3.1.7. Experiment-7

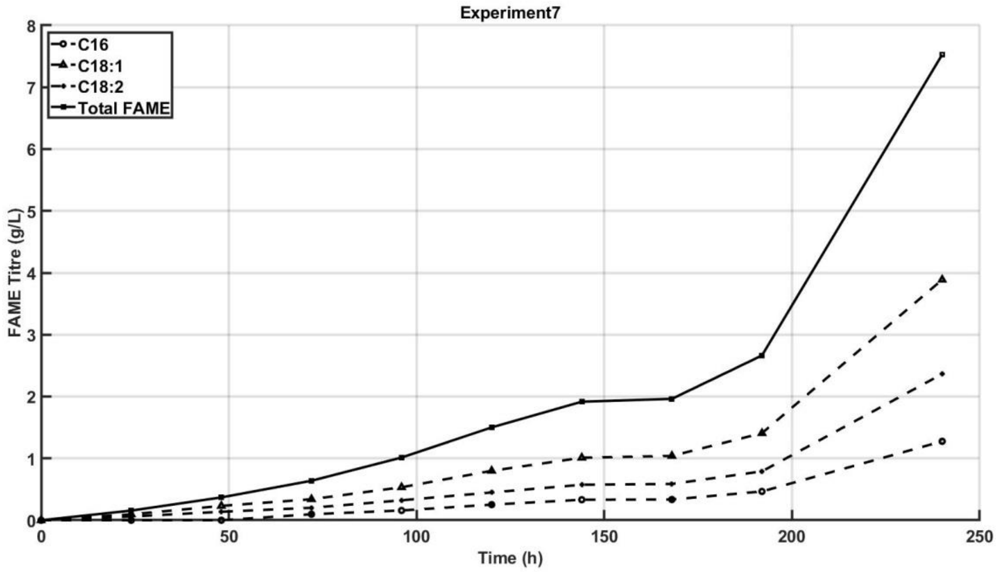

Figure 3.7 Time course profile of FAME concentration for the enzymatic methanolysis of WCO

In this study, the reaction conditions were investigated were a temperature of 53°C, *C. diffluens* (D44) lipase with a concentration (wt% by weight of oil) 28 (%w/w), and methanol to WCO molar ratio of 7:1.

As shown in Figure 3.7 the first findings of formation for methyl oleate (C18:1) and methyl linoleate (C18:2) are detected at 24 hours, whereas this is for methyl palmitate (C16:0) after 24 hours. It is seen from the figure that until 144 hours the FAME production gradually increases with increasing the reaction time. Then it is observed production remains almost constant between 144 and 168 hours. When the FAME production is investigated between 192 and 240 hours, almost 3-fold increase in concentration is observed. The reason is due to the fact that after a while the temperature will reduce the viscosity of the oil which leads to a sufficient contact at the active site of enzyme surface between the oil and the methanol.

When each of the esters are examined individually, it is observed that they all have the same pattern. Methyl oleate (C18:1) is the major component which is followed by methyl linoleate (C18:2) and methyl palmitate (C16:0), respectively. Maximum concentrations are quantified at 240 hours as 3.9, 2.3 and 1.3 g/l, respectively. It shows the maximum total FAME concentration is attained as 7.5 g/l at that time.

3.1.8. Experiment-8

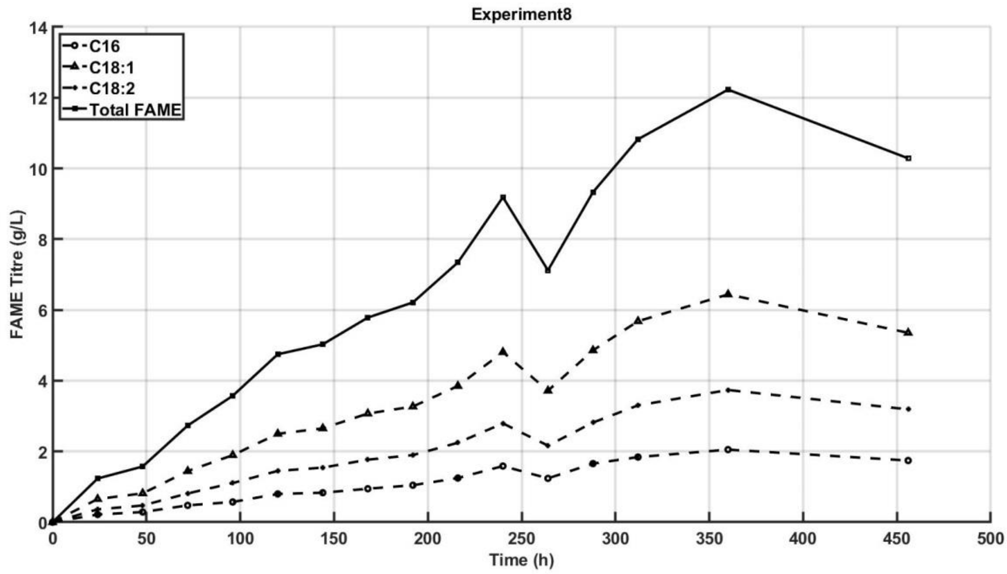

Figure 3.8 Time course profile of FAME concentration for the enzymatic methanolysis of WCO

In this work, the reaction conditions were investigated were a temperature of 53°C, *C. diffluens* (D44) lipase with a concentration (wt% by weight of oil) 46 (%w/w), and methanol to WCO molar ratio of 7:1.

It is clear from the figure that for the first 24 hours all esters have begun to be produced. Figure 3.8 represents that there is an increasing rate in methanolysis reaction until 360 hours. Only a sharp drop in total concentration at 264 hours is observed.

It shows the maximum total FAME concentration is reached as 12.2 g/l at 360 hours under this reaction conditions. After that time, the total FAME concentration drops drastically from 12.2 g/l to 10.2 g/l. As a result, the total reaction time was set at 456 hours for this experiment.

When each esters are examined individually, it is observed that they have all the same behavior. For this reaction, methyl oleate (C18:1) is the major component of the biodiesel resulted from the methanolysis of WCO which is followed by methyl linoleate (C18:2) and methyl palmitate (C16:0), respectively. Thus, the change of methyl oleate yield has the most significant effect on the total ester yield. When each ester concentrations are quantified, it is observed that the maximum values are determined at 360 hours as 6.4, 3.7 and 2.1 g/l, respectively.

3.1.9. Experiment-9

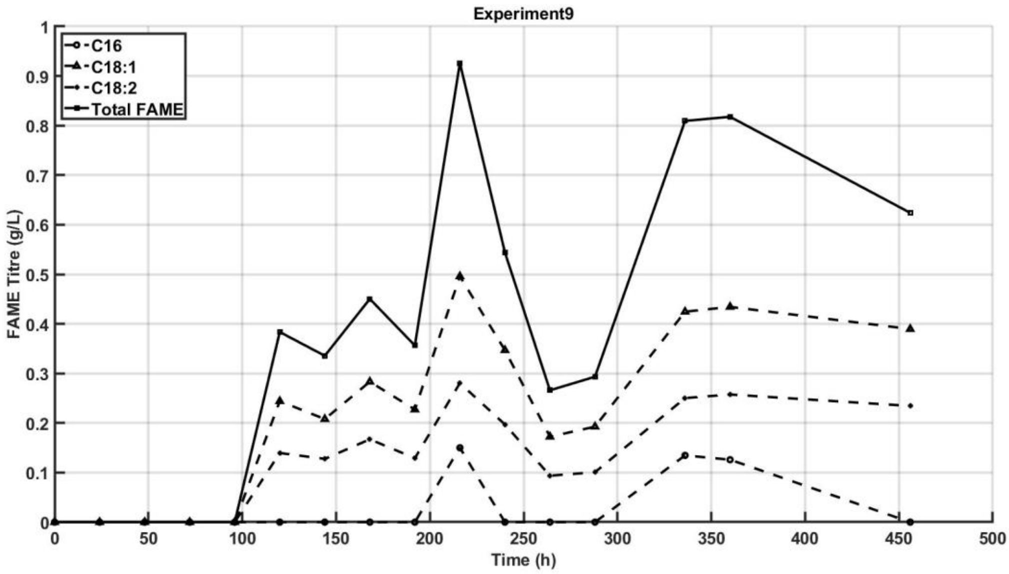

Figure 3.9 Time course profile of FAME concentration for the enzymatic methanolysis of WCO

In this study, the reaction conditions were investigated were a temperature of 25°C, *C. diffluens* (D44) lipase with a concentration (wt% by weight of oil) 32.5 (%w/w), and methanol to WCO molar ratio of 5.50:1.

The result of the experiment is shown in Figure 3.9 as the change in FAME concentration with time. Production of methyl oleate (C18:1) and methyl linoleate (C18:2) are observed after first 120 hours, whereas methyl palmitate (C16:0) is produced in a very small amount only at 216, 336 and 360 hours. It is clear that the low reaction temperature is unsufficient for the enzyme-oil-methanol interaction required to ester production. It shows the maximum total FAME concentration is reached as only 0.9 g/l at 216 hours under this reaction conditions.

3.1.10. Experiment-10

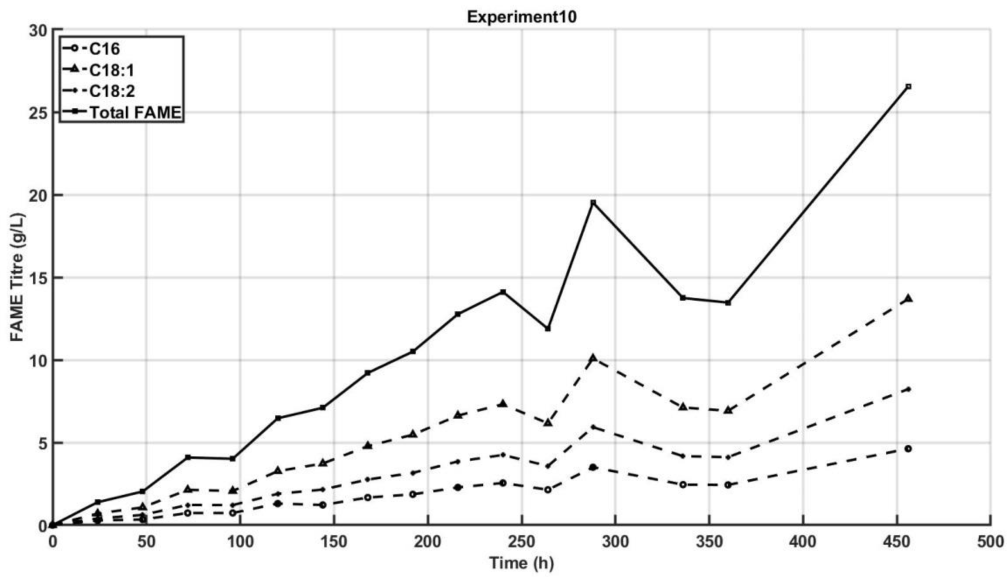

Figure 3.10 Time course profile of FAME concentration for the enzymatic methanolysis of WCO

In this work, the reaction conditions were investigated were a temperature of 60°C, *C. diffluens* (D44) lipase with a concentration (wt% by weight of oil) 32.5 (%w/w), and methanol to WCO molar ratio of 5.50:1.

It is observed from the figure that for the first 24 hours all esters have begun to be produced. As shown in the figure above enzymatic methanolysis of WCO takes place at a fluctuating rate during the reaction and maximum total FAME concentration is reached as 26.5 g/l at 456 hours.

As the total FAME production is investigated, the reaction takes place at an almost linear rate up to 240 hours whereas a slight decrease in concentrations are observed at 264 hours. After that time, the total FAME concentration attains from 12 g/l to 19.5 g/l at 288 hours. While the production remains almost constant between 336 and 360 hours, then it rises substantially and almost 2-fold increase in concentration from 13.5 g/l to 26.5 g/l is observed. The reason is due to the fact that after a while the temperature will reduce the viscosity of the oil which leads to a sufficient contact at the active site of enzyme surface between the oil and the methanol.

When each esters are examined, it is observed that they have all the same behavior. For this reaction, methyl oleate (C18:1) is the major component of the biodiesel resulted from the methanolysis of WCO which is followed by methyl linoleate (C18:2) and methyl palmitate (C16:0), respectively. When each individual ester concentrations are quantified, it is observed that the maximum values are determined at 456 hour as 13.7, 8.2 and 4.6 g/l, respectively.

3.1.11. Experiment-11

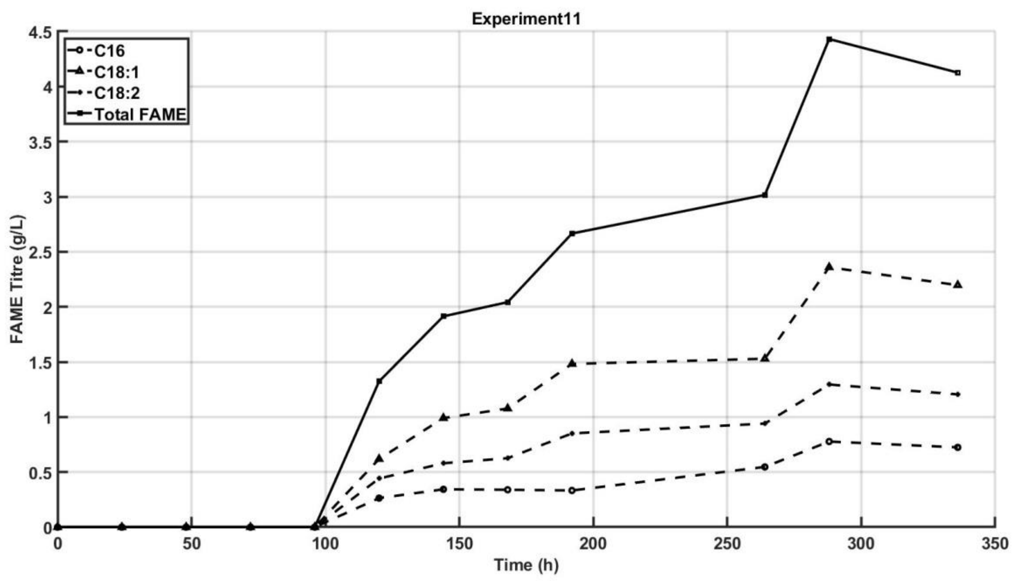

Figure 3.11 Time course profile of FAME concentration for the enzymatic methanolysis of WCO

In this work, the reaction conditions were investigated were a temperature of 42.5°C, *C. diffluens* (D44) lipase with a concentration (wt% by weight of oil) 55 (%w/w), and methanol to WCO molar ratio of 3:1.

Figure 3.11 represents that no ester production is observed for the first 96 hours. It is known the enzyme-oil-methanol interaction starts after a certain time caused by the stirring effect and temperature. Under this reaction conditions, the enzyme-oil-methanol interaction takes at least 96 hours to start the ester production because of the relatively low methanol concentration. It shows there is an increasing rate in methanolysis reaction until 288 hours and the maximum total FAME concentration is observed as 4.4 g/l. After that time, total FAME concentration slightly drops from 4.4 g/l to 4.1 g/l due to a lack of substrate for the enzyme. As a result, the total reaction time was set at 336 hours for this experiment.

For this reaction, methyl oleate (C18:1) is the major component of the biodiesel resulted from the methanolysis of WCO which is followed by methyl linoleate (C18:2) and methyl palmitate (C16:0), respectively. Thus, the change of methyl oleate yield has the most significant effect on the total ester yield. When each individual ester concentrations are quantified, the maximum values are determined at 288 hour as 2.4, 1.3 and 0.7 g/l, respectively.

3.1.12. Experiment-12

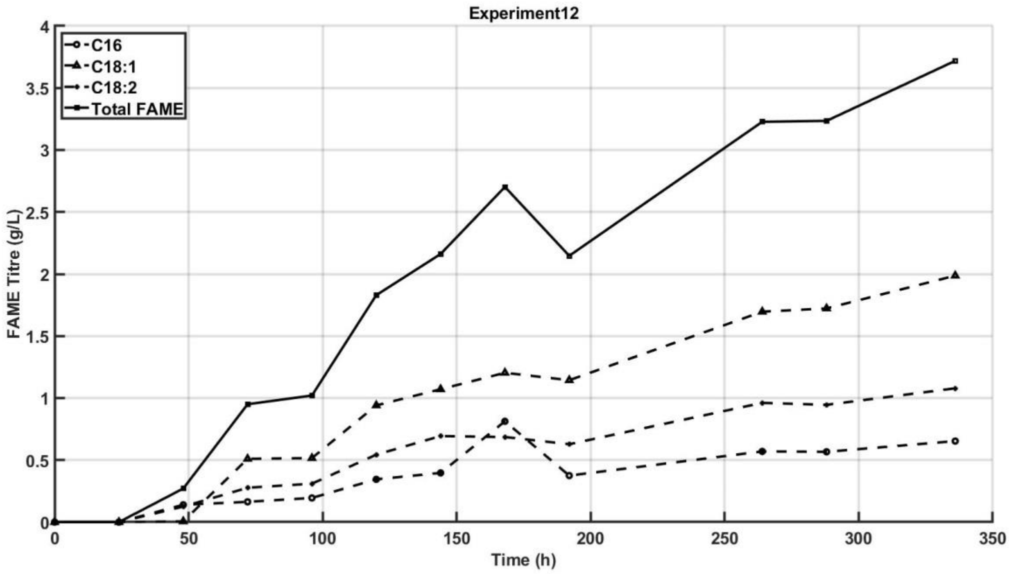

Figure 3.12 Time course profile of FAME concentration for the enzymatic methanolysis of WCO

In this work, the reaction conditions were investigated were a temperature of 42.5°C, *C. diffluens* D44 lipase with a concentration (wt% by weight of oil) 55 (%w/w), and methanol to WCO molar ratio of 8:1.

Figure 3.12 represents that no ester production is observed for the first 24 hours. Under this reaction conditions, the enzyme-oil-methanol interaction takes at least 24 hours to start the ester production. After first 24 hours, methyl palmitate (C16:0) and methyl linoleate (C18:2) are both produced as 0.1 g/l whereas production of methyl oleate (C18:1) is not significant.

Although we used relatively high amount of methanol, inhibition was not observed during the reactions due to the fact that *C. diffluens* D44 lipase was an organic solvent tolerant lipase.

The enzymatic methanolysis of WCO takes place at an increasing rate until 336 hours and it shows the maximum total FAME concentration is reached as 3.7 g/l at the same time. Only a sharp drop in concentration is observed at 192 hour, which is due to behaviour of methyl palmitate (C16:0).

When each esters are examined individually, it is observed that methanolysis reactions for methyl oleate (C18:1) and methyl linoleate (C18:2) take place at an almost linear pattern during the reaction and maximum concentrations are quantified as 2.0 g/l and 1.1 g/l at 336 hours, respectively. Unlike this, production of methyl palmitate (C16:0) has a different behaviour. The maximum concentration for methyl palmitate (C16:0) is determined as 0.8 g/l at 168 hours. Especially a sharp drop in concentration of methyl palmitate (C16:0) is observed at 192 hours.

Although for this reaction methyl oleate (C18:1) is the major component of the biodiesel which is followed by methyl linoleate (C18:2) and methyl palmitate (C16:0), the production pattern of total FAME is the same with methyl palmitate (C16:0).

3.1.13. Experiment-13

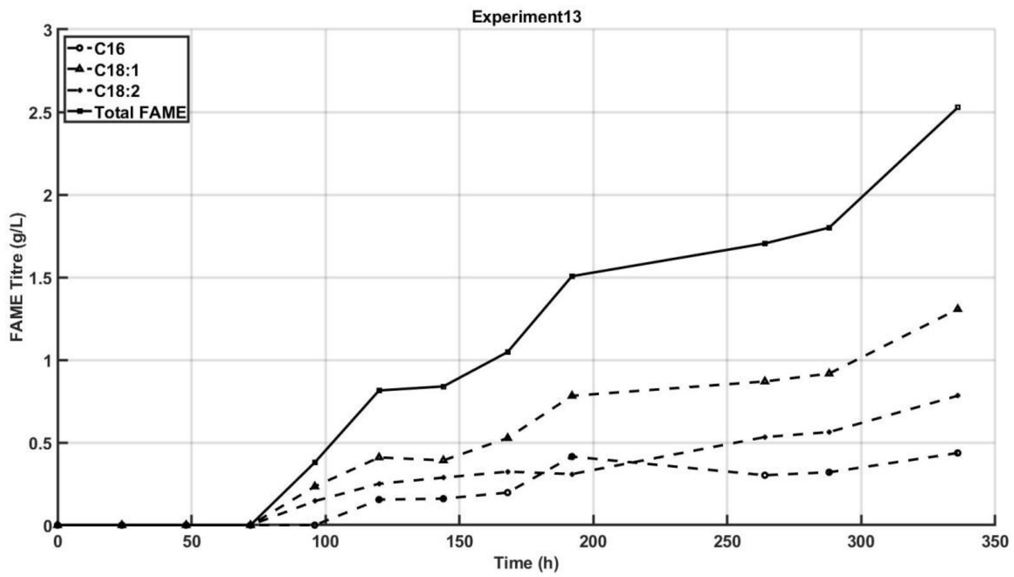

Figure 3.13 Time course profile of FAME concentration for the enzymatic methanolysis of WCO

In this work, the reaction conditions were investigated were a temperature of 42.5°C, *C. diffluens* (D44) lipase with a concentration (wt% by weight of oil) 10 (%w/w), and methanol to WCO molar ratio of 5.5:1.

It is seen from the figure that for the first 72 hours any ester production is not observed. In this reaction conditions, the enzyme-oil-methanol interaction takes at least 72 hours to start the ester production. The first findings of ester formation for methyl oleate (C18:1) and methyl linoleate (C18:2) are observed after 72 hours whereas this is for methyl palmitate (C16:0) after 96 hours.

When the total FAME production pattern is examined, it is observed that there is an increasing rate in methanolysis reaction with time. It shows the maximum total FAME concentration is attained as 2.5 g/l at 336 hours under this conditions.

When production pattern of each esters are investigated individually, it is observed that methyl oleate (C18:1) and methyl linoleate (C18:2) have almost the same behaviour like total FAME pattern whereas methyl palmitate (C16:0) has different. Methanolysis reaction for methyl palmitate (C16:0) fluctuates during the reaction which is due to analytical measurement.

For this reaction, methyl oleate (C18:1) is the major component of the biodiesel resulted from the methanolysis of WCO which is followed by methyl linoleate (C18:2) and methyl palmitate (C16:0), respectively. When each ester concentrations are quantified, it is observed that the maximum values are determined at 336 hours as 1.3, 0.8 and 0.4 g/l, respectively.

3.1.14. Experiment-14

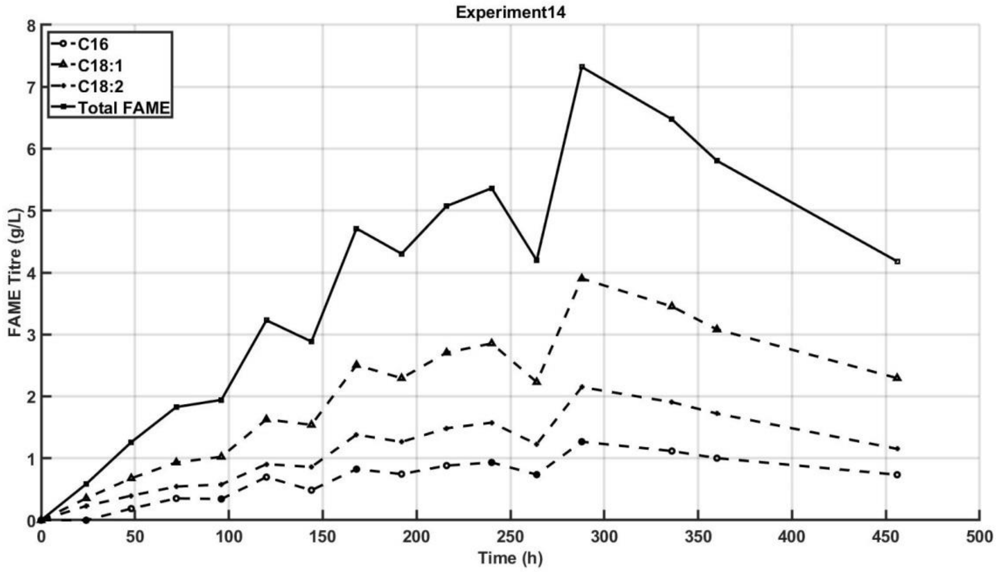

Figure 3.14 Time course profile of FAME concentration for the enzymatic methanolysis of WCO

In this work, the reaction conditions were investigated were a temperature of 42.5°C, *C. diffluens* (D44) lipase with a concentration (wt% by weight of oil) 55 (%w/w), and methanol to WCO molar ratio of 5.5:1.

It is seen from the figure, the first findings of ester formation for methyl oleate (C18:1) and methyl linoleate (C18:2) are observed at 24 hours whereas this is at 48 hours for methyl palmitate (C16:0).

Figure 3.14 represents that the reaction takes place at a fluctuating rate up to 288 hours and the maximum total FAME concentration is reached as 7.3 g/l at that time. Then the total FAME concentration gradually decreases with increasing the reaction time due to a lack of substrate for the enzyme. As a result, the total reaction time was set at 456 hours for this experiment.

When the total FAME production is investigated between 264 and 288 hours, almost 2-fold increase in total concentration is observed. The reason is due to the fact that after a while the temperature will reduce the viscosity of the oil which leads to a sufficient contact at the active site of enzyme surface between the oil and the methanol.

When each esters are examined individually, it is observed that they have all the same pattern. For this reaction, methyl oleate (C18:1) is the major component of the biodiesel resulted from the methanolysis of WCO which is followed by methyl linoleate (C18:2) and methyl palmitate (C16:0), respectively. When each individual ester concentrations are quantified, the maximum values are determined at 288 hours as 3.9, 2.1 and 1.3 g/l, respectively.

3.1.15. Experiment-15

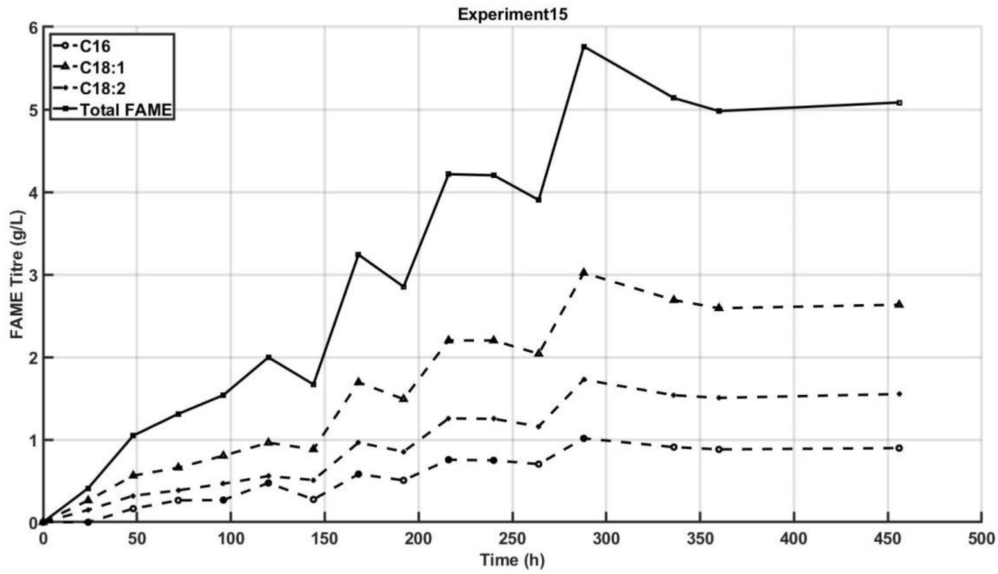

Figure 3.15 Time course profile of FAME concentration for the enzymatic methanolysis of WCO

In this work, the reaction conditions were investigated were a temperature of 42.5°C, *C. diffluens* D44 lipase with a concentration (wt% by weight of oil) 32.5 (%w/w), and methanol to WCO molar ratio of 5.5:1.

Figure 3.15 represents that the first findings of ester formation for methyl oleate (C18:1) and methyl linoleate (C18:2) are obtained at 24 hours whereas this is at 48 hours for methyl palmitate (C16:0). The reaction takes place at a fluctuating rate until 288 hours and the maximum total FAME concentration is reached as 5.8 g/l at this time. After that, the total FAME concentration drops slightly from 5.8 g/l to 5.1 g/l. As a result, the total reaction time was set at 456 hours for this experiment.

When each esters are examined individually, it is observed that they all have the same pattern. For this reaction, methyl oleate (C18:1) is the major component of the biodiesel resulted from the methanolysis of WCO which is followed by methyl linoleate (C18:2) and methyl palmitate (C16:0), respectively. Maximum concentrations are quantified at 288 hours as 3.1, 1.7 and 1.0 g/l, respectively.

3.1.16. Experiment-16

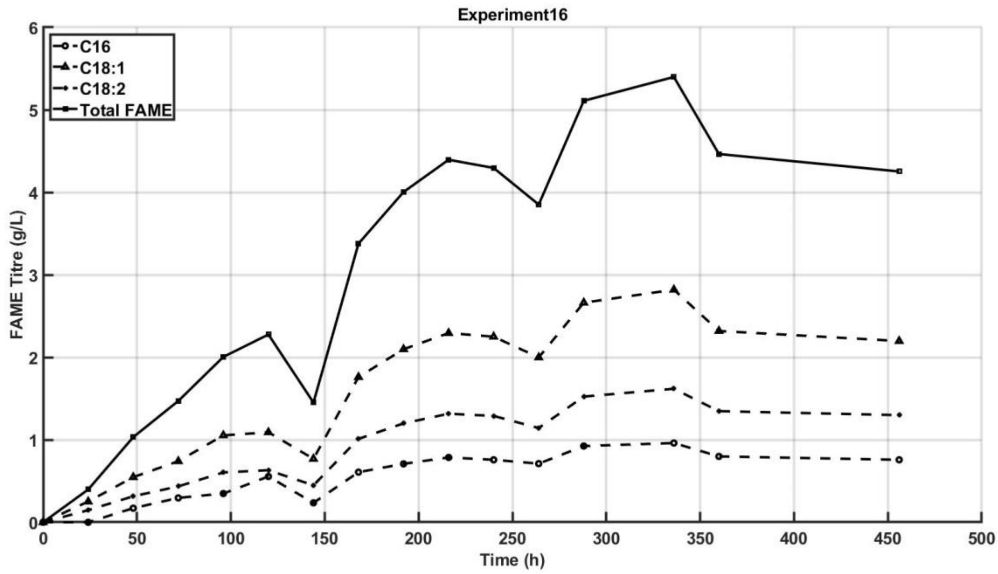

Figure 3.16 Time course profile of FAME concentration for the enzymatic methanolysis of WCO

In this work, the reaction conditions were investigated were a temperature of 42.5°C, *C. diffluens* (D44) lipase with a concentration (wt% by weight of oil) 32.5 (%w/w), and methanol to WCO molar ratio of 5.5:1.

It is presented in the Figure 3.16 that the first findings of ester formation for methyl oleate (C18:1) and methyl linoleate (C18:2) are obtained at 24 hours whereas this is at 48 hours for methyl palmitate (C16:0).

It is clear from the figure that there is an increasing rate in methanolysis reaction till 120 hours. After that time the reaction fluctuates up to 336 hours which may be due to analytical measurement and the maximum total FAME concentration is reached as 5.4 g/l at this time. Then total FAME concentration diminishes drastically from 5.4 g/l to 4.5 g/l due to a lack of substrate for the enzyme. It shows the decreasing in concentration continues and the total FAME concentration is quantified as 4.3 g/l at 456 hours as a result the total reaction time was set at 456 hours for this experiment.

When each esters are examined individually, it is observed that they all have the same pattern. For this reaction, methyl oleate (C18:1) is the major component of the biodiesel resulted from the methanolysis of WCO which is followed by methyl linoleate (C18:2) and methyl palmitate (C16:0), respectively. Maximum concentrations are quantified at 336 hours as 2.8, 1.6 and 1.0 g/l, respectively.

The results for two process metrics for all experiments are summarized in Table 3.1.

Table 3.1 FAME Titers and Productivities

Run	**FAME Titer (g/l)**	**Productivity (g/l h)**
1	2.5	0.015
2	5.1	0.014
3	1.9	0.012
4	3.1	0.009
5	6.9	0.029
6	13.6	0.038
7	7.5	0.031
8	12.2	0.034
9	0.9	0.004
10	26.5	0.058

Table 3.1 continued

Run	FAME Titer (g/l)	Productivity (g/l h)
11	4.4	0.015
12	3.7	0.011
13	2.5	0.008
14	7.3	0.025
15	5.8	0.020
16	5.4	0.016

3.2. Modelling and Optimization

3.2.1. Modelling

3.2.1.1. Model Evaluation

A statistical comparison of the two modelling methods were made using the R^2, RMSE, adj_R^2, f_stat and p_value values of the models. Table 3.1-3.3 summarize these values for the 3 models generated. Tables for all of the 48 models are presented in the appendix A part.

Table 3.2 Model-21

Estimated model parameter values		Goodness of fit	
$\boldsymbol{\beta_0}$	-1.884	R^2	0.707
$\boldsymbol{\beta_1}$	0.004	adj_R^2	0.696
$\boldsymbol{\beta_2}$	-0.074	$RMSE$	0.312
$\boldsymbol{\beta_3}$	0.025	f_stat	63.5
$\boldsymbol{\beta_4}$	0.771	p_value	4.81e-52
$\boldsymbol{\beta_5}$	-8.4511e-06		
$\boldsymbol{\beta_6}$	0.001		
$\boldsymbol{\beta_7}$	-0.0001		
$\boldsymbol{\beta_8}$	-0.071		

Model 21 pure quadratic model based on large data set for C16:0 productivity with an R^2 value of 0.707 and adj_R^2 value of 0.696 is the only model amongest the 48 models that are generated with R^2 and adj_R^2 values below 0.7. It shows that two modelling approaches both have resulted in a significant success. In addition to this, it is observed that among the all models, 28 of them are generated with R^2 and adj_R^2 values of above 0.95 whereas only 12 of them are generated with R^2 and adj_R^2 values of below 0.85.

Overall, R^2 and adj_R^2 values of the Kriging model is better than those of the low-order polynomial models.

The quality of the model fitness is verified by the R^2. The high value of R^2 indicates that the obtained statistical model had a good correlation with experimental data and the p-value indicates the probability of error and it is used to check the significance of each regression coefficient.

The Model 36 Kriging model based on small data set for total FAME titer, is the best performing model amongst the 48 models generated, with an R^2 value of 1, the adjusted adj_R^2 value of 1 and a very small p-value (3.3375e-150). It shows that the model is highly significant and sufficient to represent the actual relationship between the response and the input variables.

Table 3.3 Model-36

Estimated model parameter values		**Goodness of fit**	
$\boldsymbol{\alpha}$	-0.2343	R^2	1
$\boldsymbol{\theta_1}$	0.0891	adj_R^2	1
$\boldsymbol{\theta_2}$	0.3364	$RMSE$	1.5992e-10
$\boldsymbol{\theta_3}$	0.0250	f_stat	5.8169e+27
$\boldsymbol{\theta_4}$	0.0667	p_value	3.3375e-150

Although, Model 11 has the worst p-value (0.0424) which is still an acceptable value, this model is generated with an R^2 value of 1 and an adj_R^2 value of 0.997.

Although, Model 21 has significant p-value (4.81e-52), the model is generated with an R^2 value of 0.707 and an adj_R^2 value of 0.696.

As a result, from the point of view of p-value, Model 11 is the the lowest performing model with p- value of (0.0424). On the other hand from the point of view of R^2 and adj_R^2 values, Model 21 is the lowest performing model with the lower R^2 and adj_R^2 value.

Table 3.4 Model-11

Estimated model parameter values		Goodness of fit	
$\boldsymbol{\beta_0}$	62.455	R^2	1
$\boldsymbol{\beta_1}$	-22.064	adj_R^2	0.997
$\boldsymbol{\beta_2}$	27.315	$RMSE$	21.9
$\boldsymbol{\beta_3}$	-1.995	f_stat	341
$\boldsymbol{\beta_4}$	790.930	p_value	0.0424
$\boldsymbol{\beta_5}$	0.391		
$\boldsymbol{\beta_6}$	0.392		
$\boldsymbol{\beta_7}$	0.299		
$\boldsymbol{\beta_8}$	-2.610		
$\boldsymbol{\beta_9}$	0.434		
$\boldsymbol{\beta_{10}}$	-4.650		
$\boldsymbol{\beta_{11}}$	-0.014		
$\boldsymbol{\beta_{12}}$	-0.296		
$\boldsymbol{\beta_{13}}$	0.337		
$\boldsymbol{\beta_{14}}$	-67.118		

It is observed that, when the p-values of the 48 models are considered, except for between Model 9 and Model 16 (tables are presented in the appendix), the p-values are usually significantly low. Although the p-values are still below 0.05 for the mentioned models above, they are found to be too high to compare with the other models.

Overall, in terms of model structure the order of conformity for the system is as follows; Kriging is most appropriate, Quadratic and Pure quadratic are less convenient. This result depends on the fact that since the system is very complex and highly non-linear, consequently the pure-quadratic structure, which has the simplest mathematical structure, is seen as the most inappropriate model.

For Kriging model structure, there are actually two different approaches between small data sets and large data sets when the system is modelled. As mentioned above the small data set contains 16 points whereas the large data set contains all of the 220 data points. When the large data set is used, firstly it is observed that since the number of observations increases, the degrees of freedom increases. Secondly, there is a physical change of behavior. When the time course data is considered, the dynamic behavior becomes a concern and the dynamic feature of the system is accounted. When dynamic behavior is considered, R^2 and adj_R^2 values of Kriging model show a decline of about

10%. Model 40 Kriging model based on small data set for total FAME productivity is generated with an R^2 and an adj_R^2 values of both 1 whereas Model 48 model based on large data set for total FAME productivity is generated with an R^2 value of 0.8843 and an adj_R^2 value of 0.8822 (tables are presented in the appendix). The p-values of the models based on large data set for productivity models show an increase nearly one order of magnitude whreras it is not valid for titer models. Although the f_stat values of the models based on large data set for productivity is about 300, it is around 1000 for titer models. Moreover, R^2 and adj_R^2 values of the Kriging model based on large data set for productivity are observed to be between 0.85 and 0.9. It can be seen that from all observations, Kriging models based on large data set for productivity metrics underperform compared to the Kriging models based on large data set for titer metrics. But the resulting R^2, adj_R^2, p-value and f_stat values are indicative of acceptable model fit with the experimental data.

When the large data set is used instead of the small data set, the same underperfoming is observed in low order polynomials as in Kriging models due to dynamic behaviour. However, while the decreasing for Kriging models does not affect the accuracy of the model whereas in low order polynomial models it significantly affects because of the questionable R^2 and adj_R^2 values. It is observed that R^2 and adj_R^2 values of the low-order polynomial models for large data set are around 75%. It is seen that the R^2 and adj_R^2 values of pure-quadratic models is around %70 which is the main reason that affects accuracy for underperforming in low-order polynomial models.

Overall, the Kriging model is the best performing model amongst the 48 models generated.

Using large data set instead of small data set has an effect on the performance of the models which is explained by average p-values. Although the average R^2 and adj_R^2 values decreases dramatically from %99 to %81 when using large data set, it is observed that the average p-values of large data set (1.77E-51) are more significant. But average p-values of small data set (6.96E-03) has still an acceptable value.

The average R^2 and adj_R^2 values of FAME titer metrics for Kriging and Quadratic models are more significant than the productivity metrics of the same models whereas no significant change is observed for Pure Quadratic models. Overall, FAME titer models perform slightly better than productivity models when the R^2 and adj_R^2 values are considered.

3.2.1.2. Simulation Experiments

An important conclusion to be made with the models generated is to examine the performance of the models to simulate the physical experiments in order to evaluate the performance of the models. From engineering point of view, the Total FAME titer and its productivity are the most interested metrics. In this section, a comparison of simulation and observed value of these metrics is given as an example and comparison of these metrics of all models will be given in appendix part. In this comparison, the simulations of the experiments are compared to the actual values of the experiments along with the comparison of the models. Experiment 10 and 6 are chosen as the highest performing experiments in terms of both titer and productivity whereas Experiment 2 is chosen as relatively low performing experiment.

It is obvious that for the experiments mentioned above, models generated using large data set are much more realistic to simulate experimental progress. In all cases, Pure-quadratic, Quadratic and Kriging models deviate from actual values, especially in early periods of reaction.

This deviation is severe in low-order polynomial models based small data sets. On the other hand, for the Kriging, the deviation with models based on small data sets are worse than models based on large data sets but it is not as severe as in low-order polynomial models.

This might be due to the fact that the values that belong to the small data set are usually obtained at the in late periods of reaction where highest FAME titers are observed.

Kriging does not deviate as much as low order polynomial in small data set bacause of the zero order polynomial regression part. This explains that this structure of Kriging is better for the system. Especially with the data obtained at the end of the reactions and less data, Kriging provides a successful progress. As a result the ultimate goal is to minimize the number of experiments and obtain as much information as possible from these fewer experiments.

The advantage of Kriging to low-order polynomial is that it can acquire more information with less experiment. When using small data sets, Kriging gives less deviation than low-order polynomials. With less data set Kriging does not give much deviation as low-order polynomial. Using Kriging also helps to minimize the number of experiments. Again, in all three experiments, this acceptability of Kriging is valid for both Total FAME titer and productivity. When the number of experiments is reduced, there is a loss of information in low order polynomials. This is not as much in Kriging. More information about the system is obtained with less data in Kriging.

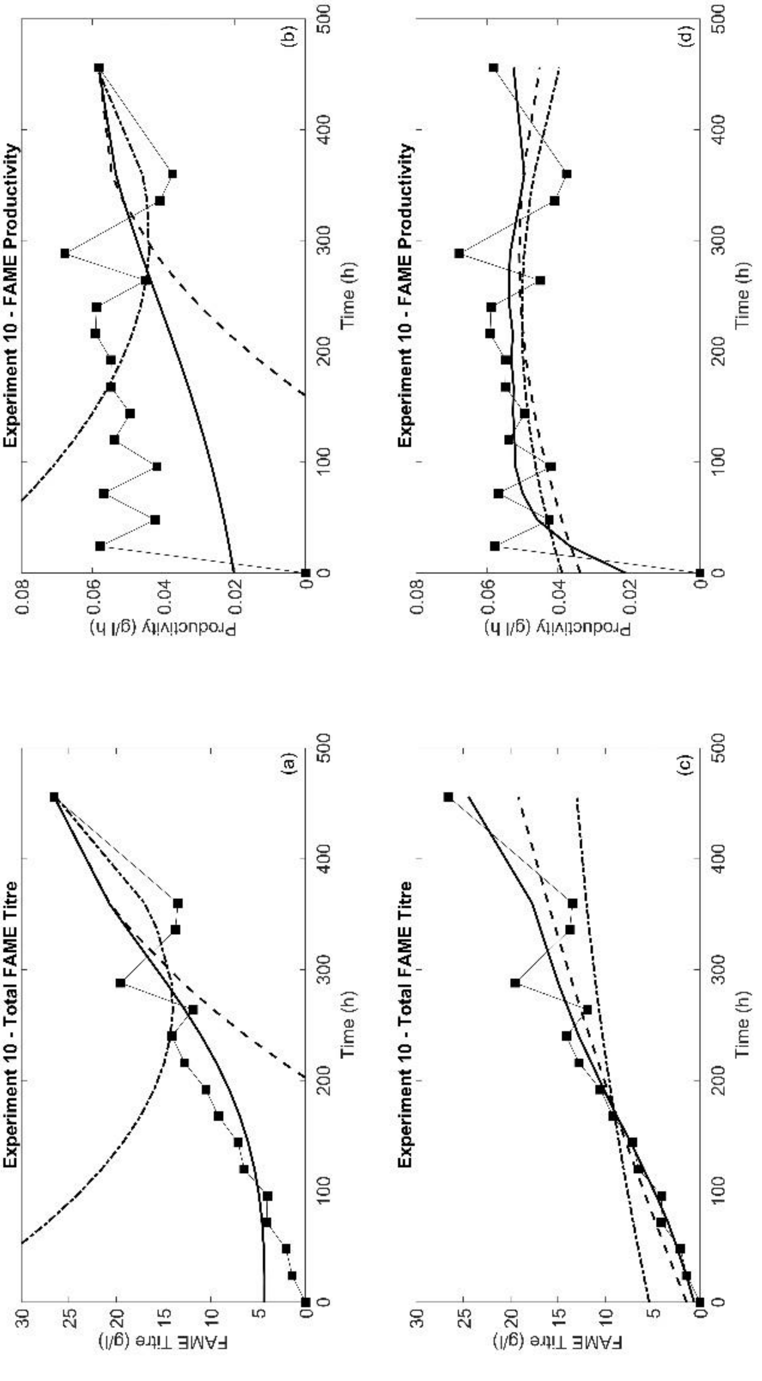

Figure 3.17 Experiment 10

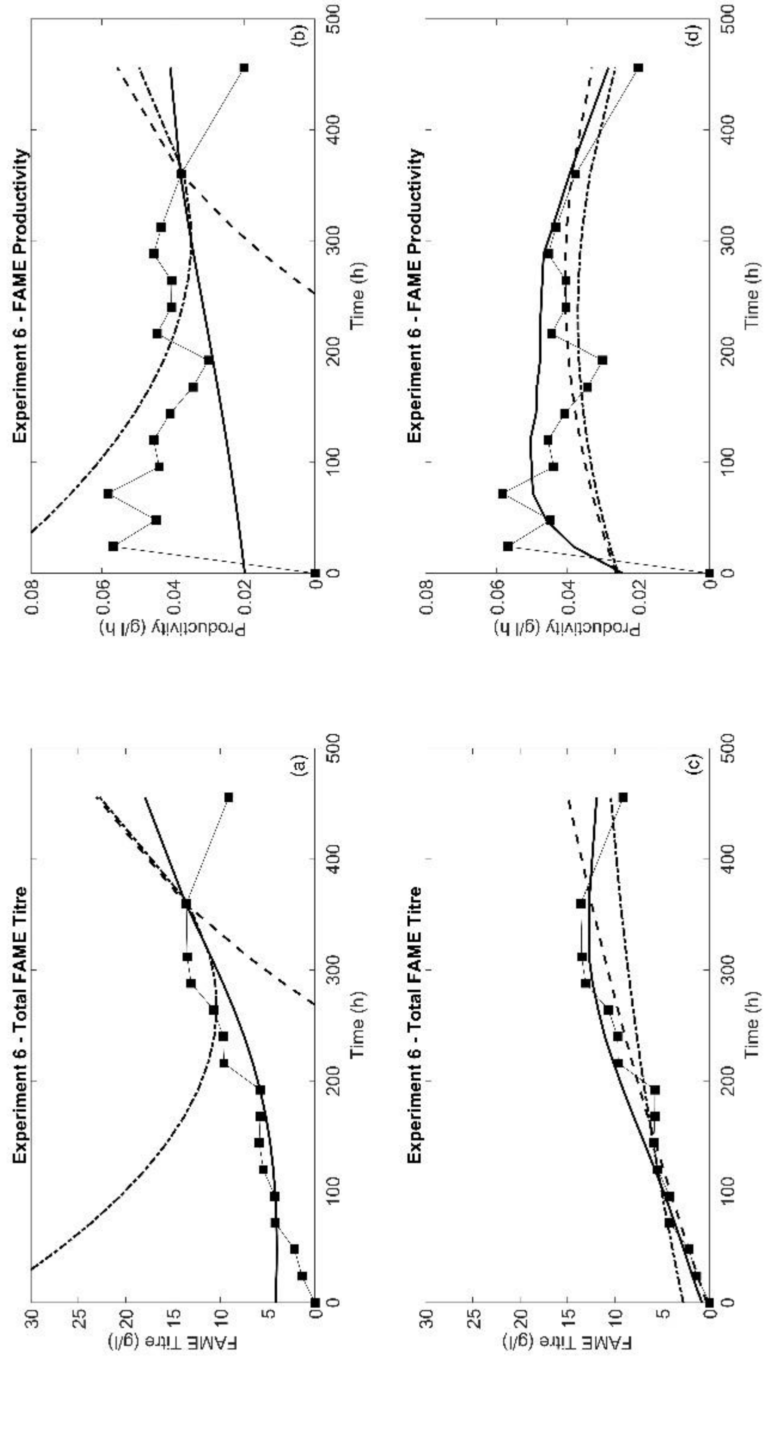

Figure 3.18 Experiment 6

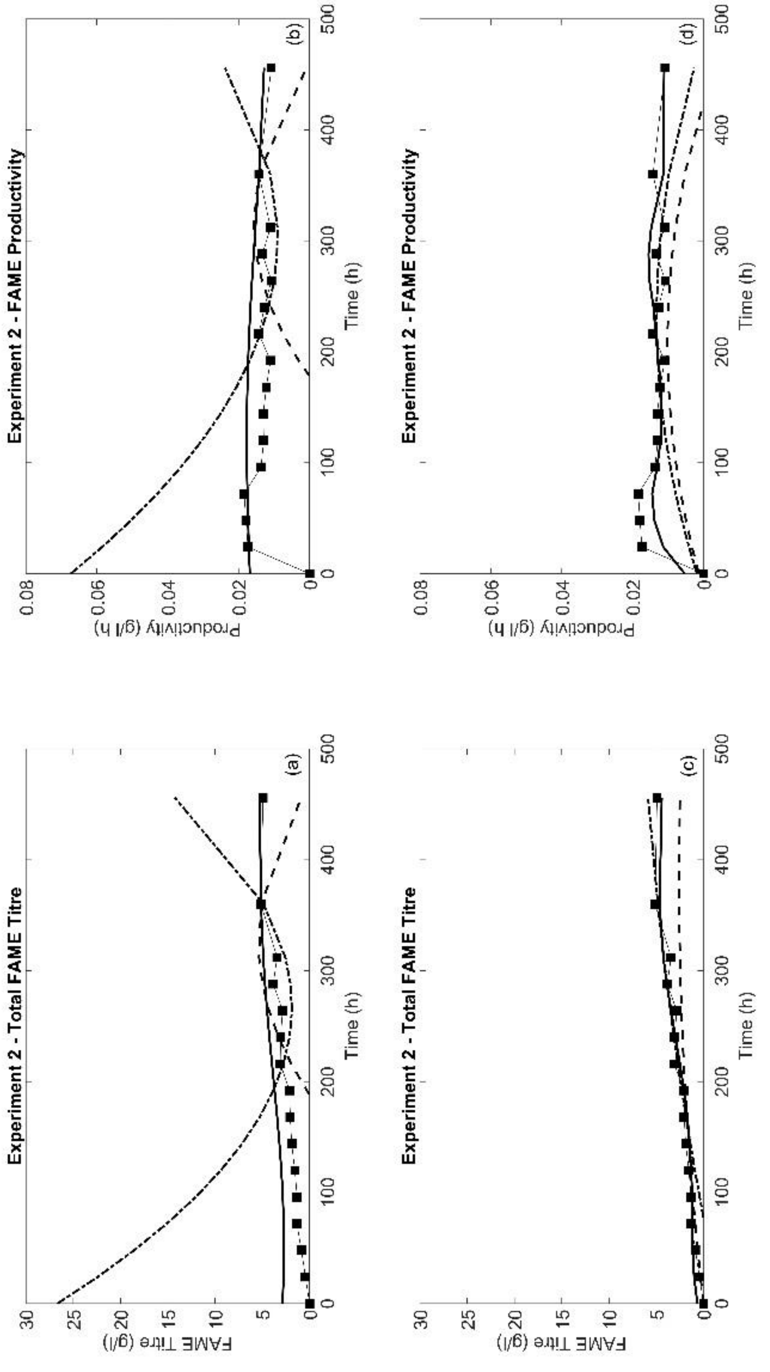

Figure 3.19 Experiment 2

3.2.2. Optimization

3.2.2.1. Single objective optimization

For low-order polynomial in all cases, except productivity optimization with the Quadratic model based on small data set, maximum amount of crude enzyme is required for maximized metrics. In the exceptional case, crude enzyme is required at a level of 10% by weight of oil for optimal metrics. In other case, optimization with Kriging model, there is a distribution from 10 to 55% in terms of crude enzyme to oil ratio (wt%). Since the Kriging model is an interpolation technique, the points between 10 and 55% can be detailed.

Table 3.5 Single-objective optimization results

Model type	Time (h)	Temperature (℃)	E:O	A:O	Opt value
1	30	60	55.00	5.25	6.42 g/l
2	30	60	55.00	5.26	18.97 g/l
3	30	60	55.00	5.26	11.24 g/l
4	30	60	55.00	5.26	183.17 g/l
5	30	60	55.00	5.23	0.02 g/l h
6	30	60	55.00	5.26	0.05 g/l h
7	30	60	55.00	5.24	0.03 g/l h
8	30	60	55.00	5.25	0.49 g/l h
9	500	60	55.00	5.29	7.23 g/l
10	500	60	55.00	5.28	23.70 g/l
11	500	60	55.00	5.30	13.33 g/l
12	500	60	55.00	5.29	221.34 g/l
13	150	60	10.00	5.95	0.02 g/l h
14	146	60	10.00	6.04	0.07 g/l h
15	105	60	10.00	5.92	0.04 g/l h
16	136	60	10.00	5.99	0.62 g/l h
17	500	60	55.00	5.33	2.51 g/l
18	500	60	55.00	5.26	7.59 g/l

Table 3.5 continued

Model type	Time (h)	Temperature (℃)	E:O	A:O	Opt value
19	500	60	55.00	5.26	4.42 g/l
20	500	60	55.00	5.27	72.60 g/l
21	238	60	55.00	5.43	0.01 g/l h
22	230	60	55.00	5.37	0.03 g/l h
23	232	60	55.00	5.37	0.02 g/l h
24	232	60	55.00	5.38	0.30 g/l h
25	500	60	55.00	4.62	3.88 g/l
26	500	60	55.00	4.47	11.91 g/l
27	500	60	55.00	4.51	6.89 g/l
28	500	60	55.00	4.51	113.41 g/l
29	263	60	55.00	5.42	0.01 g/l h
30	265	60	55.00	5.32	0.04 g/l h
31	264	60	55.00	5.39	0.02 g/l h
32	264	60	55.00	5.36	0.34 g/l h
33	500	60	34.02	5.13	4.87 g/l
34	500	60	39.58	4.87	14.40 g/l
35	500	60	34.59	5.20	8.55 g/l
36	499	60	33.93	5.12	136.96 g/l
37	482	60	42.42	5.10	0.01 g/l h
38	463	60	42.11	4.93	0.03 g/l h
39	471	60	40.50	4.90	0.02 g/l h
40	468	60	41.06	4.95	0.30 g/l h
41	499	60	14.12	7.92	6.41 g/l
42	500	60	10.88	7.99	19.57 g/l
43	500	60	10.42	5.11	10.65 g/l
44	500	60	11.66	8.00	184.06 g/l
45	58	60	54.39	3.96	0.02 g/l h
46	52	60	55.00	3.14	0.06 g/l h
47	500	50	10.09	7.73	0.04 g/l h

Table 3.5 continued

Model type	Time (h)	Temperature (℃)	E:O	A:O	Opt value
48	500	60	11.40	8.00	0.61 g/l h

For Kriging model in all cases, except Model 45 and 46, longest reaction times (500 h) are required to obtain high metrics. In exceptional case, the reaction times are required around 60 h. In low order polynomials, there is a distribution between 30 and 500 hours.

When titer versus producitivity are considered, in all cases, except Model 1 to 4, longest reaction times (500 h) are required to obtain high titer metrics.

From a different viewpoint, methanol to oil molar ratio which shows the greatest variability from 3.96 to 8.00 in terms of optimum points. This can be explained by the fact that firstly, the methanol to oil molar ratio compared to other input variables has an effect that physically increases the non-linearity on the system. Secondly, especially the methanol to oil molar ratio shows such a large oscillation, since the Kriging model is an interpolation technique, it captures the nonlinearity better and observes more clearly.

From engineering point of view, the Total FAME titer and its productivity are the most interested metrics. The maximum Total FAME titer and the productivity are observed with Quadratic model based on small data optimization set as 221.34 g/l and 0.62 g/l h, respectively. Conditions as follows; for Total FAME titer t=500 h, T=60℃, E:O=55% and A:O=5.29. For the productivity; t=136 h, T=60℃, E:O=10% and A:O=5.99.

Compared to low-order polynomial optimization, the maximum Total FAME titer and the productivity are observed with Kriging model based on large data optimization set as 184.06 g/l and 0.61 g/l h, respectively. Conditions as follows; for Total FAME titer t=500 h, T=60℃, E:O=11.66% and A:O=8.00. For the productivity; t=500 h, T=60℃, E:O=11.40% and A:O=8.00.

When the experimental values are considered, it is seen that the values are obtained resulted from above-mentioned optimizations are almost one order of magnitude larger than the experimental values. However. the direction of behavior is consistant.

The output metrics total fame titer and productivity shows that the optimal value of the output metric at that point is far from the real value. The optimization results show the direction of the optimum point within the design space. It can be seen that the results are more qualitative than quantitative.

3.2.2.2. Multi objective optimization

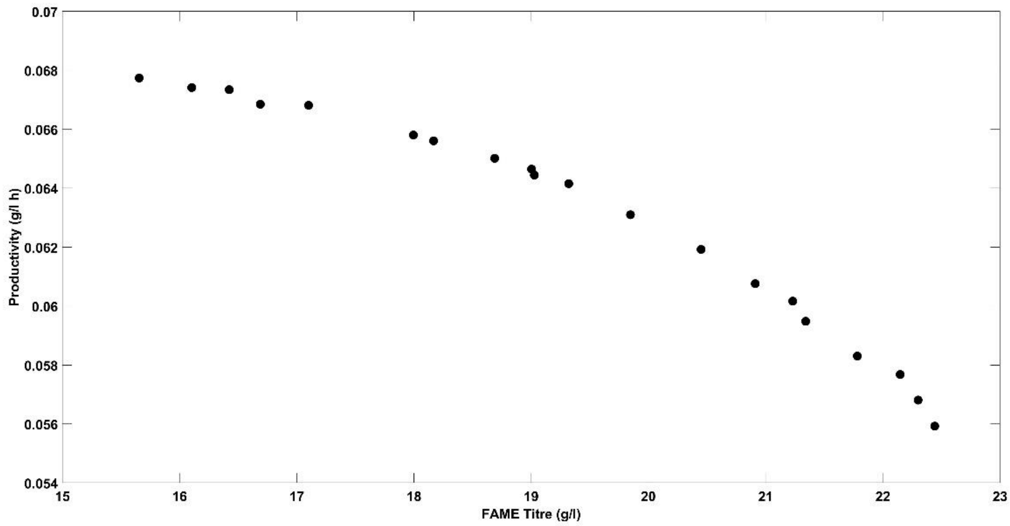

Figure 3.20 Quadratic Multi-objective Optimization

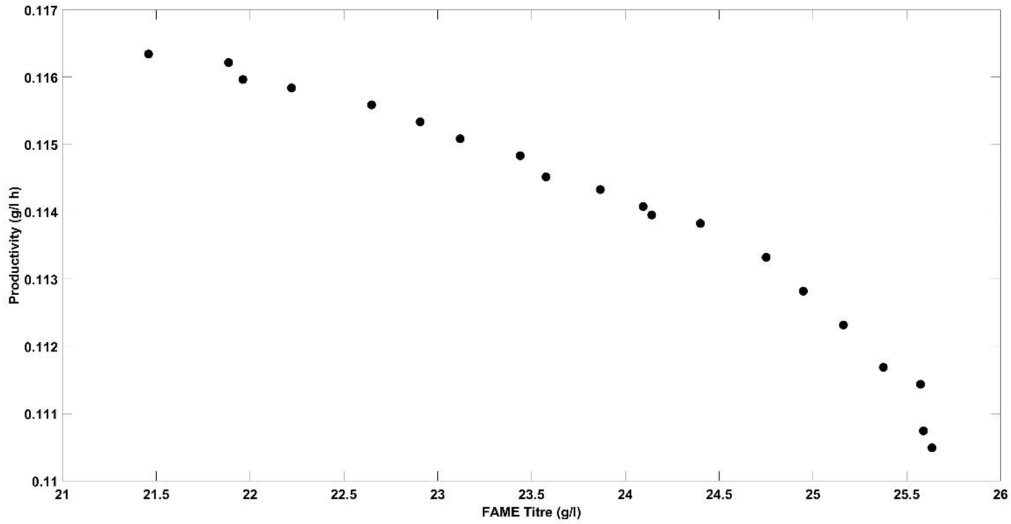

Figure 3.21 Kriging Multi-objective Optimization

Multi-objective optimization of both metrics is also performed using the two types of models. Figures 3.20 and 3.21 show the Pareto fronts generated using low-order polynomial (Quadratic) models and Kriging models, respectively. When multi-objective optimization is performed, the Pareto fronts show the numerical trade-off between the two process metrics which selected from the viewpoint of process design. More importantly, the trade-off can be visualized quantitatively. Both models show a similar trend. However the values of multi-objective optimizations with the Kriging model are observed to be more overestimated. In this stage, it is important to observe the relative relationship between the two metrics. For the multi-objective optimal Pareto front generated by the Kriging models, as the highest titer (25.63 g/l) is achieved, the lowest productivity is obtained (0.11 g / l h). The potential gain in productivity, if moved from the lowest end of the Pareto front (0.11 g/l h) to the highest (0.116 g/l h) is 5.5%. The corresponding titer loss is 16% (from 25.63 to 21.46 g/l).

In the middle point of Pareto front, the loss is as follows; titer loss is 8% (from 25.63 to 23.58 g/l), the corresponding productivity loss is 1.2% (from 0.116 to 0.1145 g/l h). In order to plan the progress of process design, these quantitative values are significant in terms of early evaluation.

Although the both models show a similar behavior, the multi-objective optimal Pareto front generated by the low-order polynomial models give a broader range. The Pareto front generated using the low-order polynomial models shows an optimal operating range of 15.7 g/l to 22.4 g/l for the titer, meaning a possible loss of 30% if operated at the minimum level. The corresponding gain in productivity is about 21% (from 0.056 to 0.068 g/l h).

The trade-off is similarly correlated for both models even though the range and the numeric values are different.

4. CONCLUSION

Commercial feasibility of biocatalytic biodiesel production using waste cooking oil as feedstock, critically depends on the availability of cheap biocatalyst. For this reason, it is important to screen, select, and develop different lipases with varying properties from different sources. After the identification of a new lipase, a set of procedures are applied to evaluate the potentiality of that lipase to be used in biodiesel productions. Most commonly, a set of time progress experiments are run under varying operational conditions to assess the performance of the enzyme. These experiments are costly in terms of time and resources. So, it is vital to make as much use of this preliminary data as possible. Another important step in the evaluation of a new lipase is its optimization towards specific targets such as maximizing yield or conversion. Conventional methods exist that have been extensively used in similar studies. These methods make use of response surface methodology which is based on modeling based on low-order quadratic polynomials.

In this study, a novel lipase is tested for its performance under varying operational conditions such as reaction temperature, methanol to oil molar ratio, and enzyme amount. Time progress data is collected for a set of different conditions according to a manually-adjusted central composite experimental design. It is observed in these experiments that the requirement of a high temperature for best performance is obvious and longer reactions times are required to obtain high FAME titers.

It is known that the WCO is suitable feedstock for biodiesel production. When WCO is analyzed as fatty acid content, it is shown palmitic C16:0 (20.4 %), oleic C18:1 (50.9 %) and linoleic C18:2 (13.5 %) acids are the most three common fatty acids. According to our results, it could be seen that the methyl esters of these three fatty acids were produced.

The collected data is also used within two modelling and optimization schemes. The first scheme is the conventional response surface methodology based on low-order polynomial models. The other scheme makes use of Kriging as an alternative. From the modelling part, it is can be concluded that one of the most important aspects of choosing the most appropriate modelling and optimization scheme is making sure the mathematical structure of the models carries as much resemblance as possible to the experimental data collected to characterize the system. Specifically, about the system studied in this work, a highly nonlinear and complex behavior is present even though the number of independent variables chosen is low. In this situation, the modelling and optimization approach based on Kriging seems to be better choice compared to the low-order polynomial models. This can be attributed to the fact that Kriging is an interpolation-based technique.

This conclusion is based on the comparison of R^2 and adj_R^2 values achieved for the different types of models generated within the study. However, another important point to add here is in regards of the p-values of the models. The comparison of p-values of the models in relation to the models generated by the small data set compared to the large data set shows that another critical factor in choosing the appropriate modelling and optimization scheme depends on the degrees of freedom of each model. The important conclusion is that as the degrees of freedom of the selected model, which depends on the difference between the number of parameters the models have and the number of experimental models, decreases the reliability with which the models can be used in further optimization tasks decreases as well.

This work is primarily an attempt to present the fact that generally accepted conventional methods of modelling and optimization based on low-order polynomial-driven response surface methodology should be challenged as there are more useful techniques which can make more efficient use of limited preliminary experimental data on biocatalytic biodiesel production systems. This work should inspire the consideration of further modelling techniques such as multivariate adaptive regression or M5 model trees to be compared as alternatives to low-order polynomial and Kriging models. Moreover, the same set of techniques should be applied to several different biocatalytic biodiesel production systems with different lipases to assess whether the level of characterization or development of the biocatalyst affects the efficiency of the different modelling schemes.

REFERENCES

Abbaszaadeh A., Ghobadian, B., Omidkhah, M.R., Najafi, G. (2012) Current biodiesel production technologies: A comparative review. Energy Conversion and Management, 63, 138–148.

Aboelazayem, O., Gadalla, M., Saha, B. (2018) Biodiesel production from waste cooking oil via supercritical methanol: Optimization and reactor simulation. Renewable Energy, 124, 144-154.

Adewale, P., Dumont, M.J., Ngadi, M. (2015) Recent trends of biodiesel production from animal fat wastes and associated production techniques. Renewable and Sustainable Energy Reviews, 45, 574–588.

Ahmed, W., Nazar, F.N., Ali, S.D., Rana, U.A., Khan U.D.S. (2015) Detailed investigation of optimized alkali catalyzed transesterification of Jatropha oil for biodiesel production. Journal of Energy Chemistry, 24, 331–336.

Aghbashloa, M., Hosseinpoura, S., Tabatabaeib, M., Soufiyan, M.M. (2019) Multi-objective exergetic and technical optimization of a piezoelectric ultrasonic reactor applied to synthesize biodiesel from waste cooking oil (WCO) using soft computing techniques. Fuel, 235, 100–112.

Aguieiras, E.C.G., Cavalcanti-Oliveira, D.E., Freire, M.G.D. (2015) Current status and new developments of biodiesel production using fungal lipases. Fuel, 159, 52–67.

Ali, C.H., Mbadinga, S.M., Liu, J.F., Yang, S.Z., Gu, J.D., Mu, B.Z. (2015) Significant enhancement of *Pseudomonas aeruginosa* FW_SH 1 lipase production using response surface methodology and analysis of its hydrolysis capability. Journal of the Taiwan Institute of Chemical Engineers, 52, 7–13.

Ali, C.H., Qureshi, A.S., Mbadinga, M.S., Liu, J.F., Yang, Z.S., Mu, B.Z. (2017) Biodiesel production from waste cooking oil using onsite produced purified lipase from *Pseudomonas aeruginosa* FW_SH-1: Central composite design approach. Renewable Energy, 109, 93-100.

Almeida, V.F.D., García-Moreno, P.J., Guadix, A., Guadix, E.M. (2015) Biodiesel production from mixtures of waste fish oil, palm oil and waste frying oil: Optimization of fuel properties. Fuel Processing Technology, 133, 152–160.

Ambat, I., Srivastava, V., Sillanpää, M. (2018) Recent advancement in biodiesel production methodologies using various feedstock: A review. Renewable and Sustainable Energy Reviews, 90, 356–369.

Amini, Z., Ilham, Z., Ong, H.C., Mazaheri, H., Chen W.H. (2017) State of the art and prospective of lipase-catalyzed transesterification reaction for biodiesel production. Energy Conversion and Management, 141, 339–353.

Andrade, T.A., Errico, M., Christensen K.V. (2017) Influence of the reaction conditions on the enzyme catalyzed transesterification of castor oil: A possible step in biodiesel production. Bioresource Technology, 243, 366–374.

Anwar, M., Rasul, M.G., Ashwath N. (2018) Production optimization and quality assessment of papaya (Carica papaya) biodiesel with response surface methodology. Energy Conversion and Management, 156, 103–112.

Aransiola, E.F., Ojumu, T.V., Oyekola, O.O., Madzimbamuto, T.F., Ikhu-Omoregbe, D.I.O. (2014) A review of current technology for biodiesel production: State of the art. Biomass and Bioenergy, 61, 276-297.

Babaki, M., Yousefi, M., Habibi, Z., Mohammadi, M. (2017) Process optimization for biodiesel production from waste cooking oil using multi-enzyme systems through response surface methodology. Renewable Energy, 105, 465-472.

Bajaj, A., Lohan, P., Jha, P.N., Mehrotra, R. (2010) Biodiesel Production through Lipase Catalyzed Transesterification: An Overview. Journal of Molecular Catalyzis B: Enzymatic, 62(1) 9–14.

Balat, M., Balat, H. (2010) Progress in biodiesel processing. Applied Energy, 87, 1815–1835.

Bankovic-Ilic, I.B., Stamenkovic, O.S., Veljkovic, V.B. Biodiesel production from non-edible plant oils. Renewable and Sustainable Energy Reviews, 16, 3621– 3647.

Borrelli, G.M., Trono, D. (2015) Recombinant Lipases and Phospholipases and Their Use as Biocatalyzts for Industrial Applications. International Journal of Molecular Sciences, 16(9), 20774-20840.

Borugadda, V.B., Goud V.V. (2012) Biodiesel production from renewable feedstocks: Status and opportunities. Renewable and Sustainable Energy Reviews, 16, 4763–4784.

Bradford MM. (1976) A rapid and sensitive method for the quantitation of microgram quantities of protein utilizing the principle of protein-dye binding. Analytical Biochemistry, 72, 248–54.

Budžaki, S., Miljić, G., Sundaram, S., Tišma, M., Hessel V. (2018) Cost analysis of enzymatic biodiesel production in small-scaled packed-bed reactors. Applied Energy, 210 268–278.

Budzaki, S., Miljic, G., Tišma, M., Sundaram, S., Hessel V. (2017) Is there a future for enzymatic biodiesel industrial production in microreactors? Applied Energy, 201, 124–134.

Canakci, M., Gerpen, V.J. (2001) Biodiesel production from oils and fats with high free fatty acids. American Society of Agricultural and Biological Engineers, 44(6), 1429–36.

Canet, A., Bonet-Ragel, K., Benaiges, M.D., Valero F. (2016) Lipase-catalyzed transesterification: Viewpoint of the mechanism and influence of free fatty acids. Biomass and Bioenergy, 85, 94-99.

Carvalho, M.S., Mendonça, M.A., Pinho, D.M.M., Resck I.S., Suarez. P.A.Z. (2012) Chromatographic Analyses of Fatty Acid Methyl Esters by HPLC-UV and GC-FID. Journal of the Brazilian Chemical Society, 23 (4), 763-769.

César, A.S., Werderits, D.E., Saraiva, G.L.O., Guabiroba, R.C.S. (2017) The potential of waste cooking oil as supply for the Brazilian biodiesel chain. Renewable and Sustainable Energy Reviews, 72, 246–253.

Chen, X., Qian, W.W., Lu X.P., Han P.F. (2012) Preparation of biodiesel catalyzed by KF/CaO with ultrasound. Natural Product Research, 26(13), 1249–1256.

Chesterfield, D.M., Rogers, P.L., Al-Zaini, E.O., Adesina, A.A. Production of biodiesel via ethanolysis of waste cooking oil using immobilised lipase. Chemical Engineering Journal, 207–208, 701–710.

Chhetri, A.B., Watts K.C., Islam M.R. (2008) Waste Cooking Oil as an Alternate Feedstock for Biodiesel Production. Energies, 1, 3-18.

Christopher, L.P., Kumar, H., Zambare V.P. (2014) Enzymatic biodiesel: Challenges and opportunities. Applied Energy, 119, 497–520.

Dharma, S., Masjuki, H.H., Ong, H.C., Sebayang, A.H., Silitonga, A.S., Kusumo, F., Mahlia, T.M.I. (2016) Optimization of biodiesel production process for mixed Jatropha curcas–Ceiba pentandra biodiesel using response surface methodology. Energy Conversion and Management, 115, 178–190.

Dhawane, S.H., Kumar, T., Halder. G. (2018) Recent advancement and prospective of heterogeneous carbonaceous catalyzts in chemical and enzymatic transformation of biodiesel. Energy Conversion and Management, 167, 176–202.

Ding, H., Ye, W., Wang, Y., Wang, X., Li, L., Liu, D., Gui, J., Song, C., Ji, N. (2018) Process intensification of transesterification for biodiesel production from palm oil: Microwave irradiation on transesterification reaction catalyzed by acidic imidazolium ionic liquids. Energy, 144, 957-967.

Ezekannagha, C.B., Ude, C.N., Onukwuli, D.O. (2017) Optimization of the methanolysis of lard oil in the production of biodiesel with response surface methodology. Egyptian Journal of Petroleum, 26, 1001–1011.

Ferella, F., Celso, G.M.D., Michelis, I.D., Stanisci, V., Vegliò, F. (2010) Optimization of the transesterification reaction in biodiesel production. Fuel 89, 36–42.

Fjerbaek, L., Christensen, V.K., Norddahl, B. (2009) A Review of the Current State of Biodiesel Production Using Enzymatic Transesterification. Biotechnology and Bioengineering, 102(5), 1298-1315.

Gaurav, A., Ng, F.T.T., Rempel G.L. (2016) A new green process for biodiesel production from waste oils via catalytic distillation using a solid acid catalyzt - Modeling, economic and environmental analysis. Green Energy & Environment 1, 62-74.

Geraili, A., Romagnoli, J.A. (2015) A Multiobjective Optimization Framework for Design of Integrated Biorefineries Under Uncertainty. American Institute of Chemical Engineers, 61(10), 3208–3222.

Ghaly, A. E., Dave, D., Brooks, M.S., Budge, S. (2010) Production of Biodiesel by Enzymatic Transesterification: Review. American Journal of Biochemistry and Biotechnology, 6(2), 54–76.

Giagkiozis, I., Fleming, P.J. (2015) Methods for multi-objective optimization: An analysis. Information Sciences, 293, 338–350.

Goharimanesh, M., Lashkaripour A., Akbari A. (2016) Optimization of Biodiesel Production Using Multi-Objective Genetic Algorithm. Journal of Applied Science and Engineering, 19(2), 117- 124.

Guldhe, A., Singh, B., Mutanda, T., Permaul, K., Bux F. (2015) Advances in synthesis of biodiesel via enzyme catalyzis: Novel and sustainable approaches. Renewable and Sustainable Energy Reviews, 41, 1447–1464.

Gumba, R.E., Saallah, S., Misson, M., Ongkudon, M.C., Anton, A. (2016) Green biodiesel production: a review on feedstock, catalyzt, monolithic reactor, and supercritical fluid technology. Biofuel Research Journal, 11, 431-447.

Gupta, R., Gupta, N., Rathi, P. (2004) Bacterial lipases: an overview of production, purification and biochemical properties. Applied Microbiol Biotechnology, 64(6), 763-781.

Haigh, F.K., Vladisavljevic, G.T., Reynolds, J.C., Nagy, Z., Saha, B. (2014) Kinetics of the pre-treatment of used cooking oilusing Novozyme 435 for biodiesel production. Chemical Engineering Research and Design, 92, 713–719.

Hajjaria, M., Tabatabaeia, M., Aghbashlod, M., Ghanavatia, H. (2017) A review on the prospects of sustainable biodiesel production: A global scenario with an emphasis on waste-oil biodiesel utilization. Renewable and Sustainable Energy Reviews, 72, 445–464.

Hama, S., Kondo, A. (2013) Enzymatic Biodiesel Production: An Overview of potential feedstocks and process development. Bioresource Technology, 135, 386–95.

Hamze, H., Akia, M., Yazdani, F. (2015) Optimization of biodiesel production from the waste cooking oil using response surface methodology. Process Safety and Environmental Protection, 94, 1–10.

Hoekman, S.K., Broch, A., Robbins, C., Ceniceros, E., Natarajan M. (2012) Review of biodiesel composition, properties, and specifications. Renewable and Sustainable Energy Reviews, 16, 143– 169.

Ismail, A.R., El-Henawy, S.B., Betiha, M.A., Amr, S.S.A., El-Gendy, N.S., Azab, M.S., Sedky, N.M. (2017) Optimization of batch Novozym435-catalyzed transesterification of waste cooking oil with methanol for biodiesel production in a solvent-free medium. Energy Sources, Part A: Recovery, Utilization, and Environmental Effects, 39(9) 911–925.

Jaeger, K.E., Dijkstra, B.W., Reetz, M.T. (1999) Bacterial biocatalyzts: molecular biology, three-dimensional structures, and biotechnological applications of lipases. Annual Review Microbiology, 53(1), 315-351.

Jia, Z., Davis, E., Muzzio, F.J., Ierapetritou, M.G. (2009) Predictive Modeling for Pharmaceutical Processes Using Kriging and Response Surface. Journal of Pharmaceutical Innovation, 4, 174–186.

José, C., Bonetto, R.D., Gambaro, L.A., Torres, M.P.G., Foresti, M.L., Ferreira, M.L., Briand, L.E. (2011) Investigation of the causes of deactivation–degradation of the commercial biocatalyzt Novozym 435 in ethanol and ethanol–aqueous media. Journal of Molecular Catalyzis B: Enzymatic, 71, 95–107.

Kamel, D.A., Farag, H.A., Amin, N.A., Zatout, A.A., Ali, R.M. (2018) Smart utilization of jatropha (Jatropha curcas Linnaeus) seeds for biodiesel production: Optimization and mechanism. Industrial Crops & Products, 111, 407–413.

Kapoor, M., Gupta, M.N. (2012) Lipase promiscuity and its biochemical applications. Process Biochemistry, 47, 555–569.

Karimi, M., Jenkins, B., Stroeve P. (2016) Multi-objective optimization of transesterifi cation in biodiesel production catalyzed by immobilized lipase. Biofuels, Bioproducts and Biorefining, 10, 804–818.

Katre, G., Raskar, S., Zinjarde, S., Kumar, V.R., Kulkarni, B.D., Kumar, A.R. (2018) Optimization of the in situ transesterification step for biodiesel production using biomass of *Yarrowia lipolytica* NCIM 3589 grown on waste cooking oil. Energy, 142, 944-952.

Kawashima, A., Matsubara, K., Honda, K. (2009) Acceleration of catalytic activity of calcium oxide for biodiesel production. Bioresource Technology, 100, 696–700.

Khuri, A. I., Mukhopadhyay, S. (2010) Response surface methodology. WIREs Computational Statistics, 2, 128-149.

Kleijnen J.P.C. (2017) Regression and Kriging metamodels with their experimental designs in simulation: A review. European Journal of Operational Research, 256, 1–16.

Knothe, G., Razon, L.F. (2017) Biodiesel fuels. Progress in Energy and Combustion Science, 58, 36–59.

Kulkarni, M.G., Gopinath, R., Meher, L.C., Dalai, A.K. (2006) Solid acid catalyzed biodiesel production by simultaneous esterification and transesterification. Green Chemistry, 8, 1056–1062.

Kusumaningtyas, R.D., Pristiyani, R., Dewajani, H. (2016) A new route of biodiesel production through chemical interesterification of jatropha oil using ethyl acetate. International Journal of ChemTech Research, 9(6), 627-634.

Lam, M.K., Lee, K.T., Mohamed A.R. (2010) Homogeneous, heterogeneous and enzymatic catalyzis for transesterification of high free fatty acid oil (waste cooking oil) to biodiesel: A review. Biotechnology Advances, 28, 500–518.

Lamba, N., Modak, M.J., Madras G. (2017) Fatty acid methyl esters synthesis from non-edible vegetable oils using supercritical methanol and methyl tert-butyl ether. Energy Conversion and Management, 138, 77–83.

Lee, H.V., Juan, J.C., Hin Y.T., Ong, H.C. (2016) Environment-Friendly Heterogeneous Alkaline-Based Mixed Metal Oxide Catalyzts for Biodiesel Production. Energies, 9(8), 611.

Leung, D.Y.C., Wu, X., Leung, M.K.H. (2010) A review on biodiesel production using catalyzed transesterification. Applied Energy, 87, 1083–1095.

Liew, W.H., Hassim, M.H., Ng D.K.S. (2014) Sustainability assessment for biodiesel production via fuzzy optimization during research and development (R&D) stage. Clean Technologies Environmental Policy, 16, 1431–1444.

Liu, X., He, H., Wang, Y., Zhu, S., Piao, X. (2008) Transesterification of soybean oil to biodiesel using CaO as a solid base catalyzt. Fuel, 87, 216–221.

Lophaven, S.N., Søndergaard, J., Nielsen, H.B. (2002) DACE A Matlab Kriging Toolbox. IMM Informatiocs and Mathematical Modelling 1–28.

Lotero, E., Liu, Y., Lopez, D.E., Suwannakarn, K., Bruce, D.A., Goodwin, J.G. (2005) Synthesis of Biodiesel via Acid Catalyzis. Industrial & Engineering Chemistry Research, 44, 5353-5363.

Mardhiah, H.H., Ong, H.C. Masjuki, H.H., Lim, S., Lee H.V. (2017) A review on latest developments and future prospects of heterogeneous catalyzt in biodiesel production from non-edible oils. Renewable and Sustainable Energy Reviews, 67, 1225–1236.

Meher, L.C., Churamani, C.P., Arif, M., Ahmed, Z., Naik, S.N. (2013) Jatrophacurcas as are new able source for bio-fuels—A review. Renewable and Sustainable Energy Reviews, 26, 397–407.

Mumtaz, M.W., Adnan, A., Anwar, F., Mukhtar, H., Raza, M.A., Ahmad, F., Rashid, U. (2012) Response Surface Methodology: An Emphatic Tool for Optimized Biodiesel Production Using Rice Bran and Sunflower Oils. Energies, 5(9), 3307–28.

Mumtaz, M.W., Mukhtar, H., Anwar, F., Saari, N. (2014) RSM Based Optimization of Chemical and Enzymatic Transesterification of Palm Oil: Biodiesel Production and Assessment of Exhaust Emission Levels. The Scientific World Journal, Article ID 526105.

Musa, I.A. (2016) The effects of alcohol to oil molar ratios and the type of alcohol on biodiesel production using transesterification process. Egyptian Journal of Petroleum, 25, 21–31.

Muthukumara, C., Praniesh, R., Navamani, P., Swathi, R., Sharmila, G., Kumar, M.N. (2017) Process optimization and kinetic modeling of biodiesel production using non-edible Madhuca indica oil. Fuel, 195, 217–225.

Narwal S.K., Gupta, R. (2013) Biodiesel production by transesterification using immobilized lipase. Biotechnology Letters, 35, 479–490.

Nejad, A.S., Zahedi, A.R. (2018) Optimization of biodiesel production as a clean fuel for thermal power plants using renewable energy source. Renewable Energy, 119, 365-374.

Pollardo, A.A., Lee, H., Lee, D., Kim, S., Kim, J. (2018) Solvent effect on the enzymatic production of biodiesel from waste animal fat. Journal of Cleaner Production, 185, 382-388.

Pourzolfaghar, H., Abnisa, F., Daud, W.M.A.W., Aroua M.K. (2016) A review of the enzymatic hydroesterification process for biodiesel production. Renewable and Sustainable Energy Reviews, 61, 245–257.

Price, J., Nordblad, M., Martel, H.H., Chrabas, B., Wang, H., Nielsen, P.M., Woodley, J.M. (2016) Scale-Up of Industrial Biodiesel Production to $40m^3$ Using a Liquid Lipase Formulation. Biotechnology and Bioengineering, 9999, 1–10.

Rafiei, S., Tangestaninejad, S., Horcajada, P., Moghadama, M., Mirkhania, V., Mohammadpoor-Baltork, I., Kardanpour, R., Zadehahmadi, F. (2018) Efficient biodiesel production using a lipase@ZIF-67 nanobioreactor. Chemical Engineering Journal, 334, 1233–1241.

Rodrigues, R.C., Volpato, G., Ayub, M.A.Z., Wada, K. (2008) Lipase-catalyzed ethanolysis of soybean oil in a solvent-free system using central composite design and response surface methodology. Journal of Chemical Technology and Biotechnology, 83, 849–854.

Saeidi, S., Jouybanpour, P., Mirvakilli, A., Iranshahi, D., Klemes J.J. (2016) A comparative study between Modified Data Envelopment Analysis and Response Surface Methodology for optimization of heterogeneous biodiesel production from waste cooking palm oil. Journal of Cleaner Production, 136 (Part B), 23-30.

Sajid, Z., Khan, F., Zhang, Y. (2016) Process simulation and life cycle analysis of biodiesel production. Renewable Energy, 85, 945-952.

Selvakumar, P., Sivashanmugam, P. (2017) Optimization of lipase production from organic solid waste by anaerobic digestion and its application in biodiesel production. Fuel Processing Technology, 165, 1–8.

Sen, B., Saraç, N., Uğur A. (2016) Partial Purification, Characterization and Biodiesel Application of *Streptomyces lienomycini* Lipase. Romanian Biotechnological Letters, 22(6), 12103-12109.

Serio, D.M., Cozzolino, M., Tesser, R., Patrono, P., Pinzari, F., Bonelli, B., Santacesaria, E. (2007) Vanadyl phosphate catalyzts in biodiesel production. Applied Catalyzis A: General, 320, 1–7.

Shieh, C.J., Liao, H.F., Lee, C.C. (2003) Optimization of lipase-catalyzed biodiesel by response surface methodology. Bioresource Technology, 88, 103–106.

Shimada, Y., Watanabe, Y., Samukawa, T., Sugihara, A., Noda, H., Fukuda, H., Tominaga, Y. (1999) Conversion of vegetable oil to biodiesel using immobilized *Candida antarctica* lipase. Journal of the American Oil Chemists' Society. 76, 789–793.

Shimada, Y., Watanabe, Y., Sugihara, A., Tominaga, Y. (2002) Enzymatic alcoholysis for biodiesel fuel production and application of the reaction to oil processing. Journal of Molecular Catalyzis B: Enzymatic, 17, 133–142.

Silva, G.F., Camargo, F.L., Ferreira, A.L.O. (2011) Application of response surface methodology for optimization of biodiesel production by transesterification of soybean oil with ethanol. Fuel Processing Technology, 92, 407–413.

Stojković, I.J., Stamenković, O.S., Povrenović, D.S., Veljković, V.B. (2014) Purification technologies for crude biodiesel obtained by alkali-catalyzed transesterification. Renewable and Sustainable Energy Reviews, 32, 1–15.

Sun, J., Chin, J.H., Zhou, W., Yu, B., Curran, P., Liu, S.Q. (2012) Biocatalytic Conversion of Coconut Oil to Natural Flavor Esters Optimized with Response Surface Methodology. Journal of the American Oil Chemists' Society, 89, 1991–1998.

Suwanno, S., Rakkan, T., Yunu, T., Paichid, N., Kimtun, P., Prasertsan, P., Sangharak, K. (2017) The Production of Biodiesel Using Residual Oil from Palm Oil Mill Effluent and Crude Lipase from Oil Palm Fruit as an Alternative Substrate and Catalyzt. Fuel, 195, 82–87.

Szczesna-Antczak, M., Kubiak, A., Antczak, T., Bielecki, S. (2009) Enzymatic Biodiesel Synthesis - Key Factors Affecting Efficiency of the Process. Renewable Energy, 34(5), 1185–94.

Tacias-Pascacio, V.G., Virgen-Ortíz, J.J., Jiménez-Pérez, M., Yates, M., Torrestiana-Sanchez, B., Rosales-Quintero, A., Fernandez-Lafuente R. (2017) Evaluation of different lipase biocatalyzts in the production of biodiesel from used cooking oil: Critical role of the immobilization support. Fuel, 200, 1–10.

Talebian-Kiakalaieh, A., Amin, N.A.S., Mazaheri, H. (2013) A review on novel processes of biodiesel production from waste cooking oil. Applied Energy, 104, 683–710.

Tan, T., Lu, J., Nie, K., Deng, L., Wang, F. (2010) Biodiesel production with immobilized lipase: A review. Biotechnology Advances, 28, 628–634.

Tang, Z.E., Lim, S., Pang, Y.L., Ong, H.C., Lee, K.T. (2018) Synthesis of biomass as heterogeneous catalyzt for application in biodiesel production: State of the art and fundamental review. Renewable and Sustainable Energy, Reviews 92, 235–253**.**

Tubino, M., Junior, J.G.R., Bauerfeldt, F.G. (2016) Biodiesel synthesis: A study of the triglyceride methanolysis reaction with alkaline catalyzts. Catalyzis Communications, 75, 6–12.

Ugur, A., Sarac, N., Boran, R., Ayaz, B., Ceylan, O., Okmen, G. (2014) New Lipase for Biodiesel Production: Partial Purification and Characterization of LipSB 25-4. ISRN Biochemistry, 2014 1–7.

Ullah, F., Dong, L., Bano, A., Peng, Q., Huang, J. (2016) Current advances in catalyzis toward sustainable biodiesel production. Journal of the Energy Institute, 89, 282-292.

Verma, P., Sharma, M.P. (2016) Comparative analysis of effect of methanol and ethanol on Karanja biodiesel production and its optimization. Fuel, 180, 164–174.

Vyas, A.P., Verma, J.L., Subrahmanyam, N. (2010) A review on FAME production processes. Fuel, 89, 1–9.

Wang, X., Qin, X., Li, D., Yang, B., Wang Y. (2017) One-step synthesis of high-yield biodiesel from waste cooking oils by a novel and highly methanol-tolerant immobilized lipase. Bioresource Technology, 235, 18–24.

Wu, L., Wei, T., Lin, Z., Zou, Y., Tong Z., Sun, J. (2016) Bentonite-enhanced biodiesel production by NaOH-catalyzed transesterification: Process optimization and kinetics and thermodynamic analysis. Fuel, 182, 920–927.

Yan, Y., Li, X., Wang, G., Gui, X., Li, G., Su, F., Wang, X., Liu, T. (2014) Biotechnological preparation of biodiesel and its high-valued derivatives: A review. Applied Energy, 113, 1614–1631.

Yılmaz, D.E., Sayar, N.A. (2015) Organic Solvent Stable Lipase from Cryptococcus Diffluens D44 Isolated from Petroleum Sludge. Journal of Molecular Catalyzis B: Enzymatic, 122, 72–79.

Yılmaz, D.E., Yalçın, H.T., Sayar, N.A. (2014) Screening of Lipase Production Among Different Microorganisms. New Biotechnology, 31, 90.

Yu, H., Yue, H., Halling, P. (2015) Optimal Experimental Design for an Enzymatic Biodiesel Production System. IFAC-PapersOnLine, 48(8) 1258–1263.

Yun, H., Wang, M., Feng, W., Tan, T. (2013) Process simulation and energy optimization of the enzyme-catalyzed biodiesel production. Energy, 54, 84-96.

Zarejousheghani, F., Kariminia, H.R., Khorasheh, F. (2016) Kinetic Modelling of Enzymatic Biodiesel Production from Castor Oil: Temperature Dependence of the Ping Pong Parameters. The Canadian Journal of Chemical Engineering, 94(3), 512-517.

Zhang, Y., Dube, M.A., McLean, D.D., Kates, M. (2003) Biodiesel production from waste cooking oil: 1. Process design and technological assessment. Bioresource Technology, 89, 1-16.

APPENDIX A

Model parameters values and Goodness of fit statistics

Table A.1 Model-1

Estimated model parameter values		**Goodness of fit**	
$\boldsymbol{\beta_0}$	41.452	R^2	0.992
$\boldsymbol{\beta_1}$	-6.667	adj_R^2	0.983
$\boldsymbol{\beta_2}$	-7.507	$RMSE$	28.2
$\boldsymbol{\beta_3}$	6.137	f_stat	111
$\boldsymbol{\beta_4}$	262.150	p_value	1.12e-06
$\boldsymbol{\beta_5}$	0.012		
$\boldsymbol{\beta_6}$	0.252		
$\boldsymbol{\beta_7}$	-0.017		
$\boldsymbol{\beta_8}$	-24.977		

Table A.2 Model-2

Estimated model parameter values		**Goodness of fit**	
$\boldsymbol{\beta_0}$	60.013	R^2	0.991
$\boldsymbol{\beta_1}$	-19.050	adj_R^2	0.982
$\boldsymbol{\beta_2}$	-28.431	$RMSE$	88.6
$\boldsymbol{\beta_3}$	19.116	f_stat	101
$\boldsymbol{\beta_4}$	796.540	p_value	1.55e-06
$\boldsymbol{\beta_5}$	0.035		
$\boldsymbol{\beta_6}$	0.827		
$\boldsymbol{\beta_7}$	-0.048		
$\boldsymbol{\beta_8}$	-75.703		

Table A.3 Model-3

Estimated model parameter values		Goodness of fit	
$\boldsymbol{\beta_0}$	228.240	R^2	0.993
$\boldsymbol{\beta_1}$	-11.413	adj_R^2	0.985
$\boldsymbol{\beta_2}$	-21.324	$RMSE$	47.4
$\boldsymbol{\beta_3}$	11.015	f_stat	126
$\boldsymbol{\beta_4}$	442.980	p_value	7.13e-07
$\boldsymbol{\beta_5}$	0.021		
$\boldsymbol{\beta_6}$	0.547		
$\boldsymbol{\beta_7}$	-0.039		
$\boldsymbol{\beta_8}$	-42.144		

Table A.4 Model-4

Estimated model parameter values		Goodness of fit	
$\boldsymbol{\beta_0}$	1648.500	R^2	0.992
$\boldsymbol{\beta_1}$	-185.650	adj_R^2	0.983
$\boldsymbol{\beta_2}$	-286.320	$RMSE$	810
$\boldsymbol{\beta_3}$	181.340	f_stat	113
$\boldsymbol{\beta_4}$	7508.400	p_value	1.06e-06
$\boldsymbol{\beta_5}$	0.347		
$\boldsymbol{\beta_6}$	8.139		
$\boldsymbol{\beta_7}$	-0.525		
$\boldsymbol{\beta_8}$	-714.120		

Table A.5 Model-5

Estimated model parameter values		Goodness of fit	
$\boldsymbol{\beta_0}$	-0.828	R^2	0.988
$\boldsymbol{\beta_1}$	-0.014	adj_R^2	0.975
$\boldsymbol{\beta_2}$	0.015	$RMSE$	0.0762
$\boldsymbol{\beta_3}$	0.027	f_stat	74.8
$\boldsymbol{\beta_4}$	0.656	p_value	4.34e-06
$\boldsymbol{\beta_5}$	2.3193e-05		
$\boldsymbol{\beta_6}$	0.0003		
$\boldsymbol{\beta_7}$	-0.0002		
$\boldsymbol{\beta_8}$	-0.062		

Table A.6 Model-6

Estimated model parameter values		Goodness of fit	
$\boldsymbol{\beta_0}$	-2.614	R^2	0.984
$\boldsymbol{\beta_1}$	-0.039	adj_R^2	0.965
$\boldsymbol{\beta_2}$	0.024	$RMSE$	0.271
$\boldsymbol{\beta_3}$	0.081	f_stat	53
$\boldsymbol{\beta_4}$	2.031	p_value	1.41e-05
$\boldsymbol{\beta_5}$	6.5416e-05		
$\boldsymbol{\beta_6}$	0.001		
$\boldsymbol{\beta_7}$	-0.0005		
$\boldsymbol{\beta_8}$	-0.193		

Table A.7 Model-7

Estimated model parameter values		**Goodness of fit**	
$\boldsymbol{\beta_0}$	-0.944	R^2	0.986
$\boldsymbol{\beta_1}$	-0.023	adj_R^2	0.969
$\boldsymbol{\beta_2}$	-0.0008	$RMSE$	0.154
$\boldsymbol{\beta_3}$	0.048	f_stat	59.7
$\boldsymbol{\beta_4}$	1.0804	p_value	9.38e-06
$\boldsymbol{\beta_5}$	3.836e-05		
$\boldsymbol{\beta_6}$	0.0009		
$\boldsymbol{\beta_7}$	-0.0003		
$\boldsymbol{\beta_8}$	-0.103		

Table A.8 Model-8

Estimated model parameter values		**Goodness of fit**	
$\boldsymbol{\beta_0}$	-21.935	R^2	0.986
$\boldsymbol{\beta_1}$	-0.384	adj_R^2	0.969
$\boldsymbol{\beta_2}$	0.192	$RMSE$	2.47
$\boldsymbol{\beta_3}$	0.789	f_stat	59.6
$\boldsymbol{\beta_4}$	18.841	p_value	9.47e-06
$\boldsymbol{\beta_5}$	0.0006		
$\boldsymbol{\beta_6}$	0.012		
$\boldsymbol{\beta_7}$	-0.005		
$\boldsymbol{\beta_8}$	-1.7953		

Table A.9 Model-9

Estimated model parameter values		Goodness of fit	
$\boldsymbol{\beta_0}$	-153.380	R^2	1
$\boldsymbol{\beta_1}$	-12.345	adj_R^2	0.998
$\boldsymbol{\beta_2}$	21.488	$RMSE$	8.55
$\boldsymbol{\beta_3}$	3.978	f_stat	696
$\boldsymbol{\beta_4}$	437.190	p_value	0.0297
$\boldsymbol{\beta_5}$	0.233		
$\boldsymbol{\beta_6}$	0.215		
$\boldsymbol{\beta_7}$	0.161		
$\boldsymbol{\beta_8}$	-1.545		
$\boldsymbol{\beta_9}$	0.240		
$\boldsymbol{\beta_{10}}$	-2.465		
$\boldsymbol{\beta_{11}}$	-0.008		
$\boldsymbol{\beta_{12}}$	-0.254		
$\boldsymbol{\beta_{13}}$	0.176		
$\boldsymbol{\beta_{14}}$	-37.497		

Table A.10 Model-10

Estimated model parameter values		Goodness of fit	
$\boldsymbol{\beta_0}$	119.210	R^2	1
$\boldsymbol{\beta_1}$	-39.263	adj_R^2	0.999
$\boldsymbol{\beta_2}$	55.992	$RMSE$	18.6
$\boldsymbol{\beta_3}$	-20.203	f_stat	1.31e+03
$\boldsymbol{\beta_4}$	1471.800	p_value	0.0216
$\boldsymbol{\beta_5}$	0.727		
$\boldsymbol{\beta_6}$	0.752		
$\boldsymbol{\beta_7}$	0.569		
$\boldsymbol{\beta_8}$	-4.687		
$\boldsymbol{\beta_9}$	0.590		
$\boldsymbol{\beta_{10}}$	-8.819		
$\boldsymbol{\beta_{11}}$	-0.031		
$\boldsymbol{\beta_{12}}$	-0.723		
$\boldsymbol{\beta_{13}}$	0.678		
$\boldsymbol{\beta_{14}}$	-123.690		

Table A.11 Model-11

Estimated model parameter values		**Goodness of fit**	
$\boldsymbol{\beta_0}$	62.455	R^2	1
$\boldsymbol{\beta_1}$	-22.064	adj_R^2	0.997
$\boldsymbol{\beta_2}$	27.315	$RMSE$	21.9
$\boldsymbol{\beta_3}$	-1.995	f_stat	341
$\boldsymbol{\beta_4}$	790.930	p_value	0.0424
$\boldsymbol{\beta_5}$	0.391		
$\boldsymbol{\beta_6}$	0.392		
$\boldsymbol{\beta_7}$	0.299		
$\boldsymbol{\beta_8}$	-2.610		
$\boldsymbol{\beta_9}$	0.434		
$\boldsymbol{\beta_{10}}$	-4.650		
$\boldsymbol{\beta_{11}}$	-0.014		
$\boldsymbol{\beta_{12}}$	-0.296		
$\boldsymbol{\beta_{13}}$	0.337		
$\boldsymbol{\beta_{14}}$	-67.118		

Table A.12 Model-12

Estimated model parameter values		**Goodness of fit**	
$\boldsymbol{\beta_0}$	141.440	R^2	1
$\boldsymbol{\beta_1}$	-368.370	adj_R^2	0.998
$\boldsymbol{\beta_2}$	523.980	$RMSE$	245
$\boldsymbol{\beta_3}$	-91.102	f_stat	706
$\boldsymbol{\beta_4}$	13500	p_value	0.0295
$\boldsymbol{\beta_5}$	6.760		
$\boldsymbol{\beta_6}$	6.805		
$\boldsymbol{\beta_7}$	5.154		
$\boldsymbol{\beta_8}$	-44.218		
$\boldsymbol{\beta_9}$	6.325		
$\boldsymbol{\beta_{10}}$	-79.676		
$\boldsymbol{\beta_{11}}$	-0.276		
$\boldsymbol{\beta_{12}}$	-6.371		
$\boldsymbol{\beta_{13}}$	5.962		
$\boldsymbol{\beta_{14}}$	-1141.5		

Table A.13 Model-13

Estimated model parameter values		Goodness of fit	
$\boldsymbol{\beta_0}$	-0.490	R^2	1
$\boldsymbol{\beta_1}$	-0.035	adj_R^2	1
$\boldsymbol{\beta_2}$	0.098	$RMSE$	0.00405
$\boldsymbol{\beta_3}$	-0.023	f_stat	1.53e+04
$\boldsymbol{\beta_4}$	1.352	p_value	0.00633
$\boldsymbol{\beta_5}$	0.0005		
$\boldsymbol{\beta_6}$	0.0006		
$\boldsymbol{\beta_7}$	0.0006		
$\boldsymbol{\beta_8}$	-0.004		
$\boldsymbol{\beta_9}$	0.001		
$\boldsymbol{\beta_{10}}$	-0.007		
$\boldsymbol{\beta_{11}}$	-2.6168e-05		
$\boldsymbol{\beta_{12}}$	-0.0008		
$\boldsymbol{\beta_{13}}$	0.0005		
$\boldsymbol{\beta_{14}}$	-0.121		

Table A.14 Model-14

Estimated model parameter values		Goodness of fit	
$\boldsymbol{\beta_0}$	-0.072	R^2	1
$\boldsymbol{\beta_1}$	-0.112	adj_R^2	0.999
$\boldsymbol{\beta_2}$	0.268	$RMSE$	0.0355
$\boldsymbol{\beta_3}$	-0.156	f_stat	1.79e+03
$\boldsymbol{\beta_4}$	4.550	p_value	0.0185
$\boldsymbol{\beta_5}$	0.001		
$\boldsymbol{\beta_6}$	0.002		
$\boldsymbol{\beta_7}$	0.002		
$\boldsymbol{\beta_8}$	-0.012		
$\boldsymbol{\beta_9}$	0.003		
$\boldsymbol{\beta_{10}}$	-0.027		
$\boldsymbol{\beta_{11}}$	-9.2905e-05		
$\boldsymbol{\beta_{12}}$	-0.002		
$\boldsymbol{\beta_{13}}$	0.002		
$\boldsymbol{\beta_{14}}$	-0.395		

Table A.15 Model-15

Estimated model parameter values		Goodness of fit	
$\boldsymbol{\beta_0}$	0.027	R^2	1
$\boldsymbol{\beta_1}$	-0.061	adj_R^2	1
$\boldsymbol{\beta_2}$	0.134	$RMSE$	0.0139
$\boldsymbol{\beta_3}$	-0.065	f_stat	4.25e+03
$\boldsymbol{\beta_4}$	2.405	p_value	0.012
$\boldsymbol{\beta_5}$	0.0008		
$\boldsymbol{\beta_6}$	0.001		
$\boldsymbol{\beta_7}$	0.001		
$\boldsymbol{\beta_8}$	-0.006		
$\boldsymbol{\beta_9}$	0.002		
$\boldsymbol{\beta_{10}}$	-0.013		
$\boldsymbol{\beta_{11}}$	-3.9412e-05		
$\boldsymbol{\beta_{12}}$	-0.0008		
$\boldsymbol{\beta_{13}}$	0.001		
$\boldsymbol{\beta_{14}}$	-0.211		

Table A.16 Model-16

Estimated model parameter values		Goodness of fit	
$\boldsymbol{\beta_0}$	-2.675	R^2	1
$\boldsymbol{\beta_1}$	-1.044	adj_R^2	1
$\boldsymbol{\beta_2}$	2.507	$RMSE$	0.129
$\boldsymbol{\beta_3}$	-1.230	f_stat	1.28e+04
$\boldsymbol{\beta_4}$	41.541	p_value	0.00693
$\boldsymbol{\beta_5}$	0.015		
$\boldsymbol{\beta_6}$	0.021		
$\boldsymbol{\beta_7}$	0.018		
$\boldsymbol{\beta_8}$	-0.118		
$\boldsymbol{\beta_9}$	0.032		
$\boldsymbol{\beta_{10}}$	-0.241		
$\boldsymbol{\beta_{11}}$	-0.0007		
$\boldsymbol{\beta_{12}}$	-0.020		
$\boldsymbol{\beta_{13}}$	0.019		
$\boldsymbol{\beta_{14}}$	-3.635		

Table A.17 Model-17

Estimated model parameter values		**Goodness of fit**	
$\boldsymbol{\beta_0}$	-202.710	R^2	0.718
$\boldsymbol{\beta_1}$	0.889	adj_R^2	0.707
$\boldsymbol{\beta_2}$	-14.545	$RMSE$	72.1
$\boldsymbol{\beta_3}$	3.338	f_stat	67
$\boldsymbol{\beta_4}$	86.554	p_value	9.03e-54
$\boldsymbol{\beta_5}$	-0.0006		
$\boldsymbol{\beta_6}$	0.261		
$\boldsymbol{\beta_7}$	-0.017		
$\boldsymbol{\beta_8}$	-8.121		

Table A.18 Model-18

Estimated model parameter values		**Goodness of fit**	
$\boldsymbol{\beta_0}$	-613.860	R^2	0.725
$\boldsymbol{\beta_1}$	2.562	adj_R^2	0.714
$\boldsymbol{\beta_2}$	-43.669	$RMSE$	211
$\boldsymbol{\beta_3}$	11.259	f_stat	69.4
$\boldsymbol{\beta_4}$	263.980	p_value	6.19e-55
$\boldsymbol{\beta_5}$	-0.001		
$\boldsymbol{\beta_6}$	0.778		
$\boldsymbol{\beta_7}$	-0.066		
$\boldsymbol{\beta_8}$	-25.110		

Table A.19 Model-19

Estimated model parameter values		**Goodness of fit**	
$\boldsymbol{\beta_0}$	-289.840	R^2	0.717
$\boldsymbol{\beta_1}$	1.450	adj_R^2	0.706
$\boldsymbol{\beta_2}$	-26.626	$RMSE$	125
$\boldsymbol{\beta_3}$	6.456	f_stat	66.9
$\boldsymbol{\beta_4}$	139.08	p_value	1.05e-53
$\boldsymbol{\beta_5}$	-0.0009		
$\boldsymbol{\beta_6}$	0.468		
$\boldsymbol{\beta_7}$	-0.041		
$\boldsymbol{\beta_8}$	-13.224		

Table A.20 Model-20

Estimated model parameter values		**Goodness of fit**	
$\boldsymbol{\beta_0}$	-5532.100	R^2	0.722
$\boldsymbol{\beta_1}$	24.513	adj_R^2	0.712
$\boldsymbol{\beta_2}$	-424.200	$RMSE$	2.03e+03
$\boldsymbol{\beta_3}$	105.270	f_stat	68.5
$\boldsymbol{\beta_4}$	2448	p_value	1.7e-54
$\boldsymbol{\beta_5}$	-0.0169		
$\boldsymbol{\beta_6}$	7.541		
$\boldsymbol{\beta_7}$	-0.628		
$\boldsymbol{\beta_8}$	-232.280		

Table A.21 Model-21

Estimated model parameter values		Goodness of fit	
$\boldsymbol{\beta_0}$	-1.884	R^2	0.707
$\boldsymbol{\beta_1}$	0.004	adj_R^2	0.696
$\boldsymbol{\beta_2}$	-0.074	$RMSE$	0.312
$\boldsymbol{\beta_3}$	0.025	f_stat	63.5
$\boldsymbol{\beta_4}$	0.771	p_value	4.81e-52
$\boldsymbol{\beta_5}$	-8.4511e-06		
$\boldsymbol{\beta_6}$	0.001		
$\boldsymbol{\beta_7}$	-0.0001		
$\boldsymbol{\beta_8}$	-0.071		

Table A.22 Model-22

Estimated model parameter values		Goodness of fit	
$\boldsymbol{\beta_0}$	-7.2384	R^2	0.718
$\boldsymbol{\beta_1}$	0.009	adj_R^2	0.707
$\boldsymbol{\beta_2}$	-0.185	$RMSE$	0.881
$\boldsymbol{\beta_3}$	0.097	f_stat	67.2
$\boldsymbol{\beta_4}$	2.642	p_value	7.73e-54
$\boldsymbol{\beta_5}$	-2.144e-05		
$\boldsymbol{\beta_6}$	0.003		
$\boldsymbol{\beta_7}$	-0.0006		
$\boldsymbol{\beta_8}$	-0.245		

Table A.23 Model-23

Estimated model parameter values		Goodness of fit	
$\boldsymbol{\beta_0}$	-3.878	R^2	0.721
$\boldsymbol{\beta_1}$	0.005	adj_R^2	0.710
$\boldsymbol{\beta_2}$	-0.110	$RMSE$	0.505
$\boldsymbol{\beta_3}$	0.054	f_stat	68.2
$\boldsymbol{\beta_4}$	1.449	p_value	2.52e-54
$\boldsymbol{\beta_5}$	-1.2216e-05		
$\boldsymbol{\beta_6}$	0.002		
$\boldsymbol{\beta_7}$	-0.0003		
$\boldsymbol{\beta_8}$	-0.134		

Table A.24 Model-24

Estimated model parameter values		Goodness of fit	
$\boldsymbol{\beta_0}$	-65.004	R^2	0.724
$\boldsymbol{\beta_1}$	0.097	adj_R^2	0.714
$\boldsymbol{\beta_2}$	-1.853	$RMSE$	8.33
$\boldsymbol{\beta_3}$	0.888	f_stat	69.3
$\boldsymbol{\beta_4}$	24.319	p_value	7.52e-55
$\boldsymbol{\beta_5}$	-0.0002		
$\boldsymbol{\beta_6}$	0.035		
$\boldsymbol{\beta_7}$	-0.005		
$\boldsymbol{\beta_8}$	-2.258		

Table A.25 Model-25

Estimated model parameter values		**Goodness of fit**	
$\boldsymbol{\beta_0}$	151.010	R^2	0.874
$\boldsymbol{\beta_1}$	-0.826	adj_R^2	0.865
$\boldsymbol{\beta_2}$	-22.354	$RMSE$	48.9
$\boldsymbol{\beta_3}$	1.589	f_stat	101
$\boldsymbol{\beta_4}$	85.895	p_value	7.23e-84
$\boldsymbol{\beta_5}$	0.044		
$\boldsymbol{\beta_6}$	0.0005		
$\boldsymbol{\beta_7}$	-0.036		
$\boldsymbol{\beta_8}$	0.015		
$\boldsymbol{\beta_9}$	-0.039		
$\boldsymbol{\beta_{10}}$	0.191		
$\boldsymbol{\beta_{11}}$	-0.0006		
$\boldsymbol{\beta_{12}}$	0.258		
$\boldsymbol{\beta_{13}}$	-0.018		
$\boldsymbol{\beta_{14}}$	-8.185		

Table A.26 Model-26

Estimated model parameter values		**Goodness of fit**	
$\boldsymbol{\beta_0}$	536.330	R^2	0.879
$\boldsymbol{\beta_1}$	-2.5407	adj_R^2	0.871
$\boldsymbol{\beta_2}$	-70.581	$RMSE$	142
$\boldsymbol{\beta_3}$	1.683	f_stat	107
$\boldsymbol{\beta_4}$	280.440	p_value	7.11e-86
$\boldsymbol{\beta_5}$	0.130		
$\boldsymbol{\beta_6}$	0.005		
$\boldsymbol{\beta_7}$	-0.111		
$\boldsymbol{\beta_8}$	0.169		
$\boldsymbol{\beta_9}$	-0.251		
$\boldsymbol{\beta_{10}}$	0.311		
$\boldsymbol{\beta_{11}}$	-0.001		
$\boldsymbol{\beta_{12}}$	0.773		
$\boldsymbol{\beta_{13}}$	-0.067		
$\boldsymbol{\beta_{14}}$	-25.371		

Table A.27 Model-27

Estimated model parameter values		Goodness of fit	
$\boldsymbol{\beta_0}$	374.630	R^2	0.876
$\boldsymbol{\beta_1}$	-1.539	adj_R^2	0.867
$\boldsymbol{\beta_2}$	-42.329	$RMSE$	83.7
$\boldsymbol{\beta_3}$	1.828	f_stat	104
$\boldsymbol{\beta_4}$	145.130	p_value	1.01e-84
$\boldsymbol{\beta_5}$	0.077		
$\boldsymbol{\beta_6}$	0.0006		
$\boldsymbol{\beta_7}$	-0.058		
$\boldsymbol{\beta_8}$	0.085		
$\boldsymbol{\beta_9}$	-0.079		
$\boldsymbol{\beta_{10}}$	0.168		
$\boldsymbol{\beta_{11}}$	-0.0009		
$\boldsymbol{\beta_{12}}$	0.463		
$\boldsymbol{\beta_{13}}$	-0.041		
$\boldsymbol{\beta_{14}}$	-13.350		

Table A.28 Model-28

Estimated model parameter values		Goodness of fit	
$\boldsymbol{\beta_0}$	5309.800	R^2	0.878
$\boldsymbol{\beta_1}$	-24.531	adj_R^2	0.870
$\boldsymbol{\beta_2}$	-676.320	$RMSE$	1.35e+03
$\boldsymbol{\beta_3}$	25.505	f_stat	106
$\boldsymbol{\beta_4}$	2557.300	p_value	1.63e-85
$\boldsymbol{\beta_5}$	1.268		
$\boldsymbol{\beta_6}$	0.031		
$\boldsymbol{\beta_7}$	-1.035		
$\boldsymbol{\beta_8}$	1.349		
$\boldsymbol{\beta_9}$	-1.853		
$\boldsymbol{\beta_{10}}$	3.359		
$\boldsymbol{\beta_{11}}$	-0.017		
$\boldsymbol{\beta_{12}}$	7.476		
$\boldsymbol{\beta_{13}}$	-0.632		
$\boldsymbol{\beta_{14}}$	-234.530		

Table A.29 Model-29

Estimated model parameter values		Goodness of fit	
$\boldsymbol{\beta_0}$	-0.189	R^2	0.727
$\boldsymbol{\beta_1}$	0.003	adj_R^2	0.709
$\boldsymbol{\beta_2}$	-0.109	$RMSE$	0.305
$\boldsymbol{\beta_3}$	-0.016	f_stat	39.1
$\boldsymbol{\beta_4}$	0.726	p_value	4.16e-50
$\boldsymbol{\beta_5}$	3.5554e-05		
$\boldsymbol{\beta_6}$	-1.6102e-05		
$\boldsymbol{\beta_7}$	-0.0001		
$\boldsymbol{\beta_8}$	0.0008		
$\boldsymbol{\beta_9}$	-0.0002		
$\boldsymbol{\beta_{10}}$	0.0001		
$\boldsymbol{\beta_{11}}$	-8.3245e-06		
$\boldsymbol{\beta_{12}}$	0.001		
$\boldsymbol{\beta_{13}}$	-0.0001		
$\boldsymbol{\beta_{14}}$	-0.071		

Table A.30 Model-30

Estimated model parameter values		Goodness of fit	
$\boldsymbol{\beta_0}$	-2.756	R^2	0.740
$\boldsymbol{\beta_1}$	0.007	adj_R^2	0.722
$\boldsymbol{\beta_2}$	-0.287	$RMSE$	0.858
$\boldsymbol{\beta_3}$	-0.014	f_stat	41.7
$\boldsymbol{\beta_4}$	2.622	p_value	3.71e-52
$\boldsymbol{\beta_5}$	0.0001		
$\boldsymbol{\beta_6}$	-4.4721e-05		
$\boldsymbol{\beta_7}$	-0.0002		
$\boldsymbol{\beta_8}$	0.002		
$\boldsymbol{\beta_9}$	-0.001		
$\boldsymbol{\beta_{10}}$	0.002		
$\boldsymbol{\beta_{11}}$	-2.1097e-05		
$\boldsymbol{\beta_{12}}$	0.003		
$\boldsymbol{\beta_{13}}$	-0.0006		
$\boldsymbol{\beta_{14}}$	-0.246		

Table A.31 Model-31

Estimated model parameter values		Goodness of fit	
$\boldsymbol{\beta_0}$	-1.035	R^2	0.744
$\boldsymbol{\beta_1}$	0.004	adj_R^2	0.727
$\boldsymbol{\beta_2}$	-0.175	$RMSE$	0.491
$\boldsymbol{\beta_3}$	-0.011	f_stat	42.6
$\boldsymbol{\beta_4}$	1.3906	p_value	6.79e-53
$\boldsymbol{\beta_5}$	6.9968e-05		
$\boldsymbol{\beta_6}$	-3.2236e-05		
$\boldsymbol{\beta_7}$	-0.0001		
$\boldsymbol{\beta_8}$	0.001		
$\boldsymbol{\beta_9}$	8.833e-05		
$\boldsymbol{\beta_{10}}$	0.001		
$\boldsymbol{\beta_{11}}$	-1.1963e-05		
$\boldsymbol{\beta_{12}}$	0.002		
$\boldsymbol{\beta_{13}}$	-0.0003		
$\boldsymbol{\beta_{14}}$	-0.134		

Table A.32 Model-32

Estimated model parameter values		Goodness of fit	
$\boldsymbol{\beta_0}$	-19.910	R^2	0.746
$\boldsymbol{\beta_1}$	0.081	adj_R^2	0.729
$\boldsymbol{\beta_2}$	-2.862	$RMSE$	8.11
$\boldsymbol{\beta_3}$	-0.209	f_stat	43.1
$\boldsymbol{\beta_4}$	23.698	p_value	2.84e-53
$\boldsymbol{\beta_5}$	0.001		
$\boldsymbol{\beta_6}$	-0.0004		
$\boldsymbol{\beta_7}$	-0.002		
$\boldsymbol{\beta_8}$	0.023		
$\boldsymbol{\beta_9}$	-0.007		
$\boldsymbol{\beta_{10}}$	0.030		
$\boldsymbol{\beta_{11}}$	-0.0002		
$\boldsymbol{\beta_{12}}$	0.035		
$\boldsymbol{\beta_{13}}$	-0.005		
$\boldsymbol{\beta_{14}}$	-2.262		

Table A.33 Model-33

Estimated model parameter values		Goodness of fit	
$\boldsymbol{\alpha}$	-0.2504	R^2	1
$\boldsymbol{\theta_1}$	0.0917	adj_R^2	1
$\boldsymbol{\theta_2}$	0.2245	$RMSE$	8.3591e-12
$\boldsymbol{\theta_3}$	0.0243	f_stat	2.5451e+27
$\boldsymbol{\theta_4}$	0.0667	p_value	3.147e-148

Table A.34 Model-34

Estimated model parameter values		Goodness of fit	
$\boldsymbol{\alpha}$	-0.4884	R^2	1
$\boldsymbol{\theta_1}$	0.0891	adj_R^2	1
$\boldsymbol{\theta_2}$	0.2245	$RMSE$	3.0692e-11
$\boldsymbol{\theta_3}$	0.0140	f_stat	1.6925e+27
$\boldsymbol{\theta_4}$	0.0445	p_value	2.967e-147

Table A.35 Model-35

Estimated model parameter values		Goodness of fit	
$\boldsymbol{\alpha}$	-0.2177	R^2	1
$\boldsymbol{\theta_1}$	0.0707	adj_R^2	1
$\boldsymbol{\theta_2}$	0.3175	$RMSE$	1.3332e-11
$\boldsymbol{\theta_3}$	0.0223	f_stat	3.2120e+27
$\boldsymbol{\theta_4}$	0.0794	p_value	8.749e-149

Table A.36 Model-36

Estimated model parameter values		Goodness of fit	
$\boldsymbol{\alpha}$	-0.2343	R^2	1
$\boldsymbol{\theta_1}$	0.0891	adj_R^2	1
$\boldsymbol{\theta_2}$	0.3364	$RMSE$	1.5992e-10
$\boldsymbol{\theta_3}$	0.0250	f_stat	5.8169e+27
$\boldsymbol{\theta_4}$	0.0667	p_value	3.337e-150

Table A.37 Model-37

Estimated model parameter values		Goodness of fit	
$\boldsymbol{\alpha}$	-0.5773	R^2	1
$\boldsymbol{\theta_1}$	0.0420	adj_R^2	1
$\boldsymbol{\theta_2}$	0.3564	$RMSE$	2.6169e-14
$\boldsymbol{\theta_3}$	0.0167	f_stat	1.2822e+27
$\boldsymbol{\theta_4}$	0.1000	p_value	1.365e-146

Table A.38 Model-38

Estimated model parameter values		Goodness of fit	
$\boldsymbol{\alpha}$	-0.5077	R^2	1
$\boldsymbol{\theta_1}$	0.0728	adj_R^2	1
$\boldsymbol{\theta_2}$	0.3564	$RMSE$	4.4384e-14
$\boldsymbol{\theta_3}$	0.0204	f_stat	4.0174e+27
$\boldsymbol{\theta_4}$	0.0749	p_value	2.555e-149

Table A.39 Model-39

Estimated model parameter values		Goodness of fit	
$\boldsymbol{\alpha}$	-0.8426	R^2	1
$\boldsymbol{\theta_1}$	0.0515	adj_R^2	1
$\boldsymbol{\theta_2}$	0.3364	$RMSE$	4.6086e-14
$\boldsymbol{\theta_3}$	0.0129	f_stat	1.3456e+27
$\boldsymbol{\theta_4}$	0.0500	p_value	1.047e-146

Table A.40 Model-40

Estimated model parameter values		Goodness of fit	
$\boldsymbol{\alpha}$	-0.5283	R^2	1
$\boldsymbol{\theta_1}$	0.0667	adj_R^2	1
$\boldsymbol{\theta_2}$	0.3175	$RMSE$	4.7641e-13
$\boldsymbol{\theta_3}$	0.0210	f_stat	3.2572e+27
$\boldsymbol{\theta_4}$	0.0707	p_value	8.102e-149

Table A.41 Model-41

Estimated model parameter values		Goodness of fit	
$\boldsymbol{\alpha}$	1.1741e+05	R^2	0.9526
$\boldsymbol{\theta_1}$	0.0022	adj_R^2	0.9517
$\boldsymbol{\theta_2}$	5.1732e-05	$RMSE$	29.2548
$\boldsymbol{\theta_3}$	1.0000e-05	f_stat	1.0821e+03
$\boldsymbol{\theta_4}$	1.0000e-05	p_value	3.843e-141

Table A.42 Model-42

Estimated model parameter values		Goodness of fit	
$\boldsymbol{\alpha}$	1.0678e+05	R^2	0.9567
$\boldsymbol{\theta_1}$	0.0023	adj_R^2	0.9559
$\boldsymbol{\theta_2}$	6.7088e-05	$RMSE$	82.7490
$\boldsymbol{\theta_3}$	1.0000e-05	f_stat	1.1845e+03
$\boldsymbol{\theta_4}$	1.0000e-05	p_value	3.577e-145

Table A.43 Model-43

Estimated model parameter values		Goodness of fit	
$\boldsymbol{\alpha}$	9.4895e+04	R^2	0.9558
$\boldsymbol{\theta_1}$	0.0022	adj_R^2	0.9549
$\boldsymbol{\theta_2}$	7.3160e-05	$RMSE$	48.8176
$\boldsymbol{\theta_3}$	1.0000e-05	f_stat	1.1554e+03
$\boldsymbol{\theta_4}$	1.0072e-05	p_value	4.634e-144

Table A.44 Model-44

Estimated model parameter values		Goodness of fit	
$\boldsymbol{\alpha}$	9.7505e+04	R^2	0.9560
$\boldsymbol{\theta_1}$	0.0022	adj_R^2	0.9552
$\boldsymbol{\theta_2}$	7.3160e-05	$RMSE$	800.6150
$\boldsymbol{\theta_3}$	1.0000e-05	f_stat	1.1635e+03
$\boldsymbol{\theta_4}$	1.0072e-05	p_value	2.249e-144

Table A.45 Model-45

Estimated model parameter values		Goodness of fit	
$\boldsymbol{\alpha}$	8.8260e+04	R^2	0.8595
$\boldsymbol{\theta_1}$	0.0022	adj_R^2	0.8569
$\boldsymbol{\theta_2}$	5.0168e-05	$RMSE$	0.2138
$\boldsymbol{\theta_3}$	1.0000e-05	f_stat	328.9924
$\boldsymbol{\theta_4}$	1.0000e-05	p_value	2.106e-90

Table A.46 Model-46

Estimated model parameter values		Goodness of fit	
$\boldsymbol{\alpha}$	-9.8888e+04	R^2	0.8796
$\boldsymbol{\theta_1}$	0.0022	adj_R^2	0.8773
$\boldsymbol{\theta_2}$	5.1732e-05	$RMSE$	0.5703
$\boldsymbol{\theta_3}$	1.0000e-05	f_stat	391.3111
$\boldsymbol{\theta_4}$	1.0000e-05	p_value	1.952e-97

Table A.47 Model-47

Estimated model parameter values		Goodness of fit	
$\boldsymbol{\alpha}$	-9.4438e+04	R^2	0.8814
$\boldsymbol{\theta_1}$	0.0022	adj_R^2	0.8792
$\boldsymbol{\theta_2}$	5.1732e-05	$RMSE$	0.3265
$\boldsymbol{\theta_3}$	1.0000e-05	f_stat	395.6292
$\boldsymbol{\theta_4}$	1.0000e-05	p_value	6.925e-98

Table A.48 Model-48

Estimated model parameter values		Goodness of fit	
$\boldsymbol{\alpha}$	-6.4004e+04	R^2	0.8843
$\boldsymbol{\theta_1}$	0.0022	adj_R^2	0.8822
$\boldsymbol{\theta_2}$	5.1732e-05	$RMSE$	5.3467
$\boldsymbol{\theta_3}$	1.0000e-05	f_stat	408.6551
$\boldsymbol{\theta_4}$	1.0000e-05	p_value	3.221e-99

APPENDIX B

Model prediction versus experimental data

In each figure ■ shows experimental data points, — ▪ shows pure quadratic model prediction, ▬ ▬ shows quadratic model prediction, ▬ shows kriging prediction.

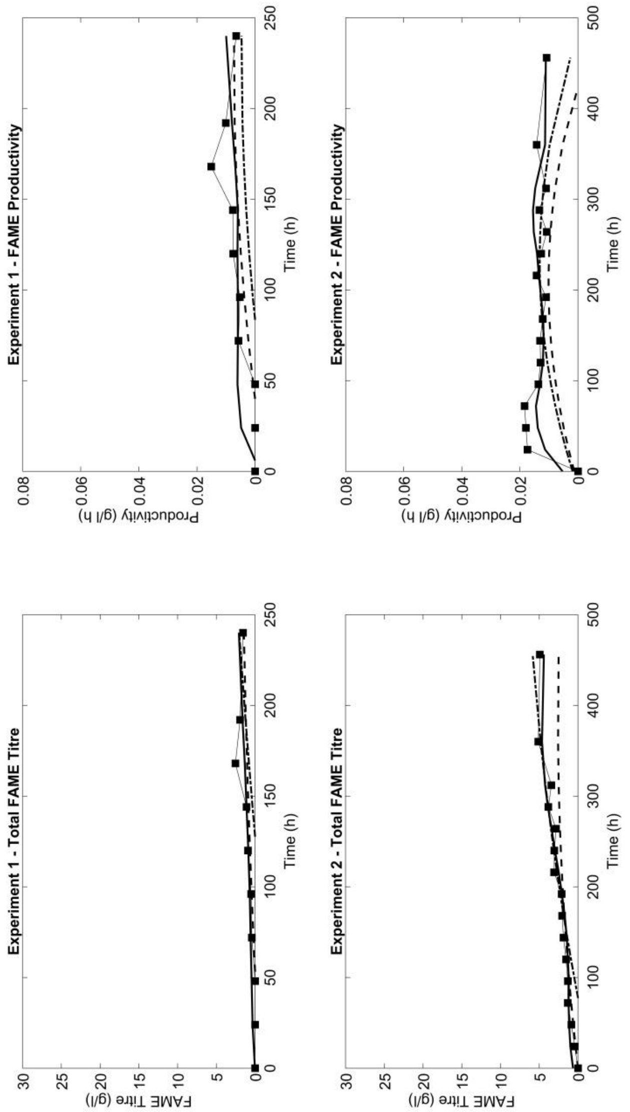

Figure B.1 Large data set

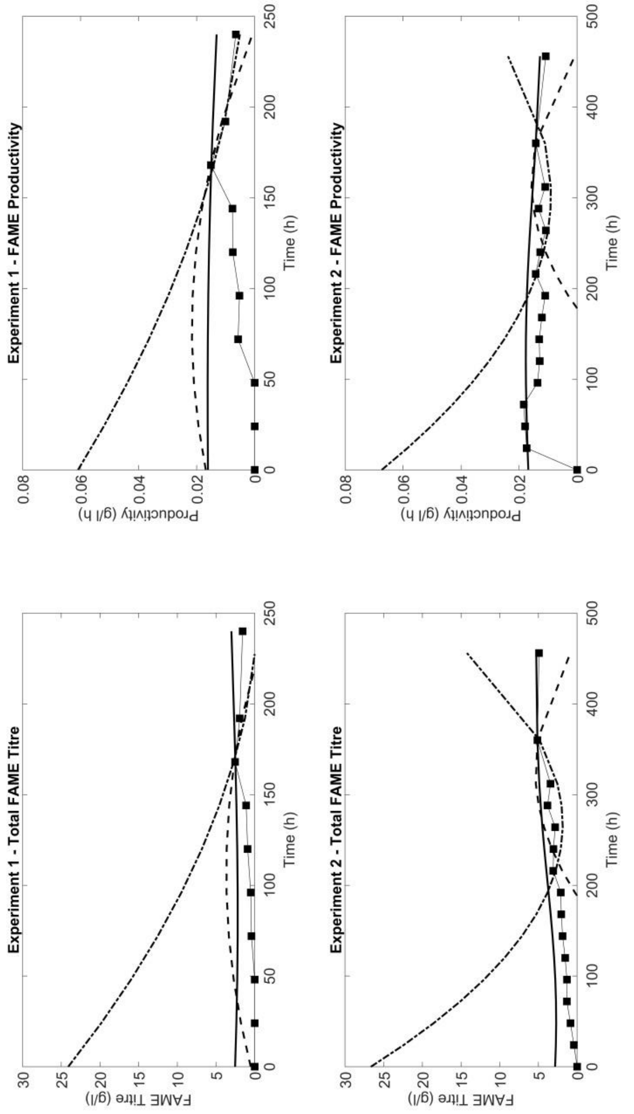

Figure B.2 Small data set

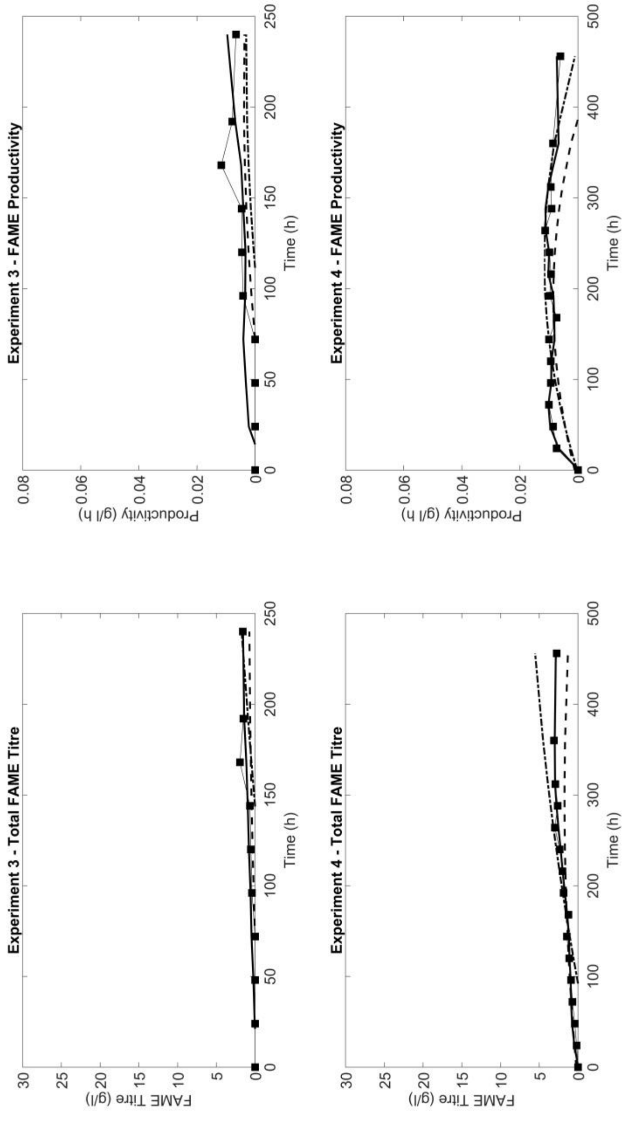

Figure B.3 Large data set

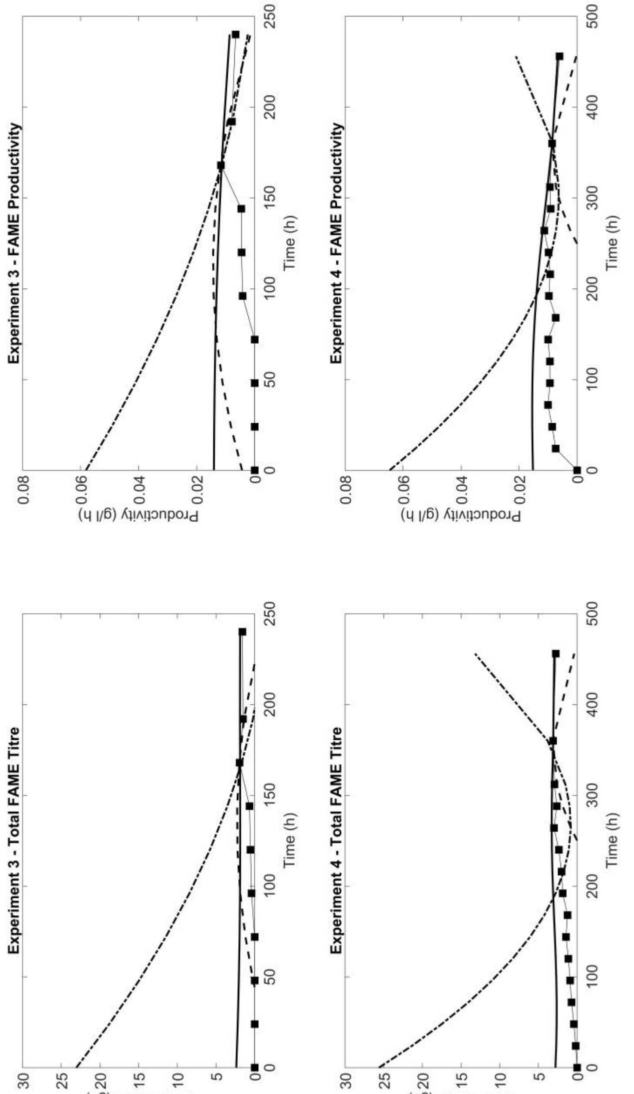

Figure B.4 Small data set

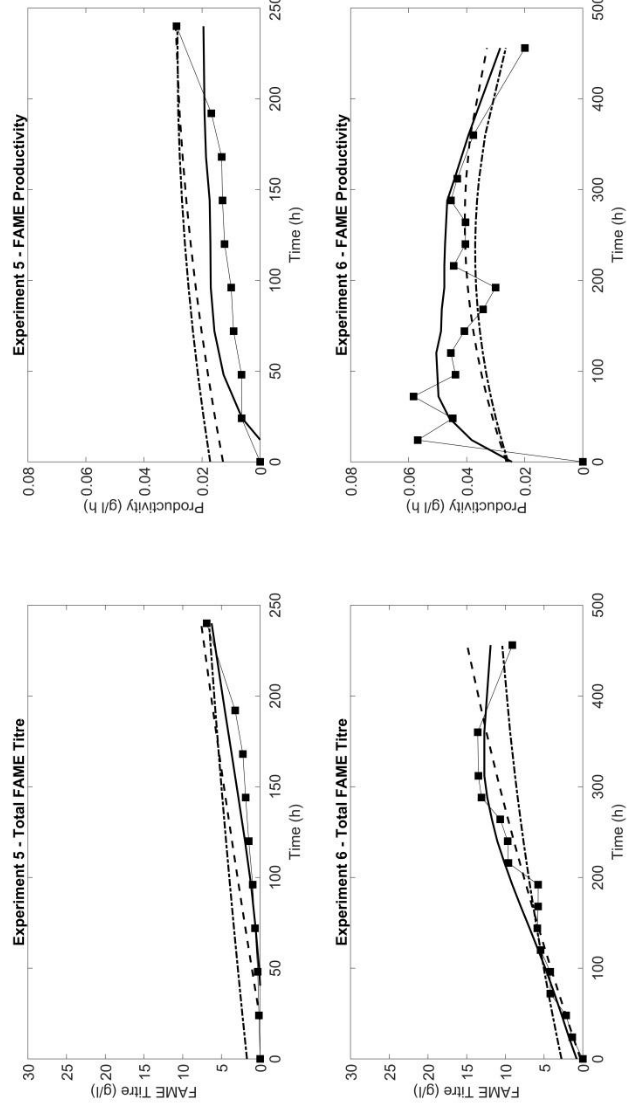

Figure B.5 Large data set

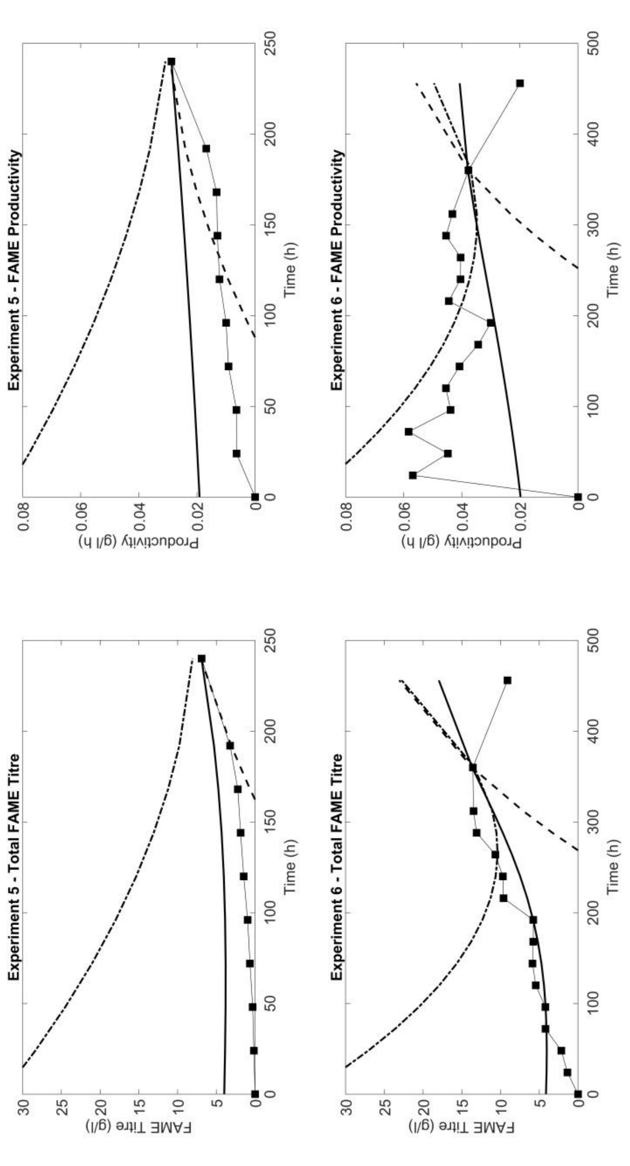

Figure B.6 Small data set

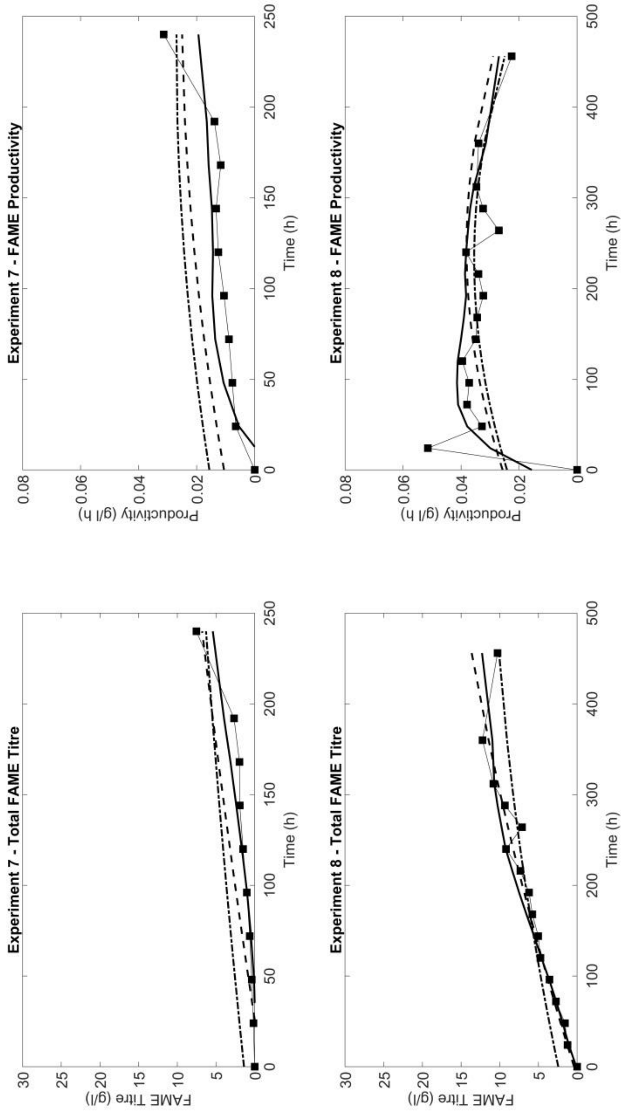

Figure B.7 Large data set

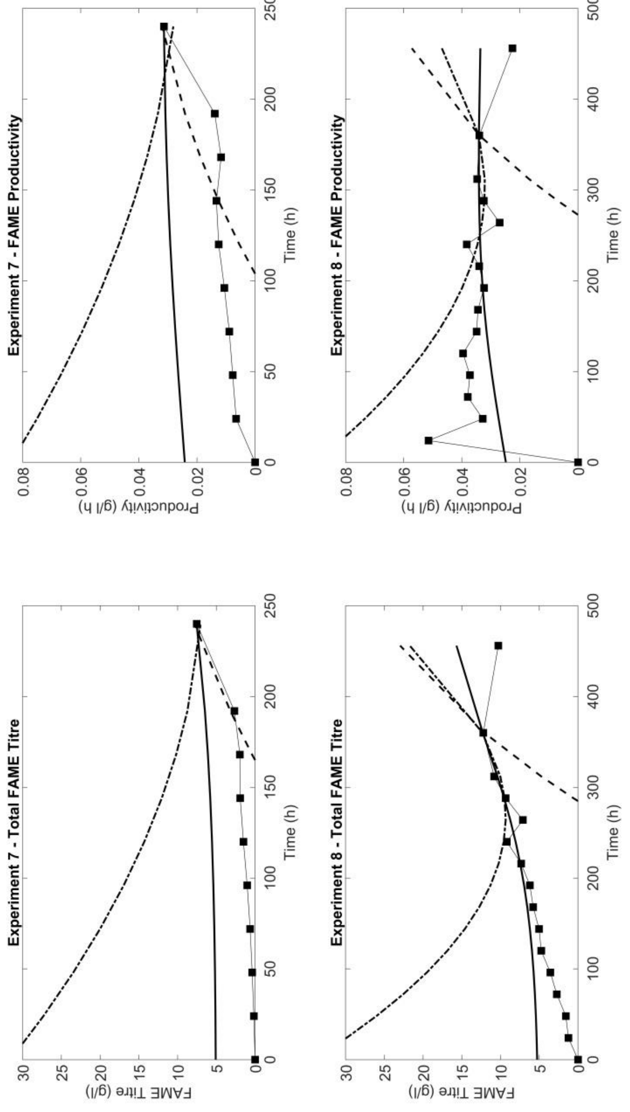

Figure B.8 Small data set

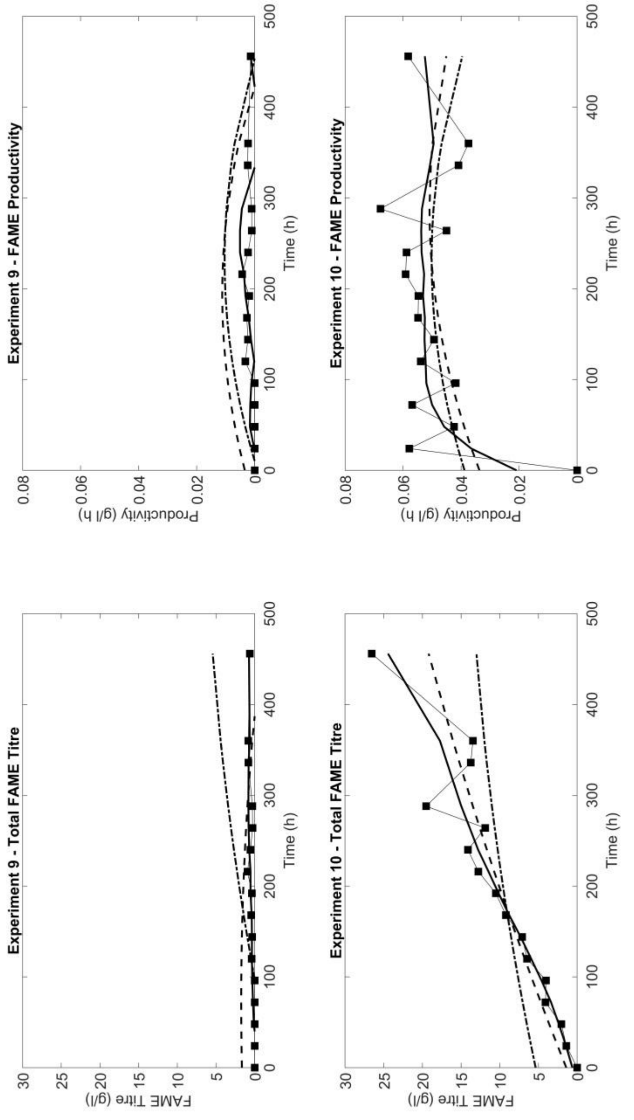

Figure B.9 Large data set

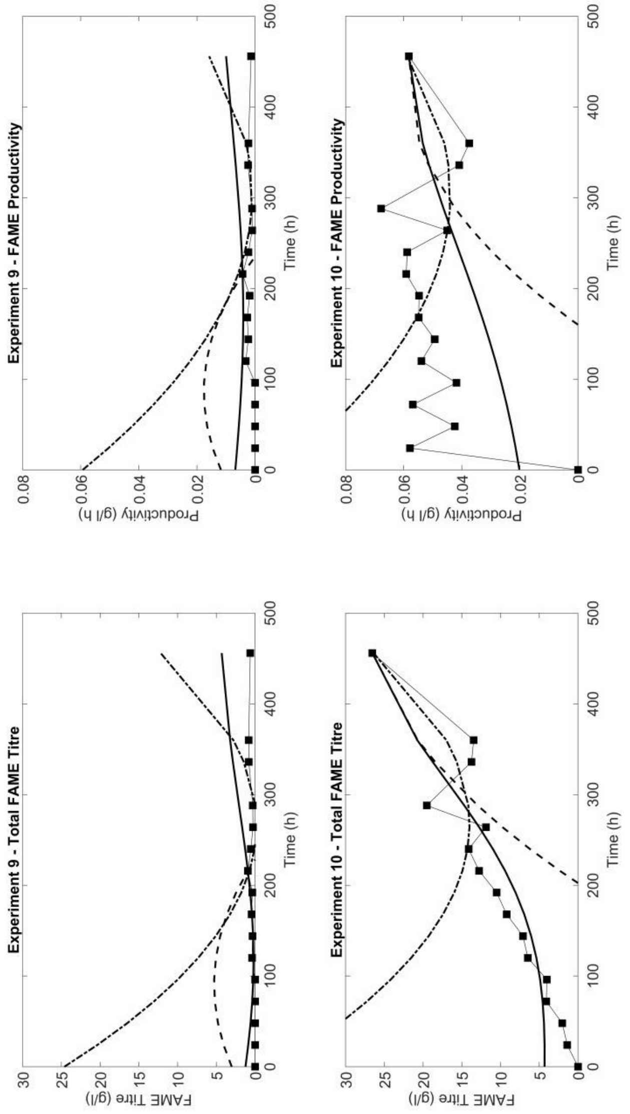

Figure B.10 Small data set

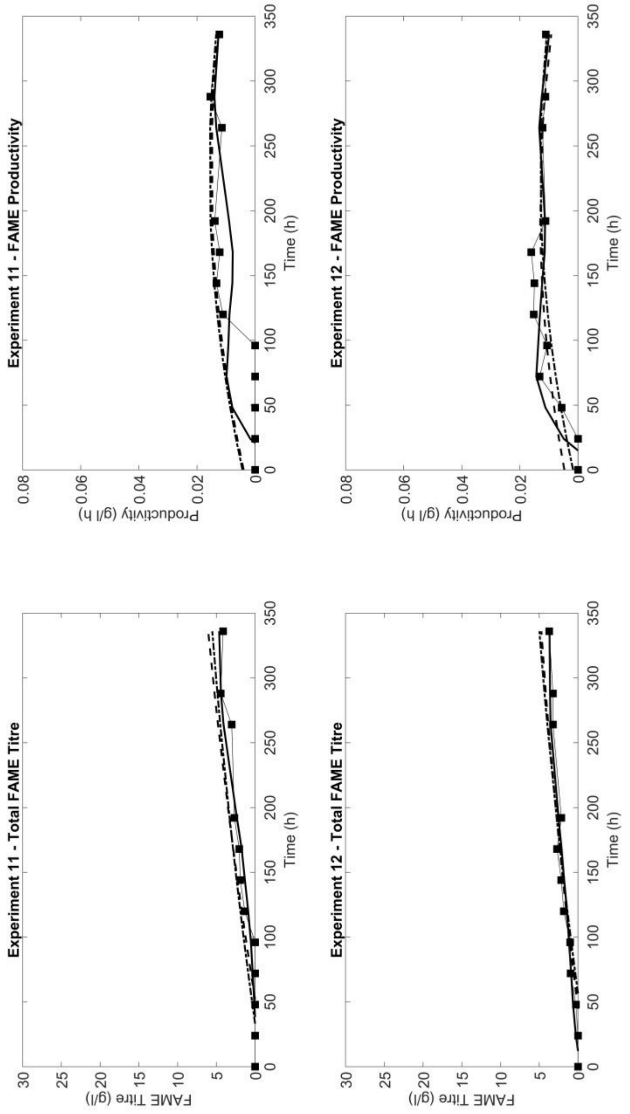

Figure B.11 Large data set

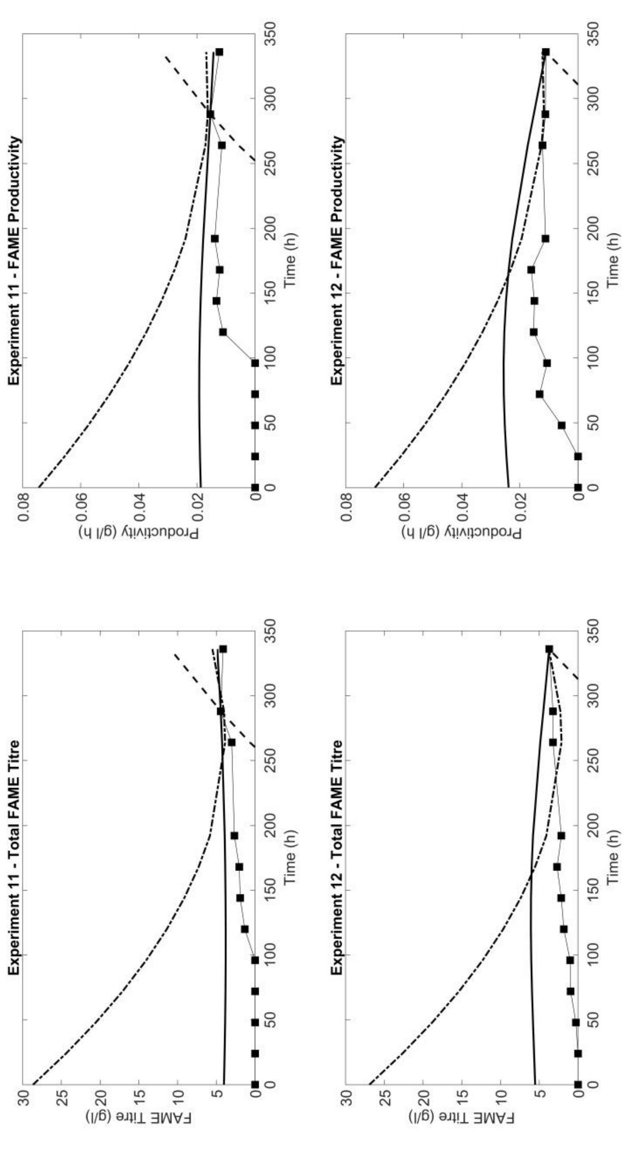

Figure B.12 Small data set

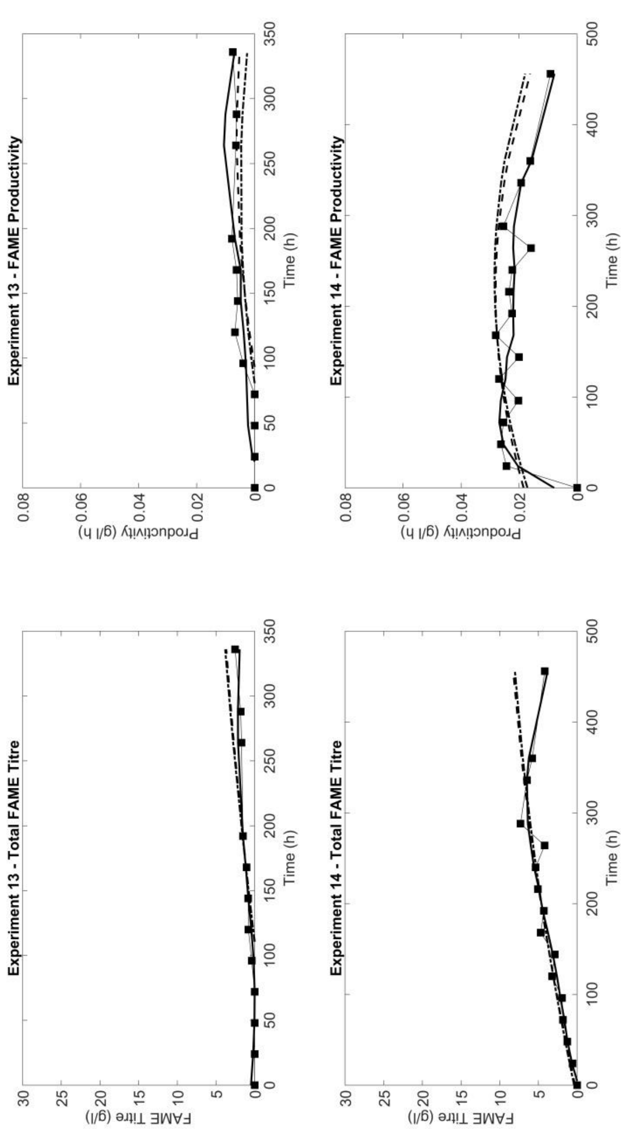

Figure B.13 Large data set

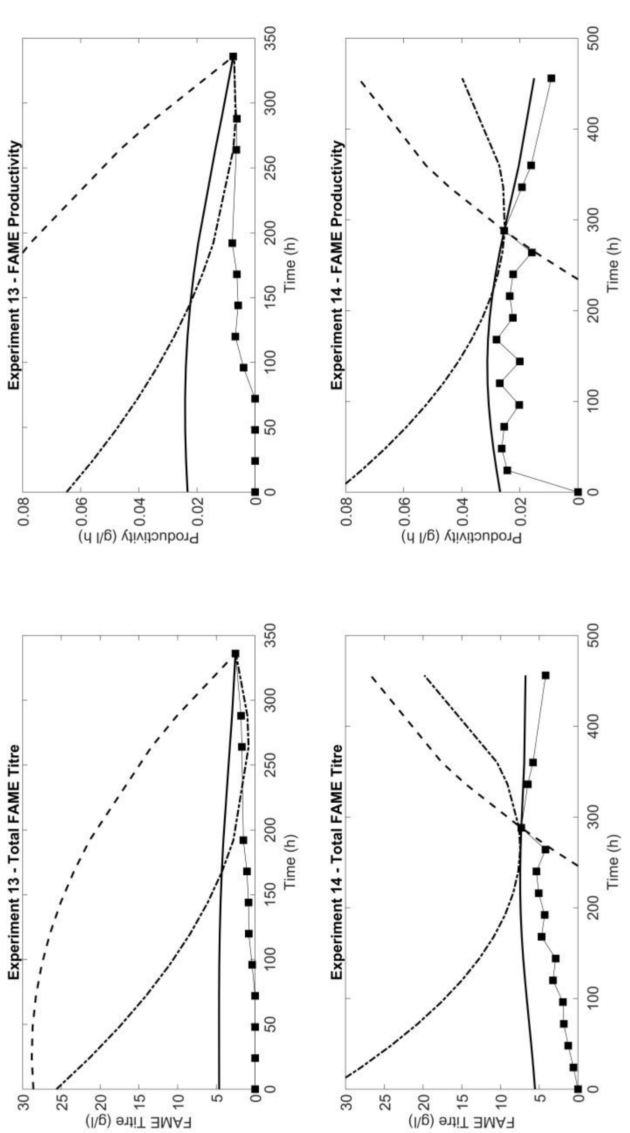

Figure B.14 Small data set

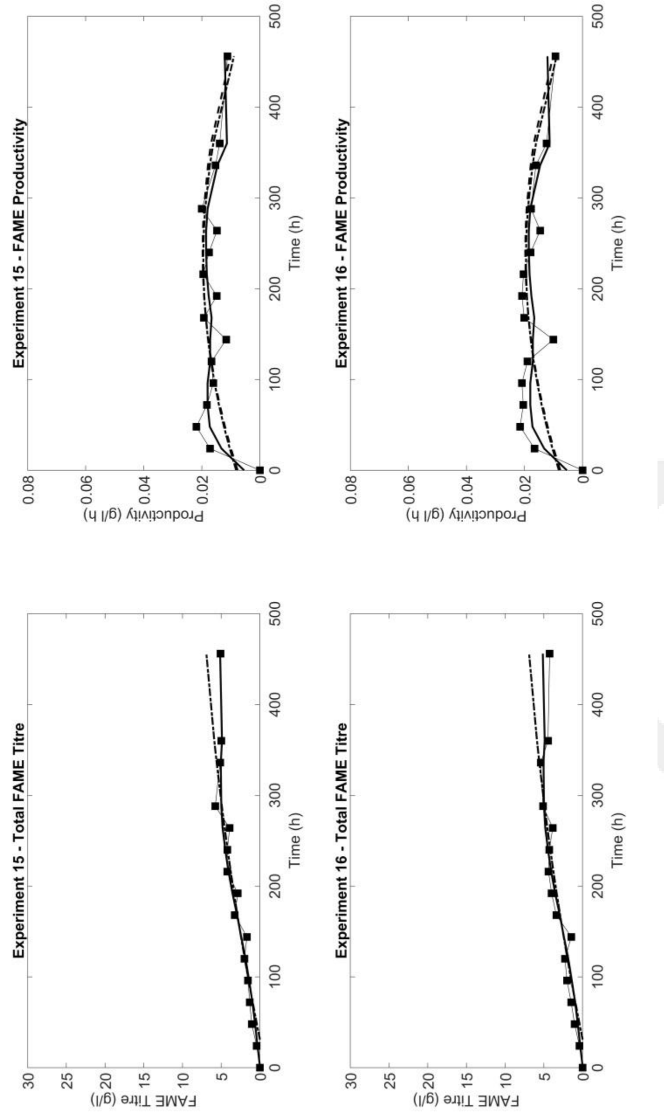

Figure B.15 Large data set

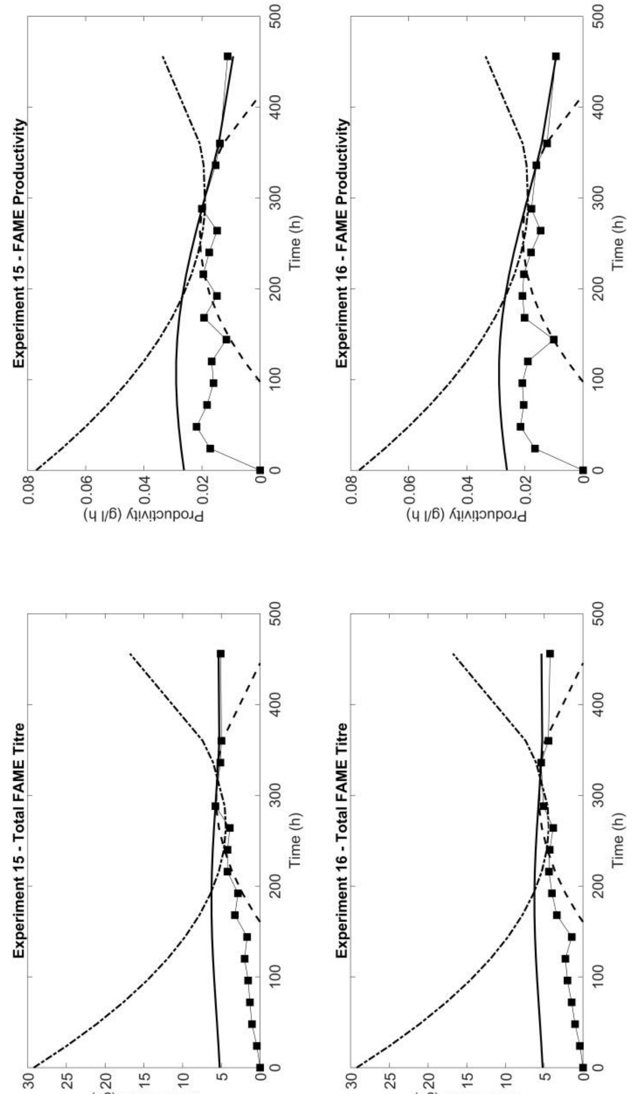

Figure B.16 Small data set

CURRICULUM VITAE

Ceyda KULA

Marmara Üniversitesi

Biyomühendislik Bölümü

34722 İstanbul, Türkiye

Telefon: +90 216 348 0292-729

e-mail: ceyda.kula@marmara.edu.tr

KİŞİSEL BİLGİLER

Doğum Tarihi : 05.08.1987

Doğum Yeri : Manisa, Türkiye.

EĞİTİM BİLGİLERİ

Doktora (2012- 2018) Marmara Üniversitesi, Fen Bilimleri Enstitüsü/Biyomühendislik Anabilim Dalı (İngilizce)

Tez Başlığı: Multi-objective optimization at a crude novel lipase catalyzed FAME production: Kriging as an alternative to RSM

Danışman: Doç. Dr. Nihat Alpagu SAYAR

Yüksek Lisans (2010-2012) Ege Üniversitesi, Fen Bilimleri Enstitüsü/Biyomühendislik Anabilim Dalı (Tezli)

Tez Başlığı: Sikloartan grubu siklokantogenol ve astragenol saponinlerinin mikrobiyal biyotransformasyonu

Danışman: Prof. Dr. Erdal BEDİR

Lisans (2005-2010) Ege Üniversitesi**,** Mühendislik Fakültesi/Biyomühendislik Bölümü

Tez Başlığı: Eczacılıkta Biyoteknoloji'nin Kullanım Alanları

Danışman: Prof. Dr. Erdal BEDİR

ÇALIŞMA BİLGİLERİ

Araştırma Görevlisi (2012-Devam) Marmara Üniversitesi/Mühendislik Fakültesi/Biyomühendislik Bölümü/Biyomühendislik Anabilim Dalı

BİLİMSEL MAKALELER

Pinar, O., Karaosmanoğlu, K., Sayar, N.A., **Kula, C**., Kazan, D. and Sayar, A.A. (2017). **Assessment of hazelnut husk as a lignocellulosic feedstock for the production of fermentable sugars and lignocellulolytic enzymes**. 3 Biotech, 7:367, 1-9.

Bedir, E., **Kula, C.,** Öner, Ö., Altaş, M., Tağ, Ö., Öngen, G. (2015). **Microbial transformation of *Astragalus* sapogenins using *Cunninghamella blakesleeana* NRRL 1369 and *Glomerella fusarioides* ATCC 9552**. Journal of Molecular Catalysis B: Enzymatic, 115, 29-34.

ULUSLARARASI BİLİMSEL TOPLANTILARDA SUNULAN BİLDİRİLER

KULA Ceyda, SAYAR Nihat Alpagu (2018). Manually-modified design of experiments for early biocatalyst evaluation – lipase-catalysed fatty acid methyl ester production. 18th Europen Congress on Biotechology (Özet Bildiri/Poster)

KULA Ceyda, SAYAR Nihat Alpagu (2016). Biodiesel production from waste cooking oil via optimised transesterification by a locally sourced lipase. Challenges in Building a Sustainable Biobased Economy, EcoBio Conference 2016 (Özet Bildiri/Poster)

KULA Ceyda, SAYAR Nihat Alpagu (2015). *Cryptococcus diffluens* D44 lipase for biodiesel production from waste cooking oil via optimized transesterification. BEC 2015 VII. Bioengineering Congress (Özet Bildiri/Poster)

KULA Ceyda, SAYAR Nihat Alpagu (2014). Lipase Catalyzed Esterification Reactions–A Kinetic Model. 16th Europen Congress on Biotechology (Özet Bildiri/Poster)

KULA Ceyda, YILMAZ Duygu Elif, YALÇIN Hüsniye Tansel, SAYAR Nihat Alpagu (2014). Characterization of Lipase Enzyme and Catalyzed Esterification Reaction as a Model System. Enzymes for Biocatalysis (Özet Bildiri/Poster)

ARAŞTIRMA PROJELERİ

Sikloartan grubu sapogenollerden hareketle potansiyel sitotoksik etkinligi yüksek moleküllerin hazırlanması, TÜBİTAK-SBAG–109S345 TÜBITAK PROJESI, Bursiyer, 2010-2013 (ULUSAL)

Lipazla katalizlenen bir esterifikasyon reaksiyonu: kinetik analizi, proses tasarımı ve proses metriklerinin değerlendirilmesi, FEN-C-DRP-080415-0124 BABKO PROJESİ, Araştırmacı, 2015-2017

KATILINAN BİLİMSEL ETKİNLİKLER

From Network To Targets: Workshop on OMIC technologies and their applications, 7-9 Haziran 2017, İstanbul, Türkiye.

New Horizons in Biocatalysis for Biomaterials (Biocat-Mat) çalıştayı, 8-12 Nisan 2014, İzmir, Türkiye.

ÖDÜLLER VE BURSLAR

TÜBİTAK-BİDEB, Bilim İnsanı Destekleme Daire Başkanlığı, 2211 Yurt İçi Doktora Burs Programı çerçevesi içerisinde, doktora eğitimi sırasında karşılıksız eğitim bursu.